Stable single molecules for quantum optics and all-optical switches

Navarro Perez, P.

Stable single molecules for quantum optics and all-optical switches

PROEFSCHRIFT

ter verkrijging van
de graad van Doctor aan de Universiteit Leiden,
op gezag van Rector Magnificus prof.mr. C.J.J.M. Stolker,
volgens besluit van het College voor Promoties
te verdedigen op donderdag 13 November 2014
klokke: 13.45 uur

door

Pedro Navarro Pérez
geboren te México City, México
in 1982

Promotiecommissie:

Promotor:	Prof. dr. M.A.G.J. Orrit	Universiteit Leiden
Overige Leden:	Prof. dr. T.J. Aartsma	Universiteit Leiden
	Dr. S. Bonnet	Universiteit Leiden
	Prof. dr. E. R. Eliel	Universiteit Leiden
	Prof. dr. E.J.J. Groenen	Universiteit Leiden
	Prof. dr. B. Kozankiewicz	Polish Academy of Sciences
	Prof. dr. J.M. van Ruitenbeek	Universiteit Leiden
	Prof. dr. V. Subramaniam	Universiteit Twente, AMOLF

The presented work is part of the research program of the Stichting voor Fundamenteel Onderzoek der Materie (FOM), which is financially supported by the Nederlandse Organisatie voor Wetenschappelijk Onderzoek (N*W*O).

Casimir PhD Series, Delft-Leiden, 2014 - 27

ISBN: 978-90-8593-200-0

TABLE OF CONTENTS

CHAPTER 1

1.1.Introduction

Over the history of computing hardware, the number of transistors in integrated circuits doubled every two years[1], as predicted by Gordon Moore, co-founder of Intel Co. His "law" has been also proven to be accurate in predicting the development of other fields of technology, such as: semiconductors, microprocessor prices related to number of transistors, memory capacity, sensors and even the number and size of pixels in digital screens. This development has dramatically enhanced the impact of digital electronics in nearly every segment of the world's economy. However, after about 40 years, this technology is approaching its limit. On the one hand, the miniaturization of silicon transistors has a physical limit given by the finite size of atoms. On the other, the maximum frequency at which silicon transistors can be driven is determined by its size and shape.

Even though Moore's law has been accurate, it has predicted its own end in a few years. However, the spectacular advances in nanosciences and nanooptics of the last 20 years have brought the realization of all-optical data processing near to us[2]. Photonic circuits, quantum computing[3] and quantum information processing[4] have risen as the most promising emerging technologies. In principle, photonic circuits would be faster and easier to integrate with telecommunication networks than conventional electronic components. Photons are good candidates for transmitting information over large distances with minimal perturbation and losses[5] because they hardly interact with each other. However, this "blessing" is at the same time a drawback when such interactions are needed to produce basic logic operations for further data manipulation.

The proposed photonic circuits will be composed of many different individual elements, each of them with a particular function. To replace the silicon chips of today by optical analogs, low-loss interconnect waveguides, optical transistors, power splitters,

optical amplifiers, optical modulators, filters, lasers and detectors have to be integrated on the same chip. Till now, just few of these devices have been realized independently[6-8]. Each of these reports required very particular experimental conditions, like low temperatures (1 K), ultra-high vacuums and/or nano lithographic fabrications. The main problem will be to integrate all the individual elements on the same chip while keeping the properties of each element unchanged.

The efforts in our research group are mostly focused in the development of all-optical transistors, amplifiers and modulators at the single molecule level. In order to develop such devices, the most fundamental element is a stable and high-efficient source of single photons with well-defined energies. Many single quantum emitters have been considered for quantum-optical applications because they produce photons in a stochastic way (one-by-one). The first isolated quantum systems were ions and neutral atoms trapped from the gas phase. But due to the experimental conditions, they might have problems for the assembly and integration on chips[9,10]. So, condensed matter systems appear more attractive and promising in the long term. Quantum dots[11] (QD's) became very popular because of their room temperature performance and long photo-stability, together with a scalable preparation. However, due to their distribution in sizes their optical properties are also very broad distributed. In particular, they present very complex blinking dynamics which would limit their use as photon sources. Another promising quantum system in condense matter are the impurity-vacancy centers (IVC's) in diamond[12]. Their robustness, photochemical stability, and room temperature operation are clear advantages, but at the same time, the very high chemical stability will make integration on chips very challenging. One disadvantage as single photon sources is the low monochromatic emission efficiencies (<1%)[8].

In this thesis, we propose that single organic molecules could be used as high efficient single photon sources and non-linear elements for developing photonic circuits and even further, use their quantum properties to develop new information technologies[5]. The first advantage of using single organic molecules is that any kind of molecule can be

designed and chemically synthetized depending on the desired application. All the molecules obtained by synthetic methods are structurally the same and they have in principle, identical physico-chemical properties. Single organic molecules can be observed at room temperature if they are immobilized in a solid matrix (solvent) and if the concentration is set to about 1-10 nM. At these conditions, the stream of single photons from a single molecule is much more monochromatic (due to quantized transitions) and the emission rates are much higher than what can be obtained from QD's and/or IVC's. The main disadvantage for these molecules is their poor photostability at room temperature due to photochemical reactions induced by the presence of oxygen.

However, when the organic molecules are embedded in a solid medium and cooled to temperatures below 10 K many of these disadvantages can be overcome. The photostability is increased mainly because the absence of diffusing oxygen. The absorption cross section of a single molecule can be increased by many orders of magnitude compared to room temperature. The fluorescence quantum yield is enhanced by the decreased intersystem crossing (ISC) rate. When the solid medium surrounding the molecule is properly chosen such that it does not present active crystal modes at the experimental temperature, the electronic excitation occur without creation or annihilation of phonons. As a result, the absorption and emission of photons occurs within a very narrow distribution of frequencies called the "zero-phonon line" (ZPL). The total number of photons per second that can be obtained within the ZPL from single molecules[13] can be at least 10^3 times higher than what can be obtained from an IVC's or a QD[11]. These photons could then be used to transport and process qubits[5] without any need to constantly decode them into more manageable forms, such as charges. Different schemes to stochastically switch on and off the emission of photons have been also explored lately[6,10,14].

Furthermore, the non-linear response of the fluorescence of a single molecule (pump beam) to a second optical excitation (probe beam) could open the way to develop all-optical transistors[15]. However, the probability of occurrence of this non-linear optical

process is in particularly low in organic dyes. Therefore, these experiments require very high intensities of electromagnetic radiation. In order to reach such high intensities the work reported by Chang et. al made use of a surface plasmon to create a very high localized field near the quantum emiter[16,16,17]. Another report by Hwang et. al described a modulation on the fluorescence of a single molecule when a second intense CW-radiation was applied on resonance with a higher vibroelectronic state[18]. The reported modulation was about 0.3%, and the effect was explained in terms of a population inversion.

Our proposed experiment can be described using scheme 1.1, which shows an energy diagram for a three-level system on a single organic molecule. First, we spectrally isolate the molecule at low temperature by exciting on-resonance the strongly-allowed optical transition (pump beam, transition $S_0 \rightarrow S_1$) while detecting the red-shifted fluorescent photons (Dashed arrow). At our conditions, the molecule behaves as a single two-level quantum system (TLS) that can be driven at any desired Rabi frequency (Ω). When the fluorescence state is optically saturated, the nonlinear response to the absorption of just one photon (Probe) into the dark triplet state (T_1) could switch-off the stream of photons with a very high efficiency.

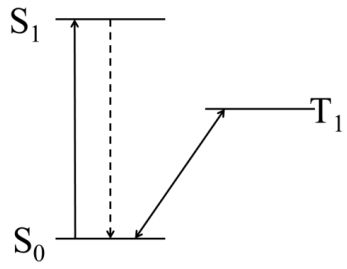

Scheme 1.1: *Energy level diagram of a three-level system. The solid arrow is the resonant excitation (pump beam) and the dotted arrow is the fluorescence. The double arrow (probe beam) shows the resonant excitation of the transition to the triplet state*

However, for the molecules studied in this thesis, the $S_0 \rightarrow T_1$ transition is strongly forbidden with an expected transition rate in the order of 10^{-10} s^{-1}. Even though

our proposed experiment is the optical response to the absorption of a single probe photon, we still need radiation intensities in the order of 1 kW cm^{-2} (I_{Probe}) to populate this T_1 state. The control of such a non-linear process on an isolated molecule could be used in the development of new all-optical transistors with high optical gains. The transistor's gain that can be obtained from the ratio of the lifetimes of the two electronic states is 10^6.

After the observation of such a non-linear effect in our single molecules, we could try to perform at least two experiments. The first idea resembles the observation made by Hans Dehmelt[19], in 1986, which reported the experimental switching process of the fluorescence of a trapped Ba^{2+} ion (reproduced from ref.19, in scheme 1.2). The changes between the on and off states probed the existence of quantum jumps within the isolated quantum emitter. The photophysical process referred as "optical shelving", corresponded to the random transition of the emissive state of the ion, into a "dark long-lived" state. This process was completely random, no active control was attempted.

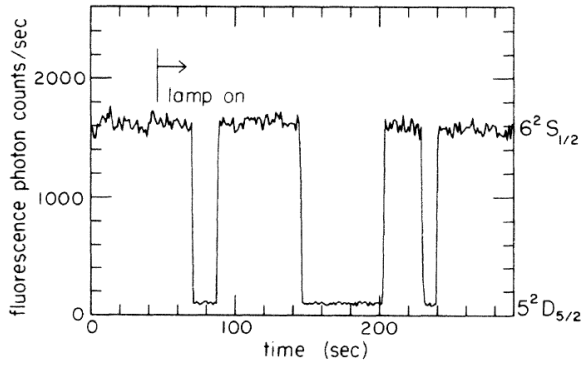

Scheme 1.2: *Fluorescence time trace of a trapped Ba^{2+} ion (As reported by Dehmelt, et.a ref.19). The fluorescence (in cps) is lost when the ion is shelved into a "dark" state and recovers after the lifetime of this state. The control beam is a continuous irradiation (lamp on).*

The second operation that can be achieved on these two-color experiments is to make the molecule transparent to the pump beam (scheme 1.3, taken from ref 2). In this case, the molecule is continuously excited on resonance with the ground→excited transition (pump, 1.3a). The excitation with the probe beam into the shelved state ("s", 1.3b) prohibits the absorption of more pump photons. As a result, during the lifetime of this "shelved" state, the molecule becomes transparent to the pump beam (scheme 1.3c). The overall process is that one probe photon induces a huge change in the absorption of the single molecule, creating a non-linear optical response.

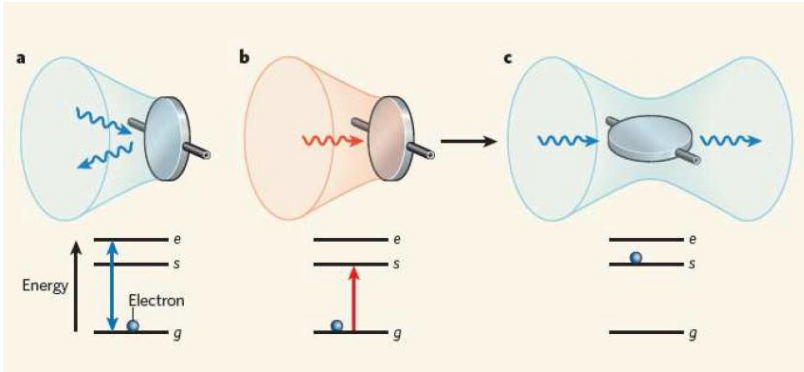

Scheme 1.3: *The "mirror" represents a single quantum emitter that scatters light. a) shows the excitation on resonance of the strong optical transition between ground (g) and excited (e) state. b) Excitation showing the transition to the shelved state (s). c) Shows that the system becomes transparent to the first beam when is in the s-state.*

In our all-optical experiment we propose an active control of the population of the emissive state by pumping the molecule into its triplet state[12,20]. In this way, we want to induce shelving of the fluorescent transition ($S_0 \rightarrow S_1$) after the absorption of just one photon into T_1. The "off" times is related to the time the molecule resides on its triplet dark state (micro-miliseconds). During this time no fluorescence is expected, however, the signal is recovered after the decay of the triplet sate into its ground state. These two beam experiments may lead to an optical triggered source of single photons[6,14]. The probability for two photons to interact with each other[15] within the same molecule is also

increased in this experiment, which could be the basics for all-optical transistor-like operations.

1.2.Single molecule spectroscopy at low temperature

The systems studied in this thesis are fluorescent molecules (guest) surrounded by condensed matter. In particular, we look at polycyclic-aromatic hydrocarbons (PAH's), which are organic molecules composed mainly of carbon and hydrogen. Owing to the sp^2 hybridization of the carbon atoms, those molecules are commonly planar and one pure *p-orbital* lies perpendicular to the plane of the molecule. These free orbitals favor the delocalization of the electrons which confers the aromatic character to these molecules.

The observation of single molecules is achieved when the fluorescent dye is highly diluted into a solvent, which in our single molecule (SM) systems is called the host. The optical properties of the guest are determined by the electrostatic solvent-guest interactions. These interactions depend on the solid-state structure and chemical properties of the host. In this thesis we report systematic studies of different single molecules (perylene, terrylene and dibenzoterrylene) embedded in different hosts (single molecular crystals with and without substituents methyl groups, poly-crystals, alkanes and polymers).

An insight into the theoretical foundations needed to describe our systems and to understand and interpret our observations is introduced now. The molecular spectra in cold matrixes can be described on the basis of the Born-Oppenheimer adiabatic approximation, which allows for the separability of degrees of freedom with different characteristic frequencies. In the adiabatic approximation the total Schrödinger equation is solved sequentially for electrons and nuclei.

First, the electronic distribution can be determined for a fixed configuration of the nuclear coordinates (on a single point). A complete electronic energy landscape can be obtained by slightly changing the nuclear coordinates. The shape of such a landscape for small amplitudes around a minimum can be described with an harmonic oscillator potential. Because the dependence of the electronic properties on the nuclear coordinates is negligible under this approximation, the electronic wavefunction can be calculated at the corresponding minimum of the harmonic potential.

For the experimental conditions of our experiments at low temperature and inside condense matter, the nuclear contribution into the total Schrödinger equation, can be again separated into different degrees of freedom if they present clearly distinguishable frequencies. One contribution corresponds to intramolecular degrees of freedom of the guest molecule, like molecular twisting, stretching, bond deformation or any other vibrational mode (optical phonon). The other contribution comes from intermolecular electrostatic interactions between the guest molecule and its surroundings (acoustic phonon).

The interactions between the guest molecule and the host are described in terms of an electron-phonon coupling. When the frequencies of the molecular vibrations of the guest are comparable to the frequencies of acoustic phonons of the host, a strong coupling between the guest and host can exist, and therefore the adiabatic approximation (separation of variables with different frequencies) does not hold anymore. In the case of some of our studied molecular crystals, the phonon frequencies are clearly different from the molecular vibration frequencies. This frequency miss-match, responsible for weak electron-phonon coupling, is the experimental condition that allows for the observation of zero-phonon lines (ZPL's) of a guest inside of a host.

Because of the optical excitation, the interactions between the host molecules and the embedded guest are different when the guest is in the ground state than when it is in the excited state. The stabilization energy of the electronic configuration of any of these

two states comes mainly from Van der Waals interactions. The guest molecule on its excited state has a stronger polarization coefficient than in the ground state, and therefore the stabilization energy for the excited state is higher. As a result, the potential energy curve for each state at thermodynamic equilibrium has slightly different nuclear coordinates. The slight change of the nuclear coordinates has implications on the curvatures of the potentials, leading to different frequencies of the normal modes.

When many impurities are embedded in a solid (Scheme 1.4) the local environments for each guest molecule are different. As a result, the stabilization energy expected for each molecule will also depend on the insertion geometry (relative orientation) of a single guest respect to the hosts surrounding it. This randomness leads to a broad distribution of resonant frequencies for innumerable guests in the spectrum of bulk solid solutions.

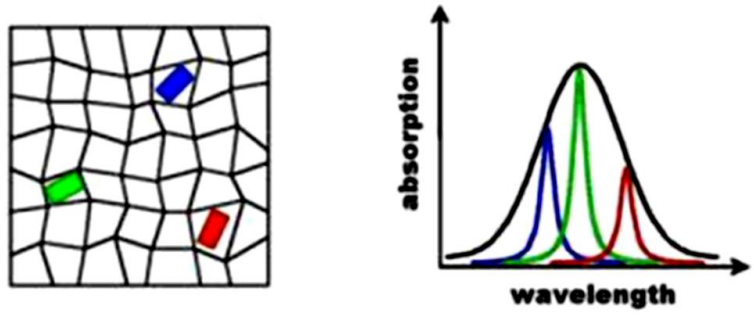

Scheme 1.4: *(Left) Representation of three molecules embedded in a solid giving rise to inhomogeneous distribution. Due to the different orientation and local surroundings of each molecule, their absorption lines are slightly shifted with respect to the others (Right).*

In principle, the probable number of insertion geometries of guest molecules within the host is extremely big (all possible combinations). This is known as the "*inhomogeneous distribution*" of the system, which is close related to the degree of crystallinity of the host. As an example of this, is that when the host is a crystalline

structure with long order range, the potential energy landscape could show well defined minima. As a result, a major number of guest molecules can occupy these potential minima, and give rise to spectroscopic insertion sites that appear in the bulk absorpt8ion or fluorescence spectra.

1.3. Zero-phonon line of a single molecule

For one single impurity, the spectral response of the electronic transition to light is expressed as the Fourier-transform of its temporal response. However, the interaction with the phonon bath at thermal equilibrium induces a modulation of the resonance frequency. In a simplified manner, the nuclear displacement can be expressed as a stochastic function that depends on thermal fluctuations giving rise to the quantized nature of phonons. The absorption spectrum, α, of a single molecule (Scheme 1.5) is defined in Eq. 1 by two contributions that depend on (ω, T), frequency and temperature:

$$\alpha(\omega,T) = \alpha_{ZPL}(\omega,T) + \alpha_{PSB}(\omega,T) \qquad \text{Eq.1}$$

The zero-phonon line (α_{ZPL}, ZPL) corresponds to a quasi-elastic scattering of the electronic excitation between states with the same vibrational modes, without any creation or annihilation of phonons in the bath. The “phonon side band” (α_{PSB}, PSB) corresponds to an inelastic scattering of the electronic transition with creation or annihilation of one or more quanta of vibrational energy. The PSB is formed by transitions that occur between two vibrational states with different quantum numbers.

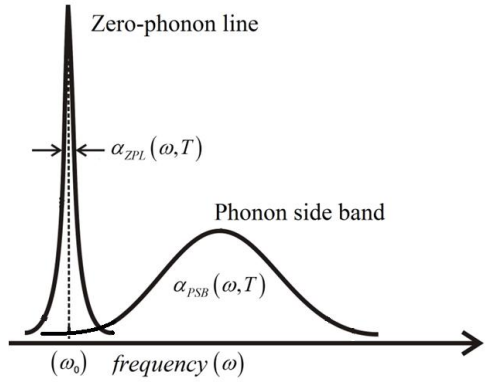

Scheme 1.5: *Absorption spectrum of a single molecule showing the ZPL and the corresponding PSB, The shape is defined by the frequency* (ω) *and the temperature (*T*). The axis shows increasing frequency towards the right side (High energy).*

The ZPL of a single molecule has a finite width (γ_0) defined by (Eq.2) the inverse of the total decay time of the coherence (T_2). This optical dephasing is governed by two terms: T_1 is the non-adiabatic process that induces decay of the population of the excited state, which determines its lifetime; and T_2^* is the pure dephasing time or "decoherence" which describes the time it takes for the electronic coherence to be dissipated by fluctuations of the phonon bath.

$$\gamma_0 = \frac{1}{\pi T_2} = \frac{1}{2\pi T_1} + \frac{1}{T_2^*} \qquad \text{Eq.2}$$

1.4.Sensitivity of single molecules

The high sensitivity of the narrow $\alpha_{ZPL}(\omega,T)$ of a SM to any chemical or physical perturbation on its local environment is the reason why the use of single fluorescent probes has become a used technique in the field of optical sensing at nanometer scale. The optical linewidth (γ) in fluorescence excitation spectra as a function of temperature (T) shown in Eq.3, is a phenomenological expression.

$$\gamma(T) = \gamma_0 + bT^{\delta} + \Delta\gamma_{LFM}\exp(-E_{act}/k_BT) \qquad \text{Eq.3}$$

Here, γ_0 is the natural lifetime-limited linewidth, bT^{δ} describes the interactions with tunneling two-level systems (TLS's) with $(\delta \approx 1)$, and $\Delta\gamma_{LFM}\exp(-E_{act}/k_BT)$ is a broadening due to dephasing by phonons and quasi-localized low-frequency vibrational modes with activation energy (E_{act}), and temperature *T*. The different contributions of the TLS's and the low-frequency modes can be determined from the line broadening of a single-molecule, which allow identifying the nature of the active phonons in the host[21]. On the one hand, a TLS jumps at comparatively low rates between two configurations. The jumping times are broadly distributed. Therefore, the effect of a TLS on the line shape of a molecular absorption are small shifts of the transition energy leading to a line broadening when many TLS's are present in the local environment. Such a broadening is called "spectral diffusion" (SD) in analogy to a diffusion of a particle in one dimension. Low frequency modes (LFM's), on the other hand, have frequencies much higher than TLS, ranging from GHz to THz. Therefore, the fluctuations induced by the LFM's in the electronic transition are averaged in the slow evolution of the optical coherence, and as a result only contribute to the pure dephasing process (T_2^*). In chapter 2 we use the ZPL to probe the activation energies of localized modes in the surrounding of an impurity.

Even when the host is selected to avoid the presence of low-frequency vibrations that interact with the optical transition of the single molecule, they are always present to

some extent, and therefore they have to be considered when studying single impurities. The use of external fields to control and produce a response of the spectral properties of the ZPL has been used for tune the resonance of the molecule to any other desired frequency[22]. The perturbation of a single molecule by the presence of an optical or an electric field will be presented to contribute the discussion of this thesis.

When any guest molecule is embedded in a transparent solid matrix (host), chemical and physical interactions with the neighbor molecules influence the observed optical properties. Matrices lacking of long-range order will generally give rise to broad distributions of electronic transition energies, and therefore to broad featureless inhomogeneous bands. Crystalline matrices, in contrast, often give rise to well-defined insertion sites where the guest molecule and its first solvent shell are matched with the rest of the crystal. This situation gives rise to narrow spectroscopic bands, as for many molecular crystals and Shpol'skii matrices of *n*-alkanes. The residual disorder of the crystalline lattices (impurities, dislocations, grain boundaries, surfaces, etc.) is responsible for the observed inhomogeneous distribution.

Electrostatic interactions between two molecules follow from the static charge distributions of these molecules. For large intermolecular distances, they vary as a power law of distance, for example as $1/r^3$ for a dipole-dipole interaction. The Van der Waals interaction results from interaction between induced dipole moments and presents a $1/r^6$ dependence. All of these forces determine the stabilization energies of the ground and excited states and therefore the energy of electronic and vibronic transitions.

In the experiments, the temperature and pressure are changed from room temperature and atmospheric pressure to 1.5 K and pressure < 10^{-5} mbar. These changes have an effect on the distances and the relative orientation of the molecules, which determines their electronic transitions. The way to describe this effect is with an electrostatic description that relates the thermodynamic properties and the polarizabilities of the host and the guest, depending on the distance[23]. The change of frequency ($d\tilde{\nu}$)

corresponding to a temperature decrease (dT) can be thought of as resulting from a volume reduction, bringing the host and guest molecules in closer proximity. The total frequency shift as a function of temperature is then related to the hydrostatic compressibility (κ) and to the thermal expansion (ϕ_{term}) of the material by[24]:

$$\frac{d\tilde{\nu}}{dT} = -\frac{3\phi_{term}}{\kappa}\left(\frac{\delta\tilde{\nu}}{\delta P}\right)_T \qquad \text{Eq.4}$$

with

$$\phi_{term} = \frac{1}{V}\left(\frac{\partial V}{\partial T}\right)_p \qquad \kappa = -\frac{1}{V}\left(\frac{\partial V}{\partial P}\right)_T$$

The temperature dependence of the compressibility factor (κ) varies less than 5 % within our experimental conditions (1.5 – 20 K)[23].

When the sample is irradiated with a laser beam, the optical linewidth can present broadening, frequency jumps or spectral shifts[25,26]. The most important parameters that determine whether or not a single-molecule system can be used as a single quantum emitter are the efficiency of the emitted photons from the single molecule within its ZPL, the stability of the resonant linewidth and the photo stability of the dye before it bleaching[27].

The increasing excitation intensity (I) induces a broadening of the homogeneous linewidth (γ_0) due to increasing thermal fluctuations on the bath. Such a relation is shown in Eq. 5, can in principle increase with no limit. We use this equation to determine at which excitation intensity the molecule starts to be saturated (I_s).

$$\gamma = \gamma_0\sqrt{1+\frac{I}{I_s}} \qquad \text{Eq.5}$$

$$R(I) = R_{\infty} \frac{I}{I + I_s} \qquad \text{Eq.6}$$

At the same time that the line becomes broader the number of emitted photons R also depends on the excitation intensity. At low intensity $I < I_s$ the rate of emitted photons increases linearly with the higher excitation intensity. However, a single two-level system has a natural lifetime of the excited state that determines a maximum emission rate. Optical saturation occurs when the rate of excitation equals the emission rate of the two-level system. Considering a three-level quantum system, three different rate constants are present, and one has the lower rate constant. This steady-state condition determines the maximum emission rate that can be obtained from the other processes. In poly-aromatic hydrocarbons (PAH's) this is the long-lived triplet state (T_1) which is populated via intersystem crossing (ISC) after optical excitation to the S_1 state with a very low probability.

The maximum number of detected photons R_{∞} measured at saturation, are well below the expected maximum emission rate (≈10^9 *hν/s*). This is mainly due to low collection efficiency of the experiment, which depends on the orientation of the excitation dipole, the orientation of the emissive dipole, total internal reflection, the numerical aperture of the collecting optics, the quantum efficiency of the detectors, all transmission of optics and electronic noise sources.

The transition energy of a single two-level system (TLS) can be tuned when applying an external voltage[28,29]. For centrosymmetric molecules like terrylene, perylene or dibenzoterrylene (Tr, Pr and DBT) the static transition dipole moment in gas phase is zero and should give rise to a quadratic dependence of the electronic transition frequency on the applied field. However, the experiments that have been performed on single molecules showed linear Stark-effect with a broad distribution of frequency shifts and broadenings[22,28,29]. The reason seems to be that when these molecules are embedded in

the solids, the presence of microscopic forces breaks their symmetry, so the statit transition dipole moment is not zero. The excitation frequency change ($\Delta\nu$) of a single molecule in an electric field ($\vec{E}$) follows the phenomenological expression:

$$h\Delta\nu = -\Delta\vec{\mu}_E \bullet f_e\vec{E} \qquad \text{Eq.7}$$

Where $\Delta\vec{\mu}_E$, is the difference between excited and ground state dipole moments. At the single molecule level the homogeneous electric field ($\vec{E}$) has to be corrected with a local field factor f_e.

1.5.Outline of the thesis

This section is organized in a way that you can connect between the main goals of the project with the main milestones founded during the development of the thesis, which gave us the reasons to perform each experiment. At the very beginning, terrylene was the selected molecule to try to develop the optical transistor because is a dye with very low intersystem crossing rate and high fluorescence quantum yield. With this, the molecule does not blink during the intensity traces, which is a requirement for our controlled "switching" experiment. Terrylene has been measured by single molecule spectroscopy (SMS) [30-32] in different matrices, and the absorption lie around 570±10 nm for the singlet state, and lifetime limited lines are also reported. However, the energy at which the lowest triplet state lies above the ground state has never been measured due to the same low intersystem crossing rate. Quantum chemical calculations predict approximately a 1 ± 0.1 eV transition energy. The other candidate was perylene, a smaller but similar dye with singlet absorption in the blue, at 445 nm. Compared to other polyaromatic molecules, perylene has been much less studied[33,34]. No lifetime-limited lines have ever been reported. However, the phosphorescent emission is known to appear at 778 nm when embedded in an anthracene crystal[35]. The need of a near infrared laser for the triplet of terrylene or in the blue for the study of the perylene singlet was a crucial element in the choice of the system and in the development of the project.

As a first action to determine the triplet energy of terrylene, we went to the Institute of Physics in Warsaw, with Prof. Kozankiewicz who is an expert in triplet state spectroscopy of PAH's. There we tried to measure the direct absorption from the ground state to the triplet state from a pure single crystal of terrylene, but without success. At the same time, the group in Warsaw was working in the preparation of crystals of 2, 3-dimethylanthracene (2, 3-DMA) co-sublimated with dibenzoterrylene (DBT). The experiments in Warsaw are a bit different from what we do in Leiden, because of different laboratory facilities. So, we proposed to take a sample of the doped crystals and perform the experiments at 1.5 K that were complementary to the experiments at 5 K that they have reported[36]. ***Chapter 2*** demonstrates the application of single-molecule confocal fluorescence spectroscopy and correlation spectroscopy (FCS) to study the physical origin of spectral diffusion in solids[37,38]. We report the spectroscopic properties of single (DBT) molecules embedded in a single crystal of 2,3-DMA. Also, we look at fluorescence correlation traces as a function of temperature and laser intensity[39]. The physical origin of the spectral diffusion and instabilities appear to be directly connected with librational degrees of freedom of the methyl groups in the host molecules together with the dipolar disorder in the crystalline structure.

Not knowing the energy of triplet terrylene, we started thinking of possible hosts in which perylene could be isolated showing narrow and stable lines (but we had no blue laser). At a conference in Hole-Burning and Single Molecule, in Tübingen (HBSM 12) I had a discussion with Prof. Naumov from Russia. He had studied terrylene in a poly-crystal of *ortho*-dichlorobenzene[40]. I found this host very interesting first because of the very high energy of the triplet (357 nm) and singlet (256 nm) which allowed for look at perylene at 447 nm, without intermolecular quenching processes. I started studying the bulk fluorescence of perylene as a function of temperature for 10 different hosts using a 405 nm diode laser. I found that in fluorene, alkane (C_{12}), *o*-DCB and also the isomer *para*-DCB, perylene showed narrow fluorescent peaks when the temperature was decreased to 5K. However, at this point we had no single frequency and tunable blue laser to perform SMS of perylene. So, we decided to look for stable terrylene in *p*-DCB

which as a solid has some advantages from its isomer *o*- DCB reported by Naumov. ***Chapter 3*** presents the complete single molecule characterization of a new system of terrylene in p-DCB at 1.5 K. The sample preparation is much simple than the co-sublimation method. It was possible to put the mixture inside glass capillaries. We found in the capillaries the formation of a very strong site at 597 nm which cannot be distinguished when we studied films in coverslips. The main result is the observation of lifetime-limited lines all over the 25 nm of the inhomogeneous distribution from 575 nm to 597 nm.

The observation of stable terrylene molecules proved that *p*-DCB is a convenient host to stabilize lifetime-limited lines, as well as *o*-DCB reported by Naumov et.al. At the same time, these positive results pushed our research again towards the triplet of terrylene. So we came with a new idea "if the transition to the triplet is so forbidden is due to optical selection rules…why not use electrons instead of photons?". So we contacted Prof. Stefan Tautz, in the Peter Grünberg Institut (PGI-3), Forschungszentrum Jülich, in Germany which perform electron energy-loss spectroscopy in some organic materials. It was a collaboration of more than one year. ***Chapter 4*** presents a complete study of the vibrational and electronic spectroscopy of terrylene made by EELS. In order to do these experiments terrylene was sublimated at 198±5°C, and thin films were grown on top of a gold Au (111) surface. The energy loss spectrum was recorded for the vibrational range of the spectrum (0-4000 cm^{-1}) and compared to the Infrared spectrum (FTIR) of Tr in a KBr pellet. The complete fluorescence from a single terrylene in *p*-DCB (CHAPTER 3) was useful to distinguish the non-IR active modes that could appear in HREELS. We look for the electronic excitation of those films using an incident beam of 12 eV. The energy for the singlet-singlet transition was found at 17200 cm^{-1} in good agreement with the optical absorption 17482 cm^{-1}. However, the determination of the energy for the singlet → triplet transition was unsuccessful. After this negative result and other non-reported attempts to determine the triplet energy of terrylene, we made the decision to go for single perylene molecules. This implied to buy a single-frequency tunable laser in the blue.

While looking for the available lasers, we started with an experiment in which the acoustic vibrations of a quartz tuning fork were coupled to the ZPL of one of our best systems: DBT in anthracene. ***Chapter 5*** shows a clear step towards the coupling between a nanomechanical resonator and a quantum emitter as proposed lately by Puller et.al[41]. First, single crystals of anthracene were doped with DBT and studied at 1.5 K. Fluorescence excitation linewidths of 32±5 MHz were observed at 785 nm wavelength as reported by Nicolet et.al[13]. Second, a commercial quartz tuning fork was studied as a function of temperature and one single mode at 32 kHz was observed with Q factor ≈40000. When the doped crystal was brought to optical contact with the tuning fork, the frequency of the fork was changed to 20 kHz and its Q factor strongly reduced. However, the linewidth of the DBT molecule remained unchanged. The tuning fork was then driven at different voltages at their main resonances (kHz). The fluorescence time traces of single DBT's were used to extract indirectly, the frequency of the fork. We found that the maximum sensitivity, which is the minimum displacement required to still has a detectable change in the signal, was about 0.14×10^{-7} nm $Hz^{-1/2}$.

The blue lasers with the spectral requirements for single molecule spectroscopy were not available from the shelf of any of the main laser suppliers in Europe. We started collaborating with Toptica to develop a tunable single-frequency laser in the blue in order to record the fluorescence excitation lines of perylene. It took few months for Toptica to develop and implement the technology on their blue pro-series. The laser diodes are made of Aluminum Nitride, and due to the external cavity had a coarse tunability of 3 nm, therefore the determination of the zero-phonon line from any of the chosen systems required a spectral accuracy in the order of ±1 nm. We looked for perylene at 1.5 K in *p*-DCB but no lasers were available for the strange 437 nm maximum. Fluorene on the other hand showed the narrower bulk emission peak, but the maximum appeared at 457 nm. Finally, *o*-DCB showed a nice narrow peak at 447 nm were diodes were available, and also at the same wavelength as reported before. ***Chapter 6*** presents for the first time the observation of lifetime-limited lines from perylene at low temperature.

Fluorescence excitation spectroscopy showed lifetime limited ZPL's of 23±5 MHz, which correspond to the expected lifetime-limited value considering a lifetime T_1 = 9 ns[42]. We report the saturation profile and line broadening as a function of excitation intensity.

Reference List

1. Moore, G. E. Cramming more components onto integrated circuits (Reprinted from Electronics, pg 114-117, April 19, 1965). *Proceedings of the Ieee* **1998,** *86* (1), 82-85.

2. Orrit, M. Nano-optics - Quantum light switch. *Nature Physics* **2007,** *3* (11), 755-756.

3. Brown, K. R. QUANTUM COMPUTING Chemistry from photons. *Nature Chemistry* **2010,** *2* (2), 76-77.

4. Paredes-Barato, D.; Adams, C. All-Optical Quantum Information Processing Using Rydberg Gates. *Phys. Rev. Lett.* **2014,** *112* (4).

5. Unrau, W.; Bimberg, D. Flying qubits and entangled photons. *Laser & Photonics Reviews* **2014,** *8* (2), 276-290.

6. Holmes, M. J.; Choi, K.; Kako, S.; Arita, M.; Arakawa, Y. Room-Temperature Triggered Single Photon Emission from a III-Nitride Site-Controlled Nanowire Quantum Dot. *Nano Letters* **2014,** *14* (2), 982-986.

7. Kumar, S.; Kristiansen, N. I.; Huck, A.; Andersen, U. L. Generation and Controlled Routing of Single Plasmons on a Chip. *Nano Letters* **2014,** *14* (2), 663-669.

8. Kennard, J.; Hadden, J.; Marseglia, L.; Aharonovich, I.; Castelletto, S.; Patton, B.; Politi, A.; Matthews, J.; Sinclair, A.; Gibson, B.; Prawer, S.; Rarity, J.; O'Brien, J. On-Chip Manipulation of Single Photons from a Diamond Defect. *Phys. Rev. Lett.* **2013,** *111* (21).

9. Darquie, B.; Jones, M. P. A.; Dingjan, J.; Beugnon, J.; Bergamini, S.; Sortais, Y.; Messin, G.; Browaeys, A.; Grangier, P. Controlled single-photon emission from a single trapped two-level atom. *Science* **2005,** *309* (5733), 454-456.

10. McKeever, J.; Boca, A.; Boozer, A. D.; Miller, R.; Buck, J. R.; Kuzmich, A.; Kimble, H. J. Deterministic generation of single photons from one atom trapped in a cavity. *Science* **2004,** *303* (5666), 1992-1994.

11. Kako, S.; Holmes, M.; Sergent, S.; Buerger, M.; As, D. J.; Arakawa, Y. Single-photon emission from cubic GaN quantum dots. *Applied Physics Letters* **2014,** *104* (1).

12. Santori, C.; Tamarat, P.; Neumann, P.; Wrachtrup, J.; Fattal, D.; Beausoleil, R. G.; Rabeau, J.; Olivero, P.; Greentree, A. D.; Prawer, S.; Jelezko, F.; Hemmer, P. Coherent

population trapping of single spins in diamond under optical excitation. *Phys. Rev. Lett.* **2006,** *97* (24).

13. Nicolet, A. A.; Hofmann, C.; Kol'chenko, M. A.; Kozankiewicz, B.; Orrit, M. Single dibenzoterrylene molecules in an anthracene crystal: Spectroscopy and photophysics. *Chemphyschem* **2007,** *8* (8), 1215-1220.

14. Brunel, C.; Lounis, B.; Tamarat, P.; Orrit, M. Triggered source of single photons based on controlled single molecule fluorescence. *Physical Review Letters* **1999,** *83* (14), 2722-2725.

15. Orrit, M. Photons pushed together. *Nature* **2009,** *460* (7251), 42-44.

16. Chang, D. E.; Sorensen, A. S.; Demler, E. A.; Lukin, M. D. A single-photon transistor using nanoscale surface plasmons. *Nature Physics* **2007,** *3* (11), 807-812.

17. Hwang, J.; Hinds, E. Dye molecules as single-photon sources and large optical nonlinearities on a chip. *New Journal of Physics* **2011,** *13*.

18. Hwang, J.; Pototschnig, M.; Lettow, R.; Zumofen, G.; Renn, A.; Goetzinger, S.; Sandoghdar, V. A single-molecule optical transistor. *Nature* **2009,** *460* (7251), 76-80.

19. Nagourney, W.; Sandberg, J.; Dehmelt, H. Shelved optical electron amplifier: Observation of quantum jumps. *Phys. Rev. Lett.* **1986,** *56* (26), 2797-2799.

20. Houel, J.; Prechtel, J. H.; Kuhlmann, A. V.; Brunner, D.; Kuklewicz, C. E.; Gerardot, B. D.; Stoltz, N. G.; Petroff, P. M.; Warburton, R. J. High Resolution Coherent Population Trapping on a Single Hole Spin in a Semiconductor Quantum Dot. *Phys. Rev. Lett.* **2014,** *112* (10).

21. Kozankiewicz, B.; Orrit, M. Single-molecule photophysics, from cryogenic to ambient conditions. *Chemical Society Reviews* **2014,** *43* (4), 1029-1043.

22. Rezus, Y.; Walt, S.; Lettow, R.; Renn, A.; Zumofen, G.; Goetzinger, S.; Sandoghdar, V. Single-Photon Spectroscopy of a Single Molecule. *Physical Review Letters* **2012,** *108* (9).

23. Kador, L.; Personov, R.; Richter, W.; Sesselmann, T.; Haarer, D. Laser Photochemistry and Hole Burning Spectroscopy in Polymers and Glasses - External-Field Effects. *Polymer Journal* **1987,** *19* (1), 61-71.

24. Sesselmann, T.; Richter, W.; Haarer, D.; Morawitz, H. Spectroscopic studies of impurity-host interactions in dye-doped polymers: Hydrostatic-pressure effects versus temperature effects. *Phys. Rev. B* **1987,** *36* (14), 7601-7611.

25. Plakhotnik, T.; Walser, D.; Renn, A.; Wild, U. P. Light induced single molecule frequency shift. *Phys. Rev. Lett.* **1996,** *77* (27), 5365-5368.

26. Plakhotnik, T.; Moerner, W. E.; Palm, V.; Wild, U. P. Single molecule spectroscopy: maximum emission rate and saturation intensity. *Optics Communications* **1995,** *114* (1ΓÇô2), 83-88.

27. Plakhotnik, T.; Moerner, W. E.; Palm, V.; Wild, U. P. Single-Molecule Spectroscopy - Maximum Emission Rate and Saturation Intensity. *Optics Communications* **1995,** *114* (1-2), 83-88.

28. Orrit, M.; Bernard, J.; Zumbusch, A.; Personov, R. I. Stark-Effect on Single Molecules in A Polymer Matrix. *Chemical Physics Letters* **1992,** *196* (6), 595-600.

29. Pirotta, M.; Renn, A.; Wild, U. P. Stark effect measurements on single perylene molecules. *Helvetica Physica Acta* **1996,** *69*, 7-8.

30. Fleury, L.; Zumbusch, A.; Orrit, M.; Brown, R.; Bernard, J. Spectral Diffusion and Individual 2-Level Systems Probed by Fluorescence of Single Terrylene Molecules in A Polyethylene Matrix. *Journal of Luminescence* **1993,** *56* (1-6), 15-28.

31. Kummer, S.; Basche, T.; Brauchle, C. Terrylene in P-Terphenyl - A Novel Single-Crystalline System for Single-Molecule Spectroscopy at Low-Temperatures. *Chemical Physics Letters* **1994,** *229* (3), 309-316.

32. Kozankiewicz, B.; Bernard, J.; Orrit, M. Single-Molecule Lines and Spectral Hole-Burning of Terrylene in Different Matrices. *Journal of Chemical Physics* **1994,** *101* (11), 9377-9383.

33. Pirotta, M.; Renn, A.; Werts, M. H. V.; Wild, U. P. Single molecule spectroscopy, perylene in the Shpol'skii matrix n-nonane. *Chemical Physics Letters* **1996,** *250* (5-6), 576-582.

34. Basche, T.; Moerner, W. E. Optical Modification of A Single Impurity Molecule in A Solid. *Nature* **1992,** *355* (6358), 335-337.

35. Walla, P. J.; Jelezko, F.; Tamarat, P.; Lounis, B.; Orrit, M. Perylene in biphenyl and anthracene crystals: an example of the influence of the host on single-molecule signals. *Chemical Physics* **1998,** *233* (1), 117-125.

36. Makarewicz, A.; Deperasinska, I.; Karpiuk, E.; Nowacki, J.; Kozankiewicz, B. Vibronic spectra of single dibenzoterrylene molecules in anthracene and 2,3-dimethylanthracene crystals. *Chemical Physics Letters* **2012,** *535*, 140-145.

37. Kulzer, F.; Orrit, M. Single-molecule optics. *Annual Review of Physical Chemistry* **2004,** *55*, 585-611.

38. Kulzer, F.; Xia, T.; Orrit, M. Single Molecules as Optical Nanoprobes for Soft and Complex Matter. *Angewandte Chemie-International Edition* **2010,** *49* (5), 854-866.

39. Tian, Y.; Navarro, P.; Kozankiewicz, B.; Orrit, M. Spectral diffusion of single dibenzoterrylene molecules in 2,3-dimethylanthracene. *Chemphyschem : a European journal of chemical physics and physical chemistry* **2012,** *13* (15), 3510-3515.

40. Gorshelev, A. A.; Naumov, A. V.; Eremchev, I. Y.; Vainer, Y. G.; Kador, L.; Koehler, J. Ortho-Dichlorobenzene Doped with Terrylene-a Highly Photo-Stable Single-Molecule System Promising for Photonics Applications. *Chemphyschem* **2010,** *11* (1), 182-187.

41. Puller, V.; Lounis, B.; Pistolesi, F. Single Molecule Detection of Nanomechanical Motion. *Physical Review Letters* **2013,** *110* (12).

42. Xu, J. H.; Shen, X. H.; Knutson, J. R. Femtosecond fluorescence upconversion study of the rotations of perylene and tetracene in hexadecane. *Journal of Physical Chemistry A* **2003,** *107* (41), 8383-8387.

CHAPTER 2

Spectral diffusion of a single molecule

The aim of this chapter is to get a deeper understanding of the physical origin of the spectral diffusion that single molecules in many solid materials have shown over the years. We use single dibenzoterrylene (DBT) molecules as a fluorescent nano-probe to extract information about the local dynamics of a single crystal of 2, 3-dimethylanthracene (2, 3-DMA). Single-molecule fluorescence excitation spectroscopy and fluorescence correlation measurements allow us to identify that the methyl groups combined with the static "dipolar disorder" present in the 2, 3-DMA may be the physical reason for such observations. Line broadening, spectral diffusion and/or frequency jumps are expected whenever the activation energies for librational degrees of freedom (acoustic phonons) or local low-frequency modes (LFM's) are active in the host at the experimental conditions (1.5 K). The presence of the methyl groups together with dipolar disorder of the host must be avoided when looking for new single molecule 'host-guest" systems with lifetime-limited linewidths and high spectral stability.

The content of this chapter is published.
Y. Tian, P. Navarro, B. Kozankiewicz and M. Orrit.
ChemPhysChem **2012,** 13, 3510-3515.

2.1.Introduction

Since the first optical detection of a single molecule at cryogenic temperature by absorption and fluorescence[1,2], single-molecule spectroscopy (SMS) has become a powerful tool for investigating structure and dynamics of condensed matter. The biggest advantage of SMS is to investigate the properties of heterogeneous systems without any ensemble averaging[3]. The properties of a single molecule depend not only on its chemical structure but also on its specific local environment. Single molecules can be thus used as probes to study the local environments at nanometer scales.

Dibenzoterrylene (DBT) was found to be a good fluorophore for SMS[4,5]. The important advantages of the DBT molecule are its photo-stability as well as its absorption in the near infrared range[6,7]. Single DBT molecules have been studied in crystal matrixes in which they are located in well-defined insertion sites with associated orientations. Lifetime-limited linewidths and a narrow inhomogeneous distribution of the zero-phonon lines (ZPLs) at low temperature were observed in these matrixes[5,7,8]. However, the molecules in the different insertion sites presented different properties, such as saturation intensity, temperature dependence and linewidth[9].

In glasses, the distribution of molecular properties is generally much broader than in crystals. The glassy disorder creates specific defects which are known as two-level systems (TLS's). These TLS's can assume two different quasi-degenerate conformations, and switch from one to the other by phonon-assisted processes. Although the TLS model was already proposed approximately 40 years ago[10,11], SMS experiments provided the first experimental evidence of the TLS's as individual entities. Single molecules thus have been used to investigate the TLS's in disordered glass matrices[12-17].

Recently, single molecules have been studied in crystals with dipolar disorder. In such crystals, the position of the host molecules at the nodes of a lattice is conserved, but each of the non-symmetric molecules can assume one of two possible orientations. The three dipolar-disordered crystals used so far have been 1,2-dichlorobenzene (1,2-DCB)[18],

2,3-dimethylnaphthalene (2,3-DMN)[19-21], and 2,3-dimethylanthracene (2,3-DMA)[22]. For terrylene in 1, 2-DCB, stable lines with lifetime-limited linewidths were observed[18]. For 2, 3-DMA and 2, 3-DMN, the two methyl groups substituted on the 2, 3 positions of the anthracene or naphthalene molecules make them non-centrosymmetric. The crystal structure of 2, 3-DMA (2, 3-DMN) resembles that of the anthracene (naphthalene) crystal, with fairly sharp Bragg reflections arising from positional order[23-25]. However, optical experiments have revealed that guest molecules doped into these crystals display active dynamics and broad inhomogeneous distributions[19,20,22,26]. Despite these earlier works at low temperature which were limited by the laser resolution (about 30 GHz), no high-resolution, low-temperature spectroscopy has been attempted yet on these systems.

In this chapter, we study single DBT molecules in 2, 3-DMA crystal at cryogenic temperatures with high spectral resolution (2 MHz). We discuss our findings on static disorder and dynamic disorder of the single molecule lines and discuss the consequences for the crystal's structure and dynamics.

2.2.Experimental

Single crystals of 2, 3-DMA (zone-refined before use) as host, doped with DBT were grown by co-sublimation in a home-built device in Warsaw under a 150 mbar argon atmosphere (scheme 1). Briefly, the 2, 3-DMA powder was heated (higher than its sublimation point ≈200^{o}C) by applying a voltage (V) through a metallic wire that surrounds the outer glass container. Another wire around the small container where the DBT was placed was heated independently with a second voltage. The doped crystals grow in the surface of the upper stopper as thin flakes. For single-molecule experiments, the sample was then cooled down to 1.25 K in a helium cryostat (Janis). For temperature-dependent experiments, the sample was set in the sample chamber and the temperature was controlled by the helium flow over the sample at very low pressure (below 10 mbar).

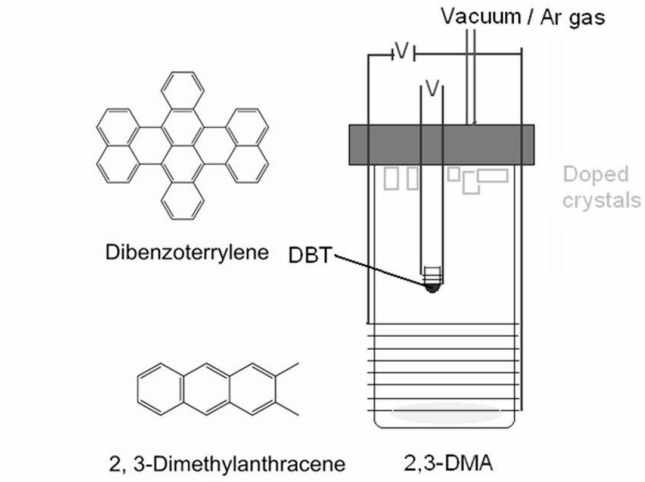

Scheme 2.1: *Glass chamber for co-sublimation of host-guest crystals for SMS. Big amount of host (23, DMA) is placed on the bottom and heated at T > sublimation. The impurity (DBT) has to be keep at very low concentration respect to the host. The vacuum reduces the vapor pressure of the molecular crystal helping sublimation. Ar or N gas keep the atmospheric pressure at desired value (150mbar) and remove impurities.*

A single-frequency Ti:Sapphire laser (Coherent 899-21) pumped by an Argon ion laser (Coherent Sabre 150) provided the excitation light at 780 nm (Scheme 2.2). A fast scanning mirror (Newport FSM-300-01) allowed us to scan the sample over about 75 × 75 μm^2. The fluorescence was collected by an objective mounted inside the cryostat (60×, NA=0.85, Edmund Optics) and detected by an avalanche photodiode (SPCM-AQR-16, Perkin-Elmer) after proper spectral and spatial filtering. In case that it is required a flip mirror in the detection path can send the fluorescence signal into a spectrograph (Princeton Instruments, i500) mounted with a CCD detector. From the fluorescence intensity traces, autocorrelation functions were obtained with a data acquisition card (TimeHarp 200, Pico Quant) and its associated software.

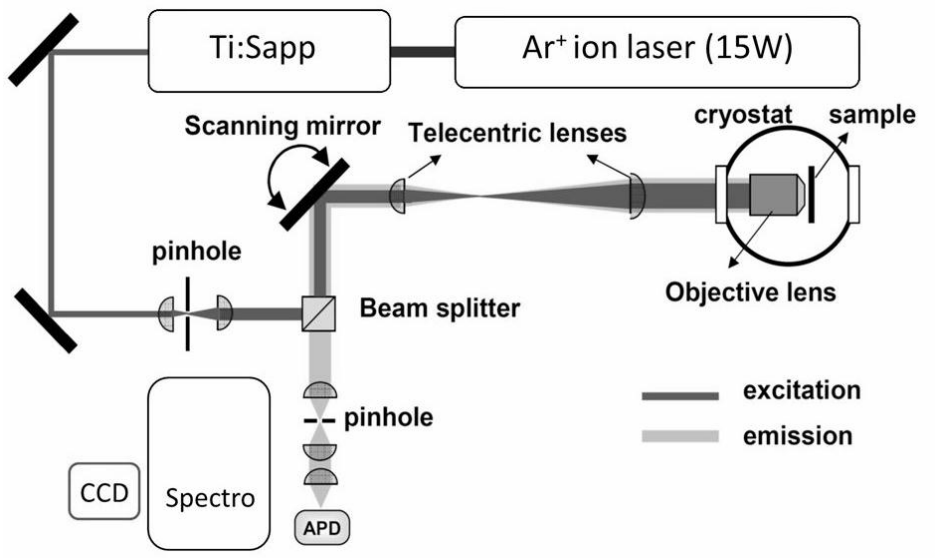

Scheme 2.2: *Optical set-up used to perform single molecule experiments inside the cryostat. The maximum conversion efficiency of TiSapp is 20 % at optimal conditions operating in single frequency. Long pass filters with cut in 810 nm were used for detect the red shifted photons, from the excitation light at 785nm.*

2.3.Results

2.3.1. Saturation intensity

We measured the fluorescence intensity and the spectral linewidth of several single DBT molecules in 2, 3-DMA as functions of the excitation intensity. The most striking observation is the large width of the molecular lines of about 1 GHz, as the insert of Figure 2.1 shows. In addition, the fluorescence (circles) becomes saturated for high excitation powers. This trend was fitted with the standard saturation expression given by Equation 5 and 6 in the introduction of this thesis.

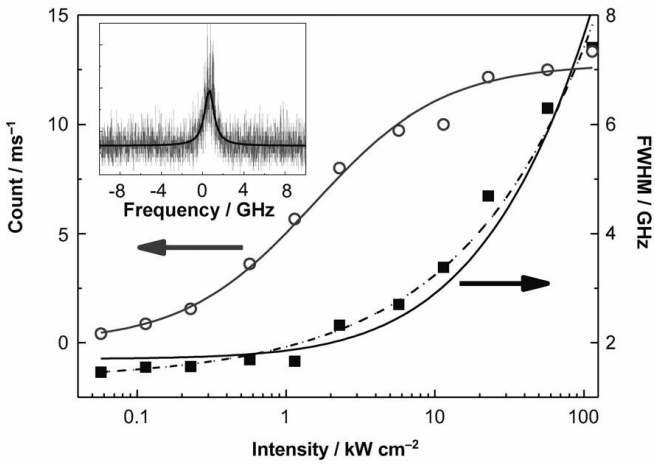

Figure 2.1: *Fluorescence intensity (○) and linewidth (■) of a single DBT molecule in 2, 3-DMA crystal versus excitation intensity. The solid lines are fits with equation (5) and (6) in introduction, for the linewidth and intensity, respectively. The dashed line is fitted considering the spectral diffusion effect. Insert: excitation spectrum of a single molecule showing FWHM =1 GHz and the solid line is a Lorentz fit.*

The linewidth (squares) shows a similar trend as seen for DBT in anthracene and was thus fitted by the corresponding expressions presented in introduction of this thesis. The obtained saturation intensity for the measured DBT molecule in 2,3-DMA (1.4 kW/cm^2) was about 1000 times higher than that of DBT in anthracene (~1 W/cm^2).[7] To understand the origin of this difference, we simulated the line broadening by saturation for two different cases, through dephasing (solid line) and through spectral diffusion (dash-dotted line), and both shown together with the results of Fig 2.1.

Both spectral diffusion (SD) and dephasing can broaden the linewidth of the molecules. Because the linewidth is larger, a larger intensity is required to achieve the same relative broadening effect. Therefore, the saturation intensity will be increased in both cases, but to different extents. Plakhotnik has proposed to separate the dephasing and the spectral diffusion effects by fitting the saturation curve of the linewidth with the

ratio of dephasing to spectral diffusion as a fit parameter[27]. However, without prior information about the natural linewidth and the transition dipole moment, it was difficult to identify these two contributions reliably. So now, we intend to show that, by using prior information about the lifetime-limited linewidth of DBT in anthracene, the difference between the contributions of spectral diffusion and dephasing can be obvious.

2.3.1.1 Line broadening by dephasing only

For a single molecule line without spectral diffusion and without pure dephasing (e.g., DBT in anthracene), the linewidth γ_0 is determined by the coherence lifetime T_2, related to the population lifetime T_1, itself including radiative k_r and non-radiative k_{nr} components:

$$\gamma_0 = \frac{1}{T_2} = \frac{1}{2T_1}, \qquad \frac{1}{T_1} = k_r + k_{nr}.$$

For the DBT molecule in the main site, the lifetime-limited linewidth (FWHM) was reported to be 32 MHz. Thus the saturation curve of the linewidth $\gamma(I)$ should follow the equation:

$$\gamma(I) = \gamma_0 \sqrt{1+\frac{I}{I_s}}, \text{ with } \gamma_0 = \pi \times 32 \text{ MHz}, \text{ and } I_s = 1.0 \text{ W/cm}^2,$$

where I is the excitation intensity and I_s is the saturation intensity. This dependence is shown as a dashed line in Fig.2.2.

For DBT in 2,3-DMA, the molecular lines are much broader than 32 MHz. If this broadening is due to pure dephasing only, and assuming that the radiative and non-radiative rates, and the transition dipole moment of DBT remain the same as in anthracene, the linewidth γ_D will be given by:

$$\gamma_D = \frac{1}{T_2} = \frac{1}{2T_1} + \frac{1}{T_2'}, \quad \text{where} \quad \frac{1}{T_2'} \quad \text{represents the pure dephasing rate.}$$

The saturation intensity can be deduced from the saturation parameter s by:

$$s = \frac{I}{I_s'} = \Omega^2 T_1 T_2 ,$$

the Rabi frequency , Ω , is related to the light electric field and transition dipole moment

by, $$\Omega = \frac{\left|\vec{\mu}_{eg} \cdot \vec{E}_0\right|}{\hbar}$$

The new saturation intensity with dephasing, I_s' is related to the previous one by:

$$I_s' = \frac{2T_1}{T_2} I_s .$$

The measured linewidth of DBT in 2,3-DMA is ~ 1 GHz. Thus, the new saturation intensity is about 30 kW/cm^2, and the saturated linewidth should follow the equation:

$$\gamma_D(I) = \gamma_D \sqrt{1 + \frac{I}{I_s'}}$$

plotted as a dotted line in Figure 2.2.

2.3.1.1. Line broadening by spectral diffusion only

If the measured linewidth is only broadened by spectral diffusion, the line shape should be the convolution of the (possibly saturated) excitation line of the molecule with the probability distribution of the spectral jumping. To perform the calculation, we assume this probability distribution to be Lorentzian, centered on ω_0 and with FWHM 2Δ . The probability density of presence of the molecular line at frequency ϖ is thus:

$$L_\Delta(\varpi, \omega_0) = \frac{1}{\pi} \frac{\Delta}{(\varpi - \omega_0)^2 + \Delta^2} .$$

The excited state population for laser excitation at ω and for resonance frequency at ϖ is:

$$p_e(\omega,\varpi) = \frac{\gamma_0^{\,2}}{2}\frac{s}{(\omega-\varpi)^2+\gamma_0^{\,2}(1+s)},$$

s being the corresponding saturation parameter. Thus, the molecular lineshape will be the convolution product of these two profiles:

$$p_e(I) = p_e(\omega,\varpi)\otimes L_\Delta(\varpi,\omega_0) = \frac{\gamma_0 s}{4\pi^2\sqrt{1+s}}\frac{\Delta+\gamma_0\sqrt{1+s}}{(\omega-\omega_0)^2+(\Delta+\gamma_0\sqrt{1+s})^2},$$

which is also a Lorentzian with linewidth $\gamma_{SD}(I) = \Delta+\gamma_0\sqrt{1+s}$.

In our case, for DBT in 2,3-DMA with a linewidth of 1 GHz, Δ = 0.97 GHz, γ_0 and I_s keeping their values as in anthracene. The saturation curve is then given by the solid line in Figure 2.2. which compares very well to the experimental data.

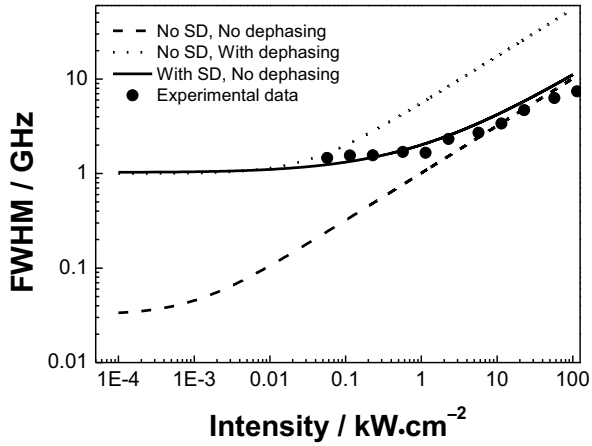

Figure 2.2. *Linewidth broadening versus excitation intensity for three different situations: natural linewidth without pure dephasing and without spectral diffusion (dashed line); pure dephasing without spectral diffusion (dotted line); spectral diffusion without pure dephasing (solid line). The dots are experimental data for DBT in 2,3-DMA.*

From these results we see that spectral diffusion leads to a much higher saturation intensity than pure dephasing. This is a strong indication that the large linewidth of single

DBT molecules in 2, 3-DMA is due to spectral diffusion. Thus, when the intensity was lower than 1 kW/cm^2 the linewidths reported hereafter were mainly determined by spectral diffusion. Saturation broadening becomes significant at excitation intensities higher than 1 kW/cm^2.

2.3.2. Linewidth distribution

We measured the excitation spectra of 34 single DBT molecules in 2, 3-DMA around 780 nm. The full-widths at half maximum (FWHM) values were deduced from Lorentzian fits, as shown in the insert of Figure 2.1. To get enough signal-to-noise ratio but avoid saturation, we used an excitation intensity of 1 kW/cm^2 for all linewidth measurements.

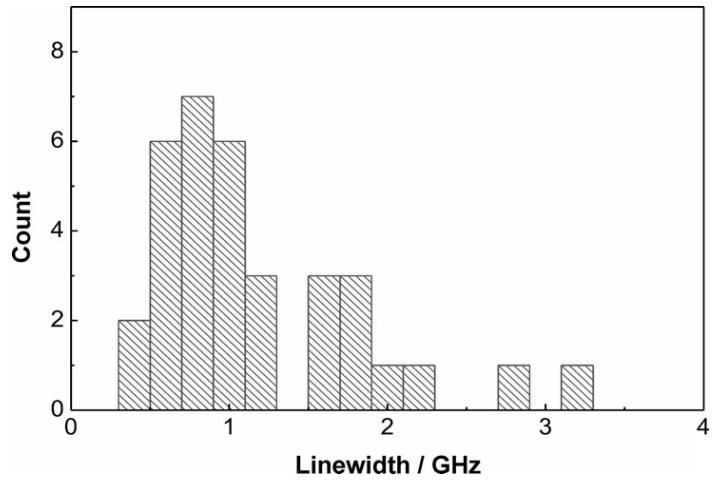

Figure 2.3: *Histogram of the linewidths of 34 DBT molecules (excitation wavelength 780 nm). An excitation intensity of 1 kW/cm^2 was used to get good signal-to-noise ratios and avoid saturation.*

The molecules were measured at 1.25 K and the histogram of their FWHMs is shown in Figure 2.3. The linewidths are widely distributed from 0.4 to 3.2 GHz with a maximum around 0.8 GHz. This average linewidth is much broader (~30 times) than the

ZPL of DBT in an anthracene crystal[7]. Saturation at our excitation intensity (1 kW/cm^2) cannot be significant in these measurements, because the reported saturation intensity (1.4 kW/cm^2) was the lowest one from all the measured molecules. Indeed, no molecules with linewidths less than 0.4 GHz was ever observed, even at very low intensities.

2.3.3. Temperature dependences of the linewidth and shift

We measured the temperature dependences of the linewidth and of the central frequency of some single DBT molecules in 2, 3-DMA in the range of 1.5–12 K, as shown in Figure 2.4. The linewidth increases with temperature (Figure 2.4 a) according to the Arrhenius law, in agreement to what has been reported for other molecules in crystals and polymer matrices[6,28,29]:

$$\gamma(T) = \gamma(0) + Ae\left(-\frac{E_a}{kT}\right)$$

Here, $\gamma(0)$ is the linewidth at zero temperature, k is the Boltzmann constant, E_a is the activation energy, and A is a constant depending on the electron–phonon coupling. Most of the molecules we measured could be fitted by using the Arrhenius equation shown above (see examples in Figure 2.4.a). The obtained activation temperatures for DBT/2,3-DMA (ranging from 20 to 26 K) are quite similar to those for DBT/anthracene[6] and for terrylenediimide (TDI)/hexadecane (HD)[29]. Vainer et al.[30] proposed a more accurate expression, including both TLSs and phonon contributions. However, the dynamic range and the accuracy of our measurements do not allow us to fit more than two parameters reliably.

The spectral shift was also observed as a function of temperature. To exclude pressure effects, we kept the sample in vacuum at constant pressure. The shifts present

different variations from molecule to molecule (see Figure 2.4.b), an observation that has previously been reported for TDI/HD by Mais et al.[29] Some lines shifted to the blue, others to the red. Again, most of the curves can be fitted with an Arrhenius equation:

$$\Delta\nu(T) = B \bullet e\left(-\frac{E_a}{kT}\right)$$

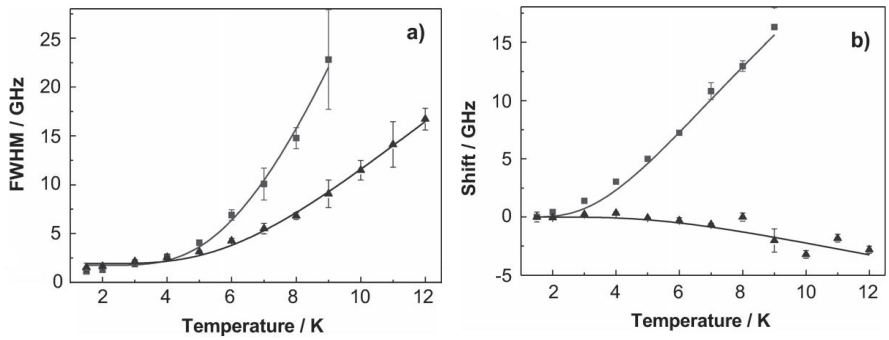

Figure 2.4: *Temperature dependence of the linewidths (a) and frequency shifts (b) of two typical single DBT molecules in 2,3-DMA. The solid lines are the fitted curves using Arrhenius equations for the linewidths and shifts, respectively.* ■ *and*▲*, correspond to two different molecules.*

The fitted activation temperature for the resonant shift varies from 10 K to 30 K from molecule to molecule but remains comparable with reported values[6,29]. The mechanism of the spectral shift is not completely clear, but there are at least two possible contributions to its temperature dependence. Firstly, the thermal expansion of the crystal changes the solvent shift, thereby shifting the optical line, and secondly, based on the second-order perturbation theory, the broadening of the optical transition by coupling to phonons and vibrations is associated to shifts of the ground and excited states, causing a shift of the optical transition.

2.3.4. Qualitative observations of spectral diffusion

DBT molecular lines were found to be very unstable in 2,3-DMA compared to anthracene. Sudden intensity jumps, known as blinking of DBT, were assigned to spectral jumping due to the coupling with surrounding TLSs, as discussed above. Both the spectral-jump sizes and rates are quite different from molecule to molecule. Some of the molecules showed spectral jumping between two different frequencies, attributable to coupling to one TLS. Some other molecules that jump between four frequencies, as shown in the examples of Figure 2.5.a & 2.5.b, appear to be coupled to two independent TLSs. More complicated cases of molecules showing noisy traces might arise from coupling to a large number of TLSs (Figure 2.5.c), or from more complex dynamics.

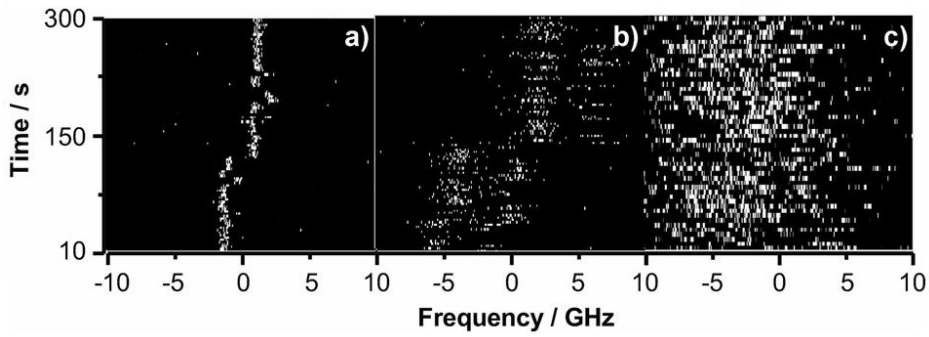

Figure 2.5: *Frequency scan over 20 GHz of single DBT molecules a) with slow spectral jumping, b) with fast spectral diffusions between four levels, and c) with very fast jumps between many different levels.*

2.3.5. Fluorescence correlation studies

To analyze the dynamics of the spectral jumps of DBT molecules in 2,3-DMA, we measured the autocorrelation functions of the fluorescence intensity for times ranging from 10 μs to 10 s. Figure 2.6.a shows the autocorrelation functions of three example molecules. As was the case for polymers,[13,31] the correlation functions can show mono, bi- or multi-exponential decays attributable to molecules coupled to one, two or more TLSs (Figure 2.6.a).

Figure 2.6.b shows a histogram of the correlation times (in ms) measured on 36 molecules at 1.25 K with an excitation intensity of 1 kW/cm^2. A significant fraction (~50%) of the molecules studied show a well-defined exponential component with a correlation decay rate of around 400 s^{-1}. The time distribution is quite broad with a clear maximum around 2.5 ms. For the few molecules which show multi-exponential decays, all components have been included in the histogram. Our traces were too short to measure reliably times longer than 1 s. The slight excess of rates around 2 s^{-1} may be due to a statistical fluctuation.

We cannot completely exclude the possibility that the component with the correlation time of 2.5 ms is due to the triplet state of DBT. However, observing the correlation due to intersystem crossing would be very difficult with an intersystem crossing-quantum yield of 10^{-7} and a lifetime of 40 μs, as reported for DBT in anthracene[7]. We do not expect the quantum yield and the lifetime of the triplet state to change much upon substitution with two methyl groups.

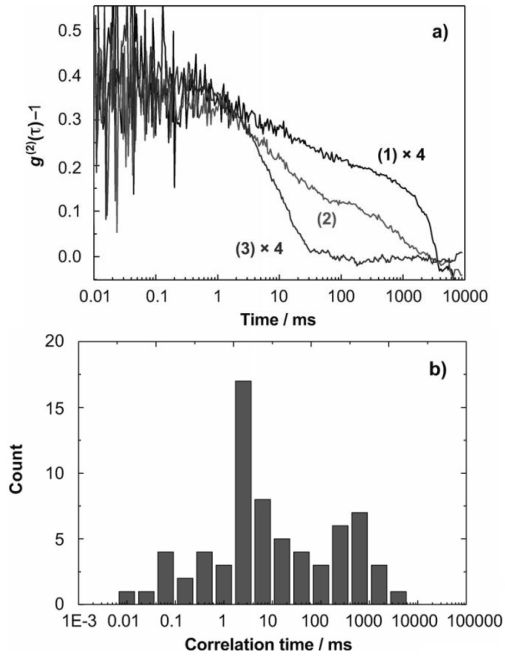

Figure 2.6: *a) Auto-correlation functions of three DBT molecules in 2,3-DMA crystals showing a multi-exponential (1), a bi-exponential (2) and mono-exponential (3) components. b) Histogram of the correlation times measured on 36 DBT molecules. All the measurements were done at 1.25 K with an excitation intensity of 1 kW/cm^2.*

2.3.6. Excitation intensity dependence of the correlations

Measuring the excitation intensity dependence of the spectral jumps was not easy for DBT/2,3-DMA due to the instability of the dye. The molecules often jumped during the measurement to a new frequency outside our scanning range (20 GHz), especially when the excitation intensity was high. Nevertheless, we successfully investigated the excitation intensity dependence for two molecules. Both of them showed bi-exponential decays (see Figure 2.7.a for one example). The two components showed different dependences on the excitation intensity. The fast component (rate~400 s^{-1}) did not seem to have any significant intensity dependence within the range from 0.5 to 200 kW/cm^2

(squares, Figure 2.7.b). The slow component (rate <20 s^{-1}) became faster with increasing excitation intensity, indicating a photo-induced spectral jumping (circles, in Figure 2.7.b).

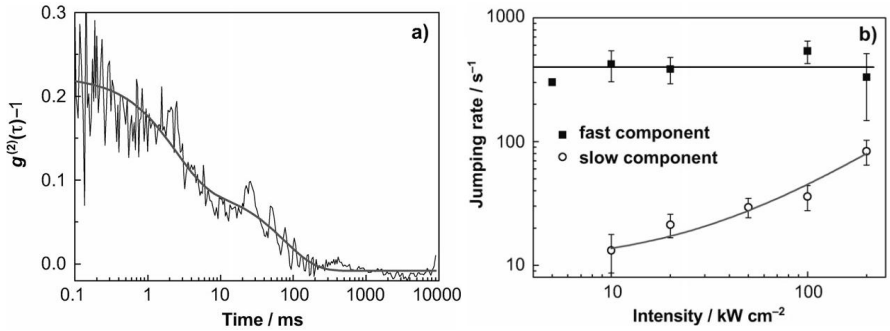

Figure 2.7: a) Correlation function of a single DBT molecule in 2,3-DMA and b) excitation intensity dependence of the fast (■) and slow (○) components. The rates were obtained by bi-exponential fitting of the correlation function. The solid lines are linear fits of the data points with a linear dependence on the intensity, $r = r_0 + aI$.

2.3.7. Temperature dependence of the correlations

We also tried to investigate the temperature dependence of the spectral jumping for several molecules within the range of 1.5–12 K. We discuss the dependence of the fast component from two representative molecules. Molecule 1 (■ in Figure 2.8) shows an increase in the jumping rate with increasing temperature up to 400 s^{-1} above 5 K, whereas molecule 2 (○ in Figure 2.8) shows a rather constant jumping rate with increasing temperature. The slower correlation component, which was observed for a few molecules, did not show any clear temperature dependence.

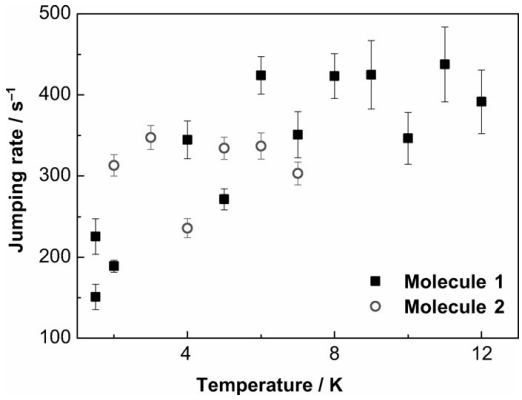

Figure 2.8: *Jumping rate of the fast component of two DBT molecules in the temperature range 1.5–12 K.*

2.4.Discussion

2.4.1. Heterogeneity

Our results present a large heterogeneity of linewidths (distributed between 0.4 and 3.2 GHz), saturation excitation intensities, spectral jumping (jump sizes and rates), and shifting behaviors. The broad distribution of ZPLs in the inhomogeneous absorption band (350 cm^{-1} wide) has also been reported earlier[22]. Such heterogeneity is generally observed for single molecules embedded in polymer matrices[32] and in another dipolar disordered crystal, 1,2-DCB[18]. Herein, the 2, 3-DMA molecules form an ordered crystal lattice. However, the non-symmetric molecules are randomly oriented, giving rise to dipolar disorder. Based on the crystal structure from DBT in anthracene[6], we assume that, here too, one DBT molecule replaces three host 2,3-DMA molecules. Moreover, we suppose that the insertion site corresponds to the main site of DBT in anthracene. Therefore, the local environment of a DBT molecule in the crystal plane should consist of ten 2,3-DMA molecules. With two different orientations for each of them, and considering the C2 symmetry of the system, there are 512 spectroscopic possibilities for degenerated local environments. Taking into account the orientations of host molecules in

the nearby planes, these multiple insertion sites lead to a broad quasi-continuum of spectroscopic sites. The heterogeneity of spectral properties we observed is consistent with the static disorder produced by the environment.

2.4.2. *Spectral diffusion*

The broad linewidth and the high saturation intensity of DBT in 2,3-DMA was the most striking and surprising observation. We safely attributed it to spectral diffusion based on saturation (Figure 2.1), time traces (Figure 2.4), and correlation studies (Figure 2.5). Generally, in crystalline matrices, single molecules are very stable. Well known examples are terrylene in naphthalene or DBT in anthracene, which show stable lines and lifetime-limited linewidths[7]. Although spectral jumping of single molecules has been observed for terrylene or pentacene in *p*-terphenyl, this crystal is a special case because of its ferro-elastic transition. Moreover, the linewidth of guest molecules remains lifetime-limited in most cases[33-35].

The spectral diffusion of DBT in 2, 3-DMA resembles that of terrylene and tetra-ter-butylterrylene (TBT) molecules in polyethylene and other polymers[13,14,31,36,37]. In many cases, the spectral diffusion of a single molecule can be described in terms of its coupling to nearby TLS's. When a TLS which is coupled to the molecule flips, the excitation spectrum jumps between two different frequencies. The jump size and rate depend on physical parameters, such as distance from the molecule, relative orientation, and temperature. For each molecule, the spectral diffusion pattern depends on the density and location of the TLS's.

2.4.3. Model for spectral diffusion

In previous literature, spectral diffusion was observed in systems with structural disorder[13,14,31,36,37] or in crystals with domain walls and other defects[27,33]. Spectral diffusion might thus appear as a general consequence of disorder. However, Gorshelev et al. recently reported stable and lifetime-limited terrylene lines in 1, 2-DCB, even though this crystal presents dipolar disorder[18]. This result is understandable because the orientations of the host molecules, albeit disordered, are fixed at low temperature and cannot give rise to flipping dynamics. Therefore, our observation of a very active spectral diffusion in another crystal with dipolar disorder is surprising. We propose that the main difference between these two dipolar crystals arises from the chemical structure of the host molecules, which includes two methyl groups in the case of 2,3-DMA but not for 1,2-DCB.

The methyl groups in 2,3-DMA present additional degrees of freedom due to the rotational flexibility around the C-CH_3 single bond, which is absent in rigid molecules like anthracene and 1,2-DCB. One of the possible dynamical processes is rotational tunneling of the methyl groups. However, rotational tunneling processes are usually very slow because of spin selection rules. Moreover, their effect on the electronic transition would be very weak if they were not directly substituted on the guest molecule[38]. Another motion able to produce spectral diffusion at low temperature would be a two-level system involving a limited rotation of the CH_3 group within its libration potential well. These reorientations can become possible due to the free space in the lattice caused by dipolar disorder.

In other words, the spectral diffusion would arise from the coexistence within the same structure of strong and weak links, which is known to give rise to complex potential energy landscapes and to additional dynamics[39]. Unexpected spectral dynamics of TBT in toluene (which also has a methyl group) has also been reported by Naumov et al[40]. By analyzing the isotope effect, they proposed that the motion of the methyl group is mainly

of librational character and probably gives rise to low-frequency vibration modes. Interestingly, the presence of methyl groups in a crystal does not appear to cause systematically additional dynamics, as was shown in the case of durene (tetramethylbenzene) [41,42]. No evidence for low-temperature dynamics was found from neutron scattering or from calculations in that work. Based on our observations and on the previous ideas, we propose that the spectral diffusion found in the dipolar-disordered crystal 2, 3-DMA originates from a combination of structural disorder of the matrix and of subtle rearrangements of the methyl groups. A systematic experiment was performed to support this conclusion, and is presented in Chapter 3.

2.5.Conclusion

We studied single DBT molecules embedded in a dipolar-disordered crystal, 2,3-DMA. We found broad linewidths, high saturation excitation intensities, as well as spectral instability. Spectral jumping was also observed and investigated further varying the excitation intensity and the temperature. The spectral diffusion and dynamic disorder in this system are believed to arise from a combination of static disorder with a slight reorientation of the methyl groups of the host 2,3-DMA molecules.

Acknowledgement

Polish Academy of Science for its invitation to visit and 4 week stay at the Institute of Physics for a fruitful introduction to single molecule spectroscopy during my first year of PhD. Prof. Boleslaw Kozankiewicz for his contributions to this work, specially the co-sublimated crystals of 2, 3-dimethyl anthracene doped with DBT.

Reference List

1. Moerner, W. E.; Kador, L. Optical-Detection and Spectroscopy of Single Molecules in A Solid. *Phys. Rev. Lett.* **1989,** *62* (21), 2535-2538.

2. Orrit, M.; Bernard, J. Single Pentacene Molecules Detected by Fluorescence Excitation in A Para-Terphenyl Crystal. *Physical Review Letters* **1990,** *65* (21), 2716-2719.

3. Moerner, W. E. A dozen years of single-molecule spectroscopy in physics, chemistry, and biophysics. *Journal of Physical Chemistry B* **2002,** *106* (5), 910-927.

4. Boiron, A. M.; Jelezko, F.; Durand, Y.; Lounis, B.; Orrit, M. Dibenzanthanthrene in n-hexadecane, dibenzoterrylene in naphthalene: Two new systems for single molecule spectroscopy. *Molecular Crystals and Liquid Crystals Science and Technology Section A-Molecular Crystals and Liquid Crystals* **1996,** *291*, 41-44.

5. Jelezko, F.; Tamarat, P.; Lounis, B.; Orrit, M. Dibenzoterrylene in naphthalene: A new crystalline system for single molecule spectroscopy in the near infrared. *Journal of Physical Chemistry* **1996,** *100* (33), 13892-13894.

6. Nicolet, A. A.; Bordat, P.; Hofmann, C.; Kol'chenko, M. A.; Kozankiewicz, B.; Brown, R.; Orrit, M. Single dibenzoterrylene molecules in an anthracene crystal: Main insertion sites. *Chemphyschem* **2007,** *8* (13), 1929-1936.

7. Nicolet, A. A.; Hofmann, C.; Kol'chenko, M. A.; Kozankiewicz, B.; Orrit, M. Single dibenzoterrylene molecules in an anthracene crystal: Spectroscopy and photophysics. *Chemphyschem* **2007,** *8* (8), 1215-1220.

8. Hofmann, C.; Nicolet, A.; Kol'chenko, M. A.; Orrit, M. Towards nanoprobes for conduction in molecular crystals: Dibenzoterrylene in anthracene crystals. *Chemical Physics* **2005,** *318* (1-2), 1-6.

9. Kulzer, F.; Xia, T.; Orrit, M. Single Molecules as Optical Nanoprobes for Soft and Complex Matter. *Angewandte Chemie-International Edition* **2010,** *49* (5), 854-866.

10. Phillips, W. A. Tunneling states in amorphous solids. *Journal of low temperature physics* **1972,** *7* (3/4), 351-360.

11. Anderson, P. W.; Halperin, B. I.; Varma, C. M. Anomalous Low-Temperature Thermal Properties of Glasses and Spin Glasses. *Philosophical Magazine* **1972,** *25* (1), 1-&.

12. Vallé, R. A. L.; Tomczak, N.; Kuipers, L.; Vancso, G. J.; van Hulst, N. F. Single Molecule Lifetime Fluctuations Reveal Segmental Dynamics in Polymers. *Phys. Rev. Lett.* **2003,** *91* (3), 038301.

13. Zumbusch, A.; Fleury, L.; Brown, R.; Bernard, J.; Orrit, M. Probing individual two-level systems in a polymer by correlation of single molecule fluorescence. *Phys. Rev. Lett.* **1993,** *70* (23), 3584-3587.

14. Boiron, A. M.; Tamarat, P.; Lounis, B.; Brown, R.; Orrit, M. Are the spectral trails of single molecules consistent with the standard two-level system model of glasses at low temperatures? *Chemical Physics* **1999,** *247* (1), 119-132.

15. Vainer, Y.; Plakhotnik, T. V.; Personov, R. I. Dephasing and diffusional linewidths in spectra of doped amorphous solids: Comparison of photon echo and single molecule spectroscopy data for terrylene in polyethylene. *Chemical Physics* **1996,** *209* (1), 101-110.

16. Naumov, A. V.; Gorshelev, A. A.; Vainer, Y. G.; Kador, L.; Kohler, J. Impurity spectroscopy at its ultimate limit: relation between bulk spectrum, inhomogeneous broadening, and local disorder by spectroscopy of (nearly) all individual dopant molecules in solids. *Phys. Chem. Chem. Phys.* **2011,** *13* (5), 1734-1742.

17. Baier, J.; Richter, M. F.; Cogdell, R. J.; Oellerich, S.; Koehler, J. Do proteins at low temperature behave as glasses? A single-molecule study. *Journal of Physical Chemistry B* **2007,** *111* (5), 1135-1138.

18. Gorshelev, A. A.; Naumov, A. V.; Eremchev, I. Y.; Vainer, Y. G.; Kador, L.; Koehler, J. Ortho-Dichlorobenzene Doped with Terrylene-a Highly Photo-Stable Single-Molecule System Promising for Photonics Applications. *Chemphyschem* **2010,** *11* (1), 182-187.

19. Deperasinska, I.; Karpiuk, E.; Banasiewicz, M.; Makarewicz, A.; Kozankiewicz, B. Single dibenzoterrylene molecules in naphthalene and 2,3-dimethylnaphthalene crystals: vibronic spectra. *Phys. Chem. Chem. Phys.* **2011,** *13* (5), 1872-1878.

20. Deperasinska, I.; Karpiuk, E.; Banasiewicz, M.; Kozankiewicz, B. On the photo-stability of single molecules. Dibenzoterrylene in 2,3-dimethylnaphthalene crystals. *Chemical Physics Letters* **2010,** *492* (1-3), 93-97.

21. Banasiewicz, M.; Wiacek, D.; Kozankiewicz, B. Structural dynamics of 2,3-dimethylnaphthalene crystals revealed by fluorescence of single terrylene molecules. *Chemical Physics Letters* **2006,** *425* (1-3), 94-98.

22. Makarewicz, A.; Deperasinska, I.; Karpiuk, E.; Nowacki, J.; Kozankiewicz, B. Vibronic spectra of single dibenzoterrylene molecules in anthracene and 2,3-dimethylanthracene crystals. *Chemical Physics Letters* **2012,** *535*, 140-145.

23. Wachtel, H.; Port, H.; Wolf, H. C. Triplet optical line profiles of orientationally disordered single crystals: 2,3-dimethylnaphthalene and 2,3-dimethylanthracene. *Chemical Physics Letters* **1987,** *135* (6), 506-510.

24. Dorr, M.; Kalus, J.; Monkenbusch, M.; Natkaniec, I.; Schmelzer, U. The lattice dynamics of a dipolar disordered crystal of 2-3-dimethylanthracene. *Physica B-Condensed Matter* **1996,** *219-20*, 368-370.

25. Dorr, M.; Gerlach, H.; Kalus, J.; Karl, N.; Monkenbusch, M.; Natkaniec, I.; Schmelzer, U.; Schmidt, W.; Stezowski, J. J.; Vorderwisch, P.; Voss, G.; Warth, M. Structure and lattice dynamics of dipolarly disordered 2,3-dimethylanthracene crystals. *Journal of Physics-Condensed Matter* **1998,** *10* (48), 10879-10899.

26. Kozankiewicz, B.; Deperasi+äska, I.; Karpiuk, E.; Banasiewicz, M.; Makarewicz, A. On photo-oxidation of single molecules. *Optical Materials* **2011,** *33* (9), 1391-1394.

27. Plakhotnik, T.; Moerner, W. E.; Palm, V.; Wild, U. P. Single-Molecule Spectroscopy - Maximum Emission Rate and Saturation Intensity. *Optics Communications* **1995,** *114* (1-2), 83-88.

28. Fleury, L.; Gruber, A.; Drabenstedt, A.; Wrachtrup, J.; Vonborczyskowski, C. Low-temperature confocal microscopy on individual molecules near a surface. *Journal of Physical Chemistry B* **1997,** *101* (40), 7933-7938.

29. Mais, S.; Basché, T.; Müller, G.; Müllen, K.; Bruchle, C. Probing the spectral dynamics of single terrylenediimide molecules in low-temperature solids. *Chemical Physics* **1999,** *247* (1), 41-52.

30. Vainer, Y.; Naumov, A., V; Kador, L. Local vibrations in disordered solids studied via single-molecule spectroscopy: Comparison with neutron, nuclear, Raman scattering, and photon echo data. *Phys. Rev. B* **2008,** *77* (22).

31. Fleury, L.; Zumbusch, A.; Orrit, M.; Brown, R.; Bernard, J. Spectral Diffusion and Individual 2-Level Systems Probed by Fluorescence of Single Terrylene Molecules in A Polyethylene Matrix. *Journal of Luminescence* **1993,** *56* (1-6), 15-28.

32. Kozankiewicz, B.; Bernard, J.; Orrit, M. Single-Molecule Lines and Spectral Hole-Burning of Terrylene in Different Matrices. *Journal of Chemical Physics* **1994,** *101* (11), 9377-9383.

33. Ambrose, W. P.; Moerner, W. E. Fluorescence Spectroscopy and Spectral Diffusion of Single Impurity Molecules in A Crystal. *Nature* **1991,** *349* (6306), 225-227.

34. Kulzer, F.; Kummer, S.; Matzke, R.; Brauchle, C.; Basché, T. Single-molecule optical switching of terrylene in p-terphenyl. *Nature* **1997,** *387* (6634), 688-691.

35. Basche, T.; Kummer, S.; Brauchle, C. Direct Spectroscopic Observation of Quantum Jumps of A Single-Molecule. *Nature* **1995,** *373* (6510), 132-134.

36. Naumov, A. V.; Vainer, Y. G.; Bauer, M.; Kador, L. Dynamics of a doped polymer at temperatures where the two-level system model of glasses fails: Study by single-molecule spectroscopy. *Journal of Chemical Physics* **2003,** *119* (12), 6296-6301.

37. Plakhotnik, T.; Donley, E. A.; Wild, U. P. Single-molecule spectroscopy. *Annual Review of Physical Chemistry* **1997,** *48*, 181-212.

38. Sigl, A.; Scharnagl, C.; Friedrich, J.; Gourdon, A.; Orrit, M. 2-methylterrylene in hexadecane: Do we see single rotational quantum jumps of methyl groups? *Journal of Chemical Physics* **2008,** *128* (4).

39. Leeson, D. T.; Wiersma, D. A.; Fritsch, K.; Friedrich, J. The energy landscape of myoglobin: An optical study. *Journal of Physical Chemistry B* **1997,** *101* (33), 6331-6340.

40. Naumov, A., V; Vainer, Y.; Kador, L. Does the standard model of low-temperature glass dynamics describe a real glass? *Physical Review Letters* **2007,** *98* (14).

41. Neumann, M. A.; Johnson, M. R.; Radaelli, P. G.; Trommsdorff, H. P.; Parker, S. F. Rotational dynamics of methyl groups in durene: A crystallographic, spectroscopic, and molecular mechanics investigation. *Journal of Chemical Physics* **1999,** *110* (1), 516-527.

42. Plazanet, M.; Johnson, M. R.; Gale, J. D.; Yildirim, T.; Kearley, G. J.; Fernández-Díaz, M. T.; Sánchez-Portal, D.; Artacho, E.; Soler, J. M.; Ordejón, P.; Garcia, A.; Trommsdorff, H. P. The structure and dynamics of crystalline durene by neutron scattering and numerical modelling using density functional methods. *Chemical Physics* **2000,** *261*, 189-203.

CHAPTER 3

Stable single-molecule lines of terrylene in polycrystalline *p*-dichlorobenzene at 1.5 K

We studied the spectroscopic properties of single terrylene (Tr) molecules in a polycrystalline matrix of *para*-dichlorobenzene (*p*-DCB) at 1.5 K. This host has been purposely chosen in order to avoid the presence of methyl groups and to remove the effect of dipolar disorder because *p*-DCB is a centrosymmetric molecule. We were able to prepare thin films on coverslips and also fill thin glass capillaries (50 - 80μm) thanks to the simplified sample preparation (compared to co-sublimation). When we studied the bulk-fluorescence as a function of temperature we found that samples grown in a glass capillary produce a very strong site at 597 nm, red-shifted by more than 700 cm^{-1} from the observed transition energy (572 nm) for terrylene in *p*-DCB prepared as a film on a coverslip. We therefore characterized each of these two sites by measuring their single-molecule spectroscopic parameters at 1.5 K. We found lifetime limited linewidths almost all over the broad inhomogeneous distribution in the same sample. The features are hallmarks of an excellent host system for low temperature spectroscopy.

The content of this chapter is published.
P. Navarro, Y. Tian, M. van Stee and M. Orrit.
ChemPhysChem **2014,** 15, 3032-3039.

3.1.Introduction

Cryogenic single-molecule spectroscopy (SMS) has become a very important field in natural science because it offers the possibility to probe an isolated quantum system optically. The information obtained from a single-molecule probe can be related to specific physical and/or chemical properties of its nano-environment. This information is mostly washed out in the ensemble averaging of bulk experiments. To probe the molecule at low temperature, a light beam excites the lowest-energy electronic transition of the one molecule which is resonant with the excitation laser. By tuning the excitation frequency, one detects the molecule's optical absorption indirectly by fluorescence excitation[1]. The spatial isolation of the molecule is achieved with an optical microscope by placing the probe molecule (guest) inside a solid (host) at low enough concentration (nM-μM). Long observation times of the line of a single molecule are possible only if the host dynamics and the associated spectral diffusion[2] of the single-molecule line are negligible in the experiments. For many interesting photonic applications[3-8] the stability of the molecule is critical, and fluctuations in local interactions between the dye and its nano-environment (host) should be avoided. In order to search for such systems it is important to understand the physical origin of inhomogeneous broadening and spectral diffusion.

An optimal detection signal requires high emission rates, high fluorescence quantum yields, low intersystem crossing rates, and high photo-stability. The observation of single molecules with sufficient signal-to-noise ratio (SNR) and spectral stability has been restricted to a few classes of host-guest systems. One of them are organic-molecular single crystals such as *para*-terphenyl, naphthalene or anthracene that have been co-sublimated with dyes like pentacene[1], terrylene[9] and dibenzoterrylene[10,11]. Also in frozen alkanes (known as Shpol'skii matrices) the SNR is high and the linewidths are narrow. However, the frequency stability of the guest molecule is closely related to the size matching between the length of the alkane chain and the guest molecule as reported for terrylene in a series of alkanes[12,13].

Another fundamental requirement is the relative position of electronic energy levels of guest and host. The host has to be selected in a way that avoids quenching processes like the intermolecular intersystem crossing reported for terrylene in anthracene[14], and presumably at work for perylene in naphthalene and anthracene[15]. The sample preparation of crystalline host-guest systems has relied on different crystallization methods like Bridgman, co-sublimation, co-precipitation, fast-freezing but the guest concentration is usually difficult to control. The co-sublimation of the two components (host and guest) has given the best results[11]. However, this method requires exhaustive purification of starting materials and therefore a large amount, which are expensive. The fragility of the obtained single-crystals (very thin flakes) can also bring complications in some applications. Therefore, a simpler and reproducible preparation method, and a simpler manipulation of the host-guest sample would help to generalize the use of single organic molecules for quantum optical experiments.

Dye-doped polymers are another class of extensively studied systems[16-18]. The sample preparation methods, e.g. spin coating, are very simple[19]. These systems show broad inhomogeneous distributions of resonant guest frequencies and spectral diffusion of the single guest molecules. The observations have been related to the structural and/or dynamic disorder of the bulk host properties. Much of the broadening and spectral diffusion of single-molecule lines at low temperature can be understood within the standard model of two-level systems[20,21] or by coupling to low-frequency vibrational modes[22] (LFM). However, the physical nature of two-level systems has not been totally clarified, and the complex dynamics cannot always be described properly with the two-level system model[23,24]. In order to better understand the origin of spectral diffusion, systematic studies have been performed by different groups in the last years[2,25-28]. In these works, the sensitivity of the narrow zero-phonon line (ZPL) of the single fluorophore was used to probe the local nature of phonon-like and tunneling excitations in disordered solids. The inhomogeneous distribution of TLSs and LFMs gives new insight into the origin of spectral diffusion and optical dephasing, which was unclear from ensemble measurements[29,30]. In particular, methyl groups in the host material appear

to enhance spectral instability of the single-molecule lines, leading to line broadening, spectral jumps and spectral diffusion[2,25-28,31].

Here, we present our findings for terrylene (guest, Tr) dispersed in a *para*-dichlorobenzene (host, *p*-DCB) polycrystal. We show that this host-guest system is suitable to perform single-molecule experiments at cryogenic temperatures (1.5 K to 5 K). Samples can be prepared as thin polycrystalline film between two glass coverslips or grown from the melt in glass capillaries. These samples show different optical properties. We identified at least three spectroscopic sites at 572, 581 and 597 nm. At the single-molecule level, we studied the stability and optical properties of the zero-phonon lines in the 572 nm normal site (NS) and in the red-shifted site at 597 nm (RS). Stable and lifetime-limited lines were observed in these sites and throughout the whole broad inhomogeneous distribution. The stability of the molecules allowed us to record the complete fluorescence spectrum from two representative single molecules, including the 0-0 ZPL, by exciting the molecules to a higher vibroelectronic state of S_1. Finally, we quantify the emission efficiency of Tr as a single-photon source through its Debye-Waller factor α_{DW}.

3.2.Experimental

3.2.1. Sample preparation

We mixed terrylene (Tr, from Chiron AS, Norway) and *para*-dichlorobenzene (*p*-DCB, Aldrich, purity 99.99%) to prepare a sample with a known concentration of 10^{-4} mol/mol (The chemical structure of both guest and host are shown as inset in Fig. 1) . For this, *p*-DCB was heated above its melting point (52 – 54 ºC) and then terrylene powder was added to create a liquid mixture with a deep pink color. With the same method, we made more diluted samples until we reached the desired concentration, around 10^{-8} mol/mol. For the coverslip sample, a small piece of the solid mixture was placed on top of a coverslip on a heating plate and melted again. We obtained a homogeneous film by pressing the liquid mixture with a second coverslip. The

"sandwich" sample was immediately removed from the heating plate and the sample re-crystallized upon cooling to room temperature, producing a film about 100 μm thick (a microscope image of the film is shown in the Supplementary Information, Fig. S1.a). Finally, the sample was transferred to the pre-cooled cryostat (200 K). For the capillary samples, we used glass capillaries (CM Scientific, UK) with a square cross section and a square hole of 80 μm × 80 μm. The thickness of the capillary wall is also 80 μm. The mixture of Tr in *p*-DCB (≈ 10^{-8} mol/mol) was melted at 52 – 54 ºC and the capillary was filled by capillary forces. The capillary was then sealed using the direct flame from a Bunsen burner. The length of the capillary (2.5 cm) and the short heating time (less than 10 s) prevented that the center of the sample melts or sublimates. Finally, the capillary was cleaned with ethanol to remove the residual solid outside.

3.2.2. Ensemble spectroscopy

Absorption spectra were recorded in a commercial spectrophotometer (Cary 50). All bulk fluorescence spectroscopy was performed in our home-built confocal fluorescence microscope inside a cryostat. It allowed us to record the evolution of the spectra with temperature from 1.5 K to room temperature. We used 532 nm as the excitation light from a diode laser (1 nm FWHM). This wavelength was removed from the detection path by the combination of a notch filter at 532 nm and a long-pass filter. The emitted photons were focused into a spectrograph (Princeton Instruments i500) equipped with three diffraction gratings (150, 500, 1200 lines/mm) and a liquid-nitrogen cooled CCD camera as the detector.

3.2.3. Single-molecule spectroscopy

We used a single-mode tunable dye laser (Coherent 699-21) operated with rhodamine-6G pumped by 5 W of 532 nm laser (Verdi V5). The output was sent to a home-built beam-scanning low-temperature fluorescence confocal microscope mounted in reflection geometry inside the cryostat. The beam was passed through a pinhole

(30 μm) to optimize its Gaussian profile. Then, the beam was expanded by a telecentric system before the cryostat to fill the back aperture of the microscope objective. We use a low-temperature microscope objective (MikroTech, N.A = 0.80) to focus the excitation light into a diffraction-limited spot with a FWHM of ~1 μm and at the same time to collect the fluorescence from the sample. In general, the laser frequency was scanned ± 10 GHz around the central wavelength (572 nm or 597 nm) to excite the 0-0 electronic transition (ZPL_{00}) resonantly and detect the red-shifted photons from all the vibrational components with an avalanche photodiode (APD, PE, SPCM-AQR - 16). For the study of the normal site of terrylene at 572 nm, the excitation light was cleaned by a band-pass filter (Omega, 590DF30) and for the red site at 597 nm we used a long-pass filter (LPF610). In order to record the complete fluorescence spectra of the single molecule from each site, the resonant frequency of the laser was tuned on resonance to a higher vibronic band, corresponding to the skeleton mode at about 250 cm^{-1}. The wavelengths were 563.9 nm for the 572 nm site and 588.5 nm for the site at 597 nm. The collected photons in each particular case were sent to a spectrometer (Horiba iHR - 320 and/or Princeton Instruments i500). All experiments were performed inside a flow-bath cryostat (Janis SVT - 200) at different temperatures (300-1.5 K) and at a residual pressure lower than 10^{-4} mbar.

3.3.Results

3.3.1. Bulk spectroscopy

Room-temperature absorption and emission spectra of a thin film of *p*-DCB doped with Tr (with a 10^{-4} mol/mol ratio) are shown in Fig.3.1. The typical absorption spectrum (circles) of Tr presents a maximum at 570.9 nm (17514 cm^{-1}) accompanied by other vibrational bands at 531.9 nm (18800 cm^{-1}) and 505 nm (19800 cm^{-1}). The strong background below 450 nm comes from scattering from the solid *p*-DCB. The fluorescence spectrum (solid line) has its maximum at 578.5 nm (17283 cm^{-1}) and the corresponding vibrational overtones at 626.8 nm (15951 cm^{-1}) and 683.2 nm(14635 cm^{-1})

are in good agreement with earlier reports[17]. The Stokes shift between absorption and emission maxima is 230 cm^{-1} and is due to relaxation of the excited state.

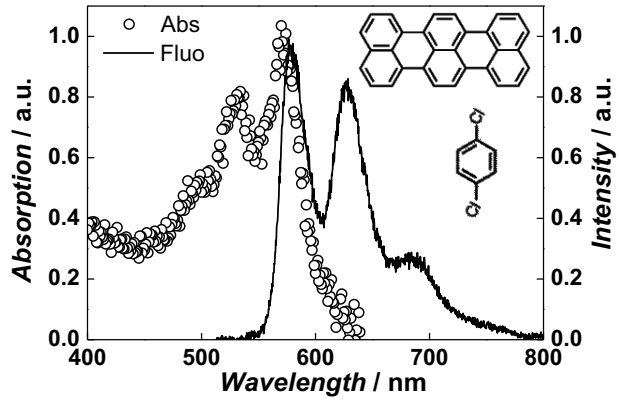

Figure 3.1: *Steady state absorption and emission spectra of a thin film of Tr/p-DCB (concentration 10^{-4} mol/mol) at room temperature.*

Coverslip sample

The fluorescence spectrum as a function of temperature for a more diluted samples (with 10^{-8} mol/mol ratio) are shown in Fig.3.2. For the coverslip sample (Fig 3.2a), the maximum wavelength shifts from 578.5 nm to 573.0 nm ($\Delta\nu \approx +167$ cm^{-1}) upon temperature change from 300 K to 1.5 K. The coverslip sample did not show any distinguishable site more than the "normal site" around 572nm. The peaks in spectrum 3.2a correspond to the vibrational components for terrylene emission.

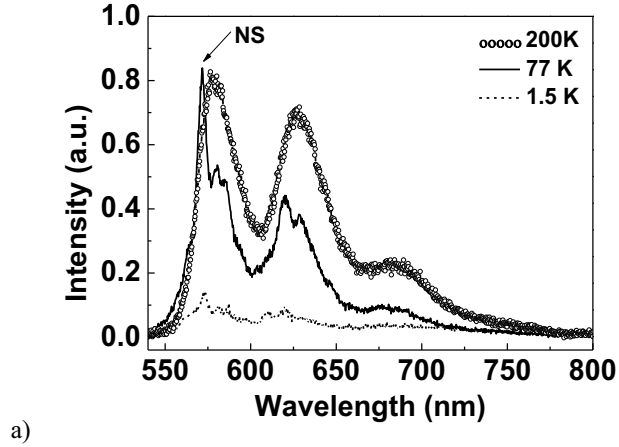

a)

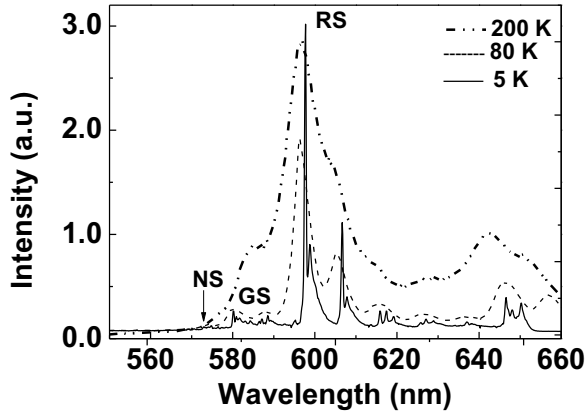

b)

Figure 3.2: *(a) Temperature dependence on the bulk fluorescence spectra of a thin film of Tr/p-DCB at 200, 77 and 1.5 K. (b) Fluorescence spectra at 200, 80 and 5 K for the capillary sample. The excitation source was 532 nm CW diode laser. The integration time was 120 s. The spectral resolution (10 cm^{-1}) was limited by the spectrograph grating (150 lines/mm). NS stands for normal site, at 572 nm in both samples. In the capillary sample, GS and RS stand for green and red site at 581 nm and 597 nm, respectively.*

Capillary sample

Coverslip samples limit our experiments to just one sample in each cooling cycle. Therefore here, we tested up to 6 samples in the same experiment by using multiple glass capillaries (or later hollow fibers) that allows to measure either different samples or different concentrations at once[32]. Capillaries used in confocal fluorescence spectroscopy were shown to increase the sensitivity down to sub-picomolar concentrations[33]. Starting from a mixture with a well-known concentration, 10^{-4} M of Tr/*p*-DCB, we obtained two other samples with concentrations ~10^{-6} and 10^{-8} M after dilution. We measured the spectra of each capillary as functions of temperature (from 200 to 5 K). The spectra shown in Fig.3.2b correspond to the sample with the lowest concentration (about 10^{-8} M) which was later used for our SM experiments. As can be seen in Fig.3.2b, the capillary influences the spectral properties of Tr, as the spectrum differs from that of Fig.3.2a. However, the observed narrow lines at low temperatures suggest well-defined spectroscopic sites, with narrow inhomogeneous distributions.

There are three main peaks in the spectrum of capillary samples. The weak site of the capillary sample, at 572 nm ("normal" site, NS, weak) is close to that found in the coverslip sample and roughly corresponds to the reported emission of Tr in polyethylene[17,34]. Then, another site appears at 581 nm ("green" site, GS, medium). Finally, the strongest site at 597 nm ("red" site, RS, strong), is red-shifted by about -732 cm^{-1}. Each of these sites has its own vibrational fingerprint, but the vibrational lines of the normal NS and green GS sites are difficult to assign because of the overlap with the spectra of the strong red site RS.

3.3.2. *Single-molecule spectroscopy*

Coverslip sample

All the experiments were performed on resonance at the red wing of the inhomogeneous band of the normal site NS. We thus could spectrally isolate single molecules within the illuminated area. Single-molecule studies on the coverslip sample were performed at a central laser wavelength of 574.2 nm. Firstly, a single-molecule signal at a given wavelength was optimized by spatially scanning the laser spot. Then, the fluorescence excitation spectrum was measured by scanning the laser frequency (±10 GHz) across the molecule's transition frequency, while detecting the red-shifted emitted photons with the APD. The selected single molecule (Fig. 3.3a) presents an excitation linewidth of 45 ± 5 MHz (at 1.5 K and $I_{exc} \leq 10$ W/cm^2) which is in good agreement with the reported value of 48 ± 5 MHz for Tr in *para*-terphenyl crystal[35]. The lifetime measurements at low temperature for Tr in *p*-terphenyl crystal reported is 4.2 ± 0.1 ns.[36] From this value is possible to predict an expected lifetime-limited value around 40 ± 8 MHz. The refractive indices and chemical structures of *p*-terphenyl and *p*-DCB (aromatics) are comparable and we therefore expect similar linewidths in both hosts. However, a real lifetime measurement is needed to prove that our linewidth is lifetime-limited.

Most of the single-molecule lines are very stable. In Fig.3.3b, we show the spectral trail of a stable molecule recorded for 15 min, in which the resonant frequency did not present any spectral jump or drift. This result is a good indication that the surrounding *p*-DCB host hardly presents interacting two-level system (TLS's) near this guest Tr molecule. However, some 10% of the molecules show blinking events (i.e., occasional jumps to a far-away frequency out of the laser range proving that these molecules are coupled to at least one TLS[23].

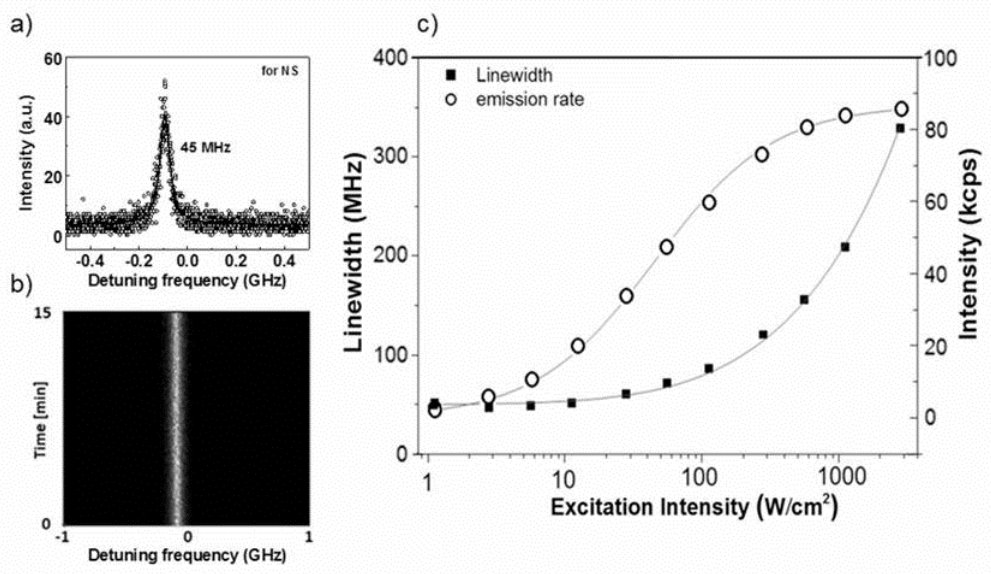

Figure 3.3: *a) Single-molecule excitation line of Tr in p-DCB (10^{-8} mol/mol) in the coverslip sample. The spectrum was recorded by detuning the laser frequency by ± 0.5 GHz around the central wavelength λ_{exc}=574.2 nm (laser linewidth ≈ 2 MHz). Temperature was 1.5 K, excitation intensity I_{exc} = 10 W/cm^2. The solid line is a Lorentzian fit. b) Stable spectral trail of the single Tr molecule for a total observation time of 15 min., including 100 spectra recorded with 3000 points and with an integration time of 3.3 ms per point. c) Linewidth (solid squares) and emission rate (open circles) as functions of excitation intensity for a single Tr molecule at 1.5 K. The emission rate at saturation is 86 ± 3 kcount/s and an I_{sat} = 45 ± 5 W/cm^2.*

We performed saturation studies on stable molecules[37]. An example of the saturation curves is shown in Fig.3.3c, presenting fluorescence detection rate (open circles, right axis) and linewidth (solid squares, left axis) as functions of excitation intensity (in log scale). On one hand, by fitting with Eq. (1), we obtain a lifetime-limited linewidth of γ_0 = 50 ± 5 MHz. The saturation intensity corresponds to 45 ± 5 W/cm^2. On the other hand, we obtained a detected emission rate at saturation of R_∞ = 86 ± 3 kcps using eq. (2).

$$\gamma = \gamma_0 \sqrt{1 + \frac{I}{I_s}} \qquad (1) \qquad R(I) = R_\infty \frac{I}{(I + I_s)} \quad . \qquad (2)$$

We analyzed the linewidth distribution of 62 single molecules measured at 1.5 K. In order to minimize saturation broadening, all the molecules were measured at a power density of 10 W/cm^2 which is lower than the saturation intensity but still gives a good signal-to-noise ratio. As can be seen in Fig.3.4, the excitation linewidths are distributed between 30 and 350 MHz. The maximum of the distribution appears at 50 ± 5 MHz, which is in good agreement with the value of 50 ± 10 MHz for Tr in *o*-DCB[38]. However, the distribution of linewidths is broader than is usually found in single crystals, as the example of DBT in anthracene shows[11]. The tail of the distribution for linewidths larger than 200 MHz could come from "jumping-molecules" that are affected by remaining structural dynamics in the local environment. Extremely low interactions with low-frequency modes can induce line broadening due to dephasing. The 10 % of the molecules that presented jumps indicate that there are still some locations within the polycrystal that are not very stable, maybe close to the grain boundaries between domains.

The complete fluorescence spectrum from a single Tr molecule in *p*-DCB at 1.5 K is presented in Fig. 3.5. For this measurement, the molecule was excited at 569.1 nm which corresponds to one of the stronger vibrational modes determined from DFT calculations[39] at 249 cm^{-1} above the ZPL_{00} found at 577.1 nm. This allowed us to collect the fluorescence photons emitted from the relaxed $S_1^{\upsilon=0}$ state, after filtering out theexcitation light. The single-molecule spectrum shows well-defined ZPL's and corresponding phonon-side bands (PSB). To quantify the fluorescence efficiency of our dye we measured the ratio of oscillator strengths of the ZPL in the fluorescence spectrum relative to the total strength of the pure electronic 0-0 fluorescence structure

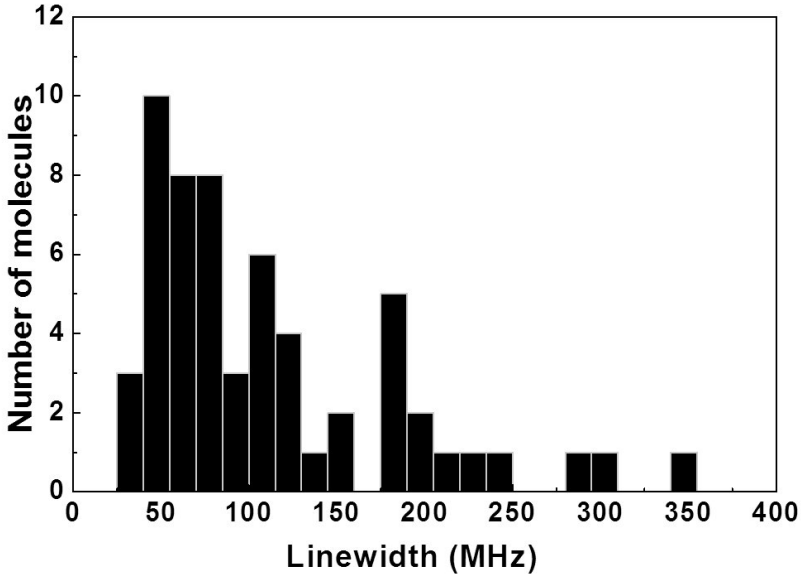

Figure 3.4: *Distribution of linewidths of 62 single-molecule lines.* I_{exc} *= 10 W/cm*^{2} *(scanned range 2 GHz with resolution of 3000 pixels and integration time of 3.3 ms/pixel).*

By integrating the area under the spectrum for the ZPL_{00} from 576.8 to 577.4 nm, and for the PSB_{00} from 577.5 to 584.3 nm, we were able to calculate an approximate Debye-Waller factor of $\alpha_{DW} = 0.33$, using Eq. 3. The integration is done only for the purely electronic part (0-0 band) of the spectrum. Therefore, the above factor does not include the Franck-Condon factors of the 0-0 transition (about 30%).

$$\frac{\int ZPL_{00}}{\int ZPL_{00} + \int PSB_{00}} = \alpha_{DW} \qquad (3)$$

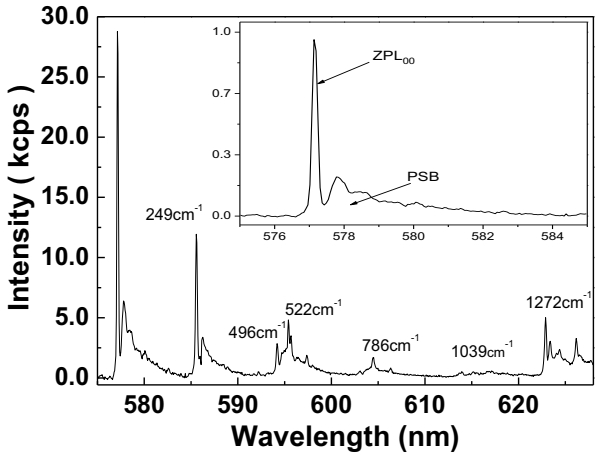

Figure 3.5: *Fluorescence spectrum of a single Tr molecule excited at 569.1 nm. The inset shows a zoom of the ZPL and its PSB. The width of the spectrum is determined by the spectrometer resolution (3 cm^{-1}).*

Table 3.1: *Main vibration frequencies of Tr in p-DCB deduced from single-molecule fluorescence spectra on a coverslip (NS) and in the capillary (RS). It is compared to Tr in polyethylene[40]. The assignment is based on published quantum chemical calculations[39].*

Mode Assignement	NS coverslip Origin at 17456cm^{-1}	RS capillary Origin at 16728cm^{-1}	DFT[39]	Tr/ PE[40]
Long-axis ring extension	249	197	278	243
In-plane ring deformation	496 522	443 500	491 597	487 534
Out-of-plane ring deform.	786 836	741 801	684 856	Not reported
Out-of-plane C-H bending	1039 1124	Out of spectrograph range	1029 1177	
in-plane C–H bending	1272 1351		1218 1352	1273 1356

Capillary sample

The experiments have been performed at a central laser wavelength of 597 nm chosen from the spectrum shown in Fig.3.2b. We checked that the image showed diffraction-limited spots. The spectrum of Fig3.6a, shows a zoom into a ±1 GHz of the ZPL of one representative Tr molecule, and the fitted linewidth of 52 ± 5 MHz corresponds to the expected lifetime-limited linewidth. Then, we recorded a spectral trail of the fluorescence excitation spectrum for a broader detuning (±10 GHz) around the central frequency (597 nm) as shown in Fig.3.6b. In the spectral trails it is possible to distinguish several stable single-molecule lines within the 20 GHz scan. No interruptions or clear spectral jumps can be seen, which indicates an absence of interacting TLS in this red site also. We also looked for single molecules in the normal site NS (572 nm) in the capillary sample and found much less molecules than in RS, in agreement with the ensemble spectrum of Fig.3.2b.

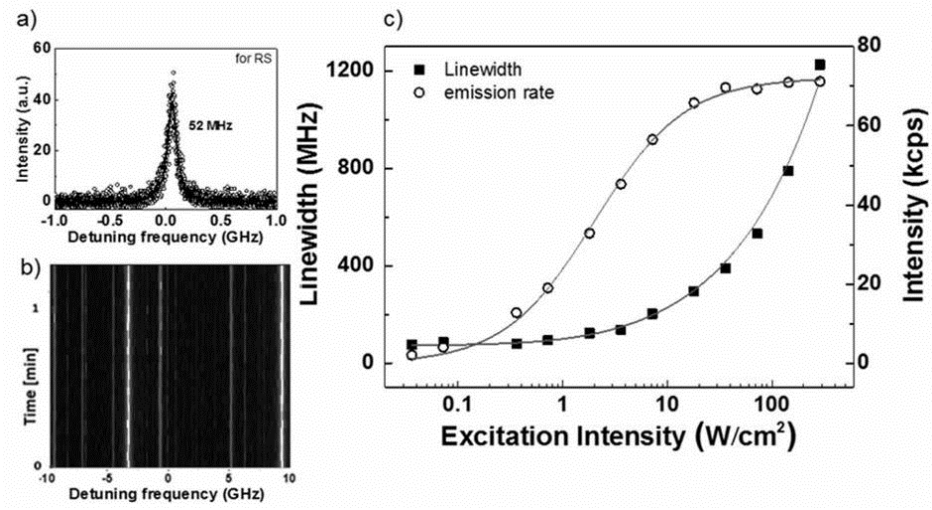

Figure 3.6: *a) Lifetime-limited fluorescence excitation spectrum of a selected single Tr molecule in the red site 597 nm (RS, at 1.5 K. b) Spectral trails showing several stable molecules in the ± 10 GHz scan (central wavelength, excitation intensity 1 W/cm^2). c) Linewidth (solid squares) and emission rate (open circles) as functions of excitation intensity for a single Tr molecule. at 1.5 K. The emission rate at saturation is 72 ± 3 kcount/s and an I_{sat} = 3.6 ± 0.5 W/cm^2.*

Then, we analyzed the saturation profile for a single molecule in the red site (Fig.3.6c), and obtained a fluorescence detection rate at saturation $R_\infty = 72 \pm 3$ kcps (open circles, right axis). The linewidth is $\gamma_0 = 79 \pm 5$ MHz, which is somewhat broader than the lifetime limit. The linewidth reaches the saturation value of $\sqrt{2}\,\gamma_0 = 111.7$ MHz at an excitation intensity of 3.6 ± 0.5 W/cm^2 and it follows the usual saturation broadening profile of eq. (1) (solid squares, left axis).

Finally, we measure the complete fluorescence spectra of a single Tr molecule with ZPL on resonance with 597nm on the RS site of the capillary sample as shown in Fig 3.7. The molecular vibrations are reported in Table 1 and compared to the vibrations found in the NS site. For the fluorescence spectrum, the excitation frequency of the laser was fixed to 16215 cm^{-1} (587.9 nm), in resonance with the vibronic transition of Tr corresponding to the strong C-C stretch mode (along the long molecular axis) at + 249 cm^{-1} above the ZPL_{00}.

In the spectrum, we found peaks that do not correspond to molecular vibrations from the molecule with its ZPL at 596.7 nm. These spurious lines marked with arrows in spectrum, may arise from other molecules excited by the 587.9 nm laser maybe on one of their higher vibronic transitions. After removing these signals, we integrated the intensities of the ZPL_{00} and the PSB_{00} and obtained a Debye-Waller factor, $\alpha_{DW} = 0.30$ which is very similar to what we have reported for the normal site (again, the 0-0 Franck-Condon factor has not been included).

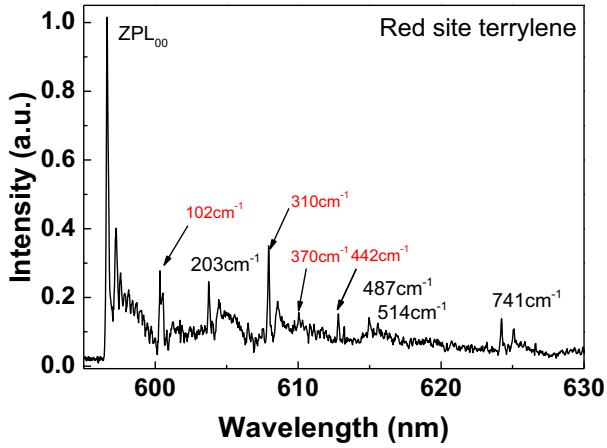

Figure 3.7: *Fluorescence spectrum of a single Tr molecule in the red site of* p-*DCB (excited at 587.9 nm). The resolution is limited by the spectrometer (3 cm^{-1}). Peaks marked with an arrow were not considered in the analysis.*

3.4.Discussion

3.4.1. Sample preparation

The main advantage of coverslip samples is that the sample can be thinner than 10 µm, which helps to reduce fluorescence background from out-of-focus molecules. However, as we could not mount more than one coverslip sample for each cooling cycle, this method is not convenient for optimizing the experimental conditions such as concentration of the sample. We can mount up to 6 thin glass capillaries (80×80 µm^2) to explore six samples within only one cooling cycle. This allowed us to measure the bulk spectrum of Tr/*p*-DCB at different concentrations and to choose the right concentration for single-molecule experiments from the same cooling cycle. In addition, compared to cylindrical capillaries, which distort the image, the square capillaries allow us to explore a larger sample area.

3.4.2. Bulk fluorescence spectra

The inhomogeneous distribution of frequencies in the bulk spectrum is related to the different local environments around each single molecule. Therefore, the intensity of each peak can give an idea of the relative number of molecules occupying that specific site. In the case of dibenzoterrylene (DBT) inserted in a single crystal of anthracene[41], even though the anthracene host presented a single crystal phase, there were at least two different ways of replacing three host molecules by a guest DBT molecule, leading to two different spectroscopic sites. In the spectrum of the capillary in Fig.3.2b three spectroscopic sites (NS, GS and RS) appear. Crystalline *p*-DCB can present three different phases at different thermodynamic conditions. X-ray crystallography has identified at least three metastable phases of *p*-DCB, called α, β and γ[42]. Under ambient pressure the most stable phase at low temperature (<100 K) is γ, followed by the α-phase from 281 K to 311 K, and between 311 and the melting point (325 K) the β-phase is more stable[43]. The crystalline γ-phase presents a monoclinic structure with two molecules per unit cell[44]. A first hypothesis is that the 3 spectroscopic sites observed in the capillary sample arise from micro-domains of α and β metastable phases included in the more thermodynamically stable γ-phase even at 1.5 K[45]. If this is the case, different crystal structures would lead to different solvent shifts and to different spectroscopic sites for the Tr molecule. A second hypothesis is that the γ-phase is the only phase present in the capillary sample at 1.5 K[46]. Since a Tr molecule has to substitute several *p*-DCB molecules in the lattice, there might be different ways of inserting it. As in the case of DBT/anthracene[41], the different insertion sites will give rise to different spectroscopic sites. Only a molecular-dynamics study could give some insight into the origin of these observed sites.

The spectral red shift of -732 cm^{-1} of Tr in *p*-DCB in the capillary is surprisingly strong. The solvent shift results from physical-chemical interactions between the host and the guest molecules, most importantly from van der Waals interactions[47]. We propose that this strong shift is due to π-π stacking between the Tr molecule and some of its *p*-DCB neighbors. For the normal site NS (572 nm), the site energy is not significantly

shifted with respect to non-aromatic hosts such as polyethylene[16] or Shpol'skii matrixes[18]. The π-π stacking would thus be nearly absent for the NS but very pronounced for the red site RS. Fluorescence spectroscopy experiments in supersonic beams report a -134 cm^{-1} red shift attributed to very strong π-π interactions in one-to-one complexes between *p*-DCB and perylene[48], a lighter analog of Tr. The red shift of -732 cm^{-1} would correspond roughly to π-π stacking interactions with four p-DCB molecules.

3.4.3. Single-molecule spectra

The sensitivity of ZPL's to their nano-environment allows us to test the structural stability of *p*-DCB. Stable single-molecule lines appeared all over the inhomogeneous distribution (in the 3 sites NS, GS and RS at intermediate wavelengths between 572 and 597 nm). The spectroscopic properties of single molecules in both sites (NS and RS) are comparable. The excitation linewidth distribution for the NS (572 nm), 50±5 MHz, is in very good agreement from the 50±10 MHz found for the similar system Tr in *o*-DCB[38]. The lifetime-limited value expected from the reported[36] lifetime in the aromatic matrix *p*-terphenyl, 4.2 ± 0.1 ns would be 40±8 MHz.

We have shown spectral trails demonstrating the frequency stability of the ZPL as a function of time. Over typical observation times of 15 min, 90% of the single molecules showed no spectral jumps or drifts. For the remaining 10% of molecules, clear jumps were perfectly resolved in our observation window, proving the presence of a few well-defined TLS's which might be interesting for solid-state dynamic studies[23,24,26]. The saturation profiles are very similar for both sites. The difference in saturation intensity may arise from different experimental adjustments and from different orientations of the molecules[37]. Observed saturation intensities of Tr range from 0.2 - 0.3 W/cm^2 in Shpols'kii matrixes[13] (dodecane, tetradecane and hexadecane) to 3.5 ± 1 W/cm^2 in *o*-DCB[38], and to 20 ± 2 W/cm^2 in *p*-terphenyl single crystal[9].

3.4.4. Comparison of single-molecule fluorescence spectra in NS and RS

We can make a quantitative comparison using the Debye-Waller factor of α_{DW} = 0.33± 0.05 for Tr in *p*-DCB in the NS and α_{DW} = 0.30± 0.05 for the RS. For dibenzoanthanthrene (DBATT) in a methylmethacrylate (MMA) crystal[49] a factor =0.4 was reported. This property could find interesting applications for many quantum optical experiments as a single photon source[5,50].

To complement the analysis of our system, we compare (In Table 3.1) the complete fluorescence spectra from two different single molecules representing in the NS and RS spectroscopic sites. The ground state vibrational frequencies give us information about possible molecular host-induced distortions and perturbations in the two sites. Table 1 summarizes the main vibrations of the two single molecules, and compares them to previous reports for Tr in polyethylene[40] and to DFT calculations[39] in gas phase. All vibrations in NS present higher frequency than in RS, corresponding to a stronger spring constant of the bond vibration, usually caused by application of an effective local hydrostatic pressure[51]. However, the red shift of RS compared to NS indicates a larger solvent shift, and therefore an increase in effective local pressure. This discrepancy between electronic and vibrational frequency shifts is surprising. It suggests that the red shift of RS follows from a strongly anisotropic strain field, possibly caused by the strong π-π stacking interactions postulated above.

3.5.Conclusion

The spectroscopic differences between the Tr/*p*-DCB samples prepared in different ways (coverslip sample and capillary sample) are clear but their physical origin is still unclear. It is known that the spectroscopic sites observed in crystalline organic host-guest systems depend very much on the crystallization conditions. Confinement and shape of the growth vessel may select growth of certain seeds with favorable orientations, thereby influencing the spectroscopic sites observed[52]. We have proved that *para*-

dichlorobenzene is a suitable matrix for isolate single terrylene molecules at low temperatures, and probably for other guests as well. This property is verified for a broad range of wavelengths (from 572 to 597 nm at least). We also simplified the sample preparation method that allows having a better control of the real dye (guest) concentration. Such simple sample preparation appears very convenient for many quantum optical experiments such as coupling to nano-mechanical resonators[8], coupling to plasmonic antennas[53] or uses as single-photon sources[7].

Acknowledgments

We thank to Marijn van Stee for his contribution to this work from May 2013 – April 2014, as part of his Master thesis. We also thank to Stichting Fundamenteel Onderzoek der Materie (FOM) project # L2105, which is part of the N*W*O, for the financial support of this thesis.

Reference List

1. Orrit, M.; Bernard, J. Single Pentacene Molecules Detected by Fluorescence Excitation in A Para-Terphenyl Crystal. *Physical Review Letters* **1990,** *65* (21), 2716-2719.

2. Tian, Y.; Navarro, P.; Kozankiewicz, B.; Orrit, M. Spectral diffusion of single dibenzoterrylene molecules in 2,3-dimethylanthracene. *Chemphyschem : a European journal of chemical physics and physical chemistry* **2012,** *13* (15), 3510-3515.

3. Hwang, J.; Pototschnig, M.; Lettow, R.; Zumofen, G.; Renn, A.; Goetzinger, S.; Sandoghdar, V. A single-molecule optical transistor. *Nature* **2009,** *460* (7251), 76-80.

4. Lettow, R.; Rezus, Y.; Renn, A.; Zumofen, G.; Ikonen, E.; Goetzinger, S.; Sandoghdar, V. Quantum Interference of Tunably Indistinguishable Photons from Remote Organic Molecules. *Physical Review Letters* **2010,** *104* (12).

5. Trebbia, J. B.; Tamarat, P.; Lounis, B. Indistinguishable near-infrared single photons from an individual organic molecule. *Physical Review A* **2010,** *82* (6).

6. Rezus, Y.; Walt, S.; Lettow, R.; Renn, A.; Zumofen, G.; Goetzinger, S.; Sandoghdar, V. Single-Photon Spectroscopy of a Single Molecule. *Physical Review Letters* **2012,** *108* (9).

7. Hwang, J.; Hinds, E. Dye molecules as single-photon sources and large optical nonlinearities on a chip. *New Journal of Physics* **2011,** *13*.

8. Puller, V.; Lounis, B.; Pistolesi, F. Single Molecule Detection of Nanomechanical Motion. *Physical Review Letters* **2013,** *110* (12).

9. Kummer, S.; Basche, T.; Brauchle, C. Terrylene in P-Terphenyl - A Novel Single-Crystalline System for Single-Molecule Spectroscopy at Low-Temperatures. *Chemical Physics Letters* **1994,** *229* (3), 309-316.

10. Jelezko, F.; Tamarat, P.; Lounis, B.; Orrit, M. Dibenzoterrylene in naphthalene: A new crystalline system for single molecule spectroscopy in the near infrared. *Journal of Physical Chemistry* **1996,** *100* (33), 13892-13894.

11. Nicolet, A. A.; Hofmann, C.; Kol'chenko, M. A.; Kozankiewicz, B.; Orrit, M. Single dibenzoterrylene molecules in an anthracene crystal: Spectroscopy and photophysics. *Chemphyschem* **2007,** *8* (8), 1215-1220.

12. Palewska, K.; Lipinski, J.; Sworakowski, J.; Sepiol, J.; Gygax, H.; Meister, E. C.; Wild, U. P. Total Luminescence Spectroscopy of Terrylene in Low-Temperature Shpol'skii Matrices. *Journal of Physical Chemistry* **1995,** *99* (46), 16835-16841.

13. Vacha, M.; Liu, Y.; Nakatsuka, H.; Tani, T. Inhomogeneous and single molecule line broadening of terrylene in a series of crystalline n-alkanes. *Journal of Chemical Physics* **1997,** *106* (20), 8324-8331.

14. Nicolet, A.; Kol'chenko, M. A.; Kozankiewicz, B.; Orrit, M. Intermolecular intersystem crossing in single-molecule spectroscopy: Terrylene in anthracene crystal. *Journal of Chemical Physics* **2006,** *124* (16).

15. Walla, P. J.; Jelezko, F.; Tamarat, P.; Lounis, B.; Orrit, M. Perylene in biphenyl and anthracene crystals: an example of the influence of the host on single-molecule signals. *Chemical Physics* **1998,** *233* (1), 117-125.

16. Orrit, M.; Bernard, J.; Zumbusch, A.; Personov, R. I. Stark-Effect on Single Molecules in A Polymer Matrix. *Chemical Physics Letters* **1992,** *196* (6), 595-600.

17. Tchenio, P.; Myers, A. B.; Moerner, W. E. Optical Studies of Single Terrylene Molecules in Polyethylene. *Journal of Luminescence* **1993,** *56* (1-6), 1-14.

18. Kozankiewicz, B.; Bernard, J.; Orrit, M. Single-Molecule Lines and Spectral Hole-Burning of Terrylene in Different Matrices. *Journal of Chemical Physics* **1994,** *101* (11), 9377-9383.

19. Wirtz, A. C.; Dokter, M.; Hofmann, C.; Groenen, E. J. J. Spincoated polyethylene films for single-molecule optics. *Chemical Physics Letters* **2006,** *417* (4-6), 383-388.

20. Phillips, W. A. Tunneling states in amorphous solids. *Journal of low temperature physics* **1972,** *7* (3/4), 351-360.

21. Suarez, A.; Silbey, R. Study of A Microscopic Model for 2-Level System Dynamics in Glasses. *Journal of Physical Chemistry* **1994,** *98* (30), 7329-7336.

22. Vainer, Y. G.; Naumov, A. V.; Bauer, M.; Kador, L. Dispersion of the local parameters of quasilocalized low-frequency vibrational modes in a low-temperature glass: Direct observation via single-molecule spectroscopy. *Journal of Chemical Physics* **2005,** *122* (24).

23. Boiron, A. M.; Tamarat, P.; Lounis, B.; Brown, R.; Orrit, M. Are the spectral trails of single molecules consistent with the standard two-level system model of glasses at low temperatures? *Chemical Physics* **1999,** *247* (1), 119-132.

24. Naumov, A., V; Vainer, Y.; Kador, L. Does the standard model of low-temperature glass dynamics describe a real glass? *Physical Review Letters* **2007,** *98* (14).

25. Vainer, Y.; Naumov, A. V.; Bauer, M.; Kador, L. Isotope effect in the linewidth distribution of single-molecule spectra in doped toluene at 4.2;K. *Journal of Luminescence* **2007,** *127* (1), 213-217.

26. Eremchev, I. Y.; Vainer, Y. G.; Naumov, A. V.; Kador, L. Low-temperature dynamics in amorphous polymers and low-molecular-weight glasses-what is the difference? *Physical Chemistry Chemical Physics* **2011,** *13* (5), 1843-1848.

27. Kosciesza, R.; Luzina, E.; Wiacek, D.; Dresner, J.; Kozankiewicz, B. Photo-stability of single terrylene molecules in 2,3-dimethylnaphthalene crystals. *Molecular Physics* **2009,** *107* (18), 1889-1895.

28. Makarewicz, A.; Deperasinska, I.; Karpiuk, E.; Nowacki, J.; Kozankiewicz, B. Vibronic spectra of single dibenzoterrylene molecules in anthracene and 2,3-dimethylanthracene crystals. *Chemical Physics Letters* **2012,** *535*, 140-145.

29. Vainer, Y.; Naumov, A., V; Bauer, M.; Kador, L. Experimental evidence of the local character of vibrations constituting the Boson peak in amorphous solids. *Physical Review Letters* **2006,** *97* (18).

30. Vainer, Y.; Naumov, A., V; Kador, L. Local vibrations in disordered solids studied via single-molecule spectroscopy: Comparison with neutron, nuclear, Raman scattering, and photon echo data. *Phys. Rev. B* **2008,** *77* (22).

31. Naumov, A. V. Low-temperature spectroscopy of organic molecules in solid matrices: from the Shpol'skii effect to laser luminescent spectromicroscopy for all effectively emitting single molecules. *Physics-Uspekhi* **2013,** *56* (6), 605-622.

32. Hussels, M.; Konrad, A.; Brecht, M. Confocal sample-scanning microscope for single-molecule spectroscopy and microscopy with fast sample exchange at cryogenic temperatures. *Review of Scientific Instruments* **2012,** *83* (12).

33. Zhu, Y.; Chen, N.; Li, Q.; Fang, Q. Improving the sensitivity of confocal laser induced fluorescence detection to the sub-picomolar scale for round capillaries by laterally shifting the laser focus point. *Analyst* **2013,** *138* (16), 4642-4648.

34. Fleury, L.; Zumbusch, A.; Orrit, M.; Brown, R.; Bernard, J. Spectral Diffusion and Individual 2-Level Systems Probed by Fluorescence of Single Terrylene Molecules in A Polyethylene Matrix. *Journal of Luminescence* **1993,** *56* (1-6), 15-28.

35. Kulzer, F.; Kummer, S.; Matzke, R.; Brauchle, C.; Basche, T. Single-molecule optical switching of terrylene in p-terphenyl. *Nature* **1997,** *387* (6634), 688-691.

36. Harms, G. S.; Irngartinger, T.; Reiss, D.; Renn, A.; Wild, U. P. Fluorescence lifetimes of terrylene in solid matrices. *Chemical Physics Letters* **1999,** *313*, 533-538.

37. Plakhotnik, T.; Moerner, W. E.; Palm, V.; Wild, U. P. Single molecule spectroscopy: maximum emission rate and saturation intensity. *Optics Communications* **1995,** *114*, 83-88.

38. Gorshelev, A. A.; Naumov, A. V.; Eremchev, I. Y.; Vainer, Y. G.; Kador, L.; Koehler, J. Ortho-Dichlorobenzene Doped with Terrylene-a Highly Photo-Stable Single-Molecule System Promising for Photonics Applications. *Chemphyschem* **2010,** *11* (1), 182-187.

39. Deperasinska, I.; Zehnacker, A.; Lahmani, F.; Borowicz, P.; Sepiol, J. Fluorescence studies of terrylene in a supersonic jet: Indication of a dark electronic state below the allowed transition. *Journal of Physical Chemistry A* **2007,** *111* (20), 4252-4258.

40. Tchenio, P.; Myers, A. B.; Moerner, W. E. Vibrational Analysis of the Dispersed Fluorescence from Single Molecules of Terrylene in Polyethylene. *Chemical Physics Letters* **1993,** *213* (3-4), 325-332.

41. Nicolet, A. A.; Bordat, P.; Hofmann, C.; Kol'chenko, M. A.; Kozankiewicz, B.; Brown, R.; Orrit, M. Single dibenzoterrylene molecules in an anthracene crystal: Main insertion sites. *Chemphyschem* **2007,** *8* (13), 1929-1936.

42. Boese, R.; Kirchner, M. T.; Dunitz, J. D.; Filippini, G.; Gavezzotti, A. Solid-state behaviour of the dichlorobenzenes: Actual, semi-virtual and virtual crystallography. *Helvetica Chimica Acta* **2001,** *84* (6), 1561-1577.

43. Thiery, M. M.; Rerat, C. Calculation of crystal and molecular structures of the temperature and pressure polymorphs of *para*-dichlorobenzene p-C6H4Cl2. *Journal of Chemical Physics* **2003,** *118* (24), 11100-11110.

44. Housty, J.; Clastre, J. Structure cristalline de la forme triclinique du *para*-dichlorobenzene. *Acta Cryst.* **1957,** *10* (11), 695-698.

45. Wheeler, G. L.; Colson, S. D. Intermolecular Interactions in Polymorphic *p*-Dichlorobenzene Crystals - Alpha, Beta, and Gamma Phases at 100 Degrees K. *Journal of Chemical Physics* **1976,** *65* (4), 1227-1235.

46. Frasson, E.; Garbuglio, C.; Bezzi, S. Structure of the monoclinic form of *p*-dichlorobenzene at low temperature. *Acta Cryst.* **1959,** *12* (2), 126-129.

47. Kador, L.; Personov, R.; Richter, W.; Sesselmann, T.; Haarer, D. Laser Photochemistry and Hole Burning Spectroscopy in Polymers and Glasses - External-Field Effects. *Polymer Journal* **1987,** *19* (1), 61-71.

48. Pryor, B. A.; Andrews, P. M.; Palmer, P. M.; Topp, M. R. Perylene complexes with *p*-dichlorobenzene and related species: Comparison of rotational coherence data with structure calculations. *Chemical Physics Letters* **1997,** *267* (5-6), 531-538.
49. Walser, A.; Renn, A.; Goetzinger, S.; Sandoghdar, V. Lifetime-limited zero-phonon spectra of single molecules in methyl methacrylate. *Chemical Physics Letters* **2009,** *472* (1-3), 44-47.

50. Brunel, C.; Lounis, B.; Tamarat, P.; Orrit, M. Triggered source of single photons based on controlled single molecule fluorescence. *Physical Review Letters* **1999,** *83* (14), 2722-2725.

51. Sesselmann, T.; Richter, W.; Haarer, D.; Morawitz, H. Spectroscopic studies of impurity-host interactions in dye-doped polymers: Hydrostatic-pressure effects versus temperature effects. *Phys. Rev. B* **1987,** *36* (14), 7601-7611.

52. Ha, J. M.; Hamilton, B. D.; Hillmyer, M. A.; Ward, M. D. Alignment of Organic Crystals under Nanoscale Confinement. *Crystal Growth & Design* **2012,** *12* (9), 449.

53. Yuan, H.; Khatua, S.; Zijlstra, P.; Yorulmaz, M.; Orrit, M. Thousand-fold Enhancement of Single-Molecule Fluorescence Near a Single Gold Nanorod. *Angewandte Chemie-International Edition* **2013,** *52* (4), 1217-1221.

CHAPTER 4

Electron energy loss of terrylene deposited on Au (111): Vibrational and electronic spectroscopy

We have investigated the vibrational and electronic properties of terrylene by high-resolution electron energy-loss spectroscopy (HREELS), Fourier-transform infrared spectroscopy and low-temperature single molecule fluorescence spectroscopy. Terrylene thin films were sublimated in ultra-high vacuum on Au (111) surface in order to record the HREEL spectra. Polycrystalline *para*-dichlorobenzene was used as a matrix to isolate a single terrylene molecule at 1.5 K, and record its fluorescence spectrum. The infrared spectrum together with the vibrational components from the fluorescence spectrum were used for the assignment and identification of the active modes found in HREELS. Finally, we report a loss signal around 17,000 cm^{-1} (2.1 eV) for the first singlet electronic excited state in agreement with optical spectroscopy. Some of the vibrational degrees of freedom either IR- or Raman-active modes can be found in the HREEL spectra provided they fulfil the surface selection rules. Energy-loss spectroscopy could be used as a complementary technique to explore some other degrees of freedom which are not accessible by optical means.

The content of this chapter is accepted for publication.
P. Navarro, F. Bocquet, I. Deperasinska, G. Pirug, S.Tautz and M. Orrit.
Journal of Physical Chemistry **C**.

4.1. Introduction

High- resolution energy-loss spectroscopy (HREELS) is a spectroscopic technique completely different to our optical techniques (SMS). On this technique, an electron beam is used as the excitation source instead of a stream of photons. It is a valuable method to characterize organic thin films because it is highly surface sensitive and induces little radiation damage[1]. From the spectral features in HREELS it is possible to learn about the orientation of molecules in organic thin films, such as Langmuir-Blodget films and polymer films. Loss signals bring information about molecular degrees of freedom that are excited at the surface or at the interface. Many studies are focused on the vibrational degrees of freedom of the selected molecule[2]. However, the electronic properties of organic semiconductor films[3,4] (molecular exciton band gap) have also been measured with HREELS, using an electron beam with moderately high energy (10 eV or higher) as excitation, and looking for energy losses in the range of 1 – 5 eV (8000 – 40000 cm^{-1}) where these transitions occur. These observations can be compared with optical spectroscopy in solution[5]. There have been also some reports of the observation of low-lying triplet states from organic semiconductor films, in particular naphthalene[6].

Organic semiconductors based on polyaromatic hydrocarbons (PAH's) have been used in the development of novel molecular electronic and photonic devices, such as organic light emitting diodes (OLED's), photovoltaic solar cells, optical switches and field-effect transistors[7-9]. The performance of these devices is determined by the complex combination of electronic and structural properties of the materials[10]. The electronic band gap of the semiconductor plays an important role in the electron and hole mobility[11] in organic field-effect transistors (OFET's). The interfacial and intermolecular interactions are strong driving forces that influence the final structure of the film, and therefore play a very important role in the properties of electronic devices such as the electroluminescence of some LED's[12-15].

The terrylene (Tr) molecule has a maximum absorption peak at the center of the visible spectra around 570 ± 10 nm, which corresponds to 2.1 ± 0.04 eV (band-gap on silicon, >1 eV). Terrylene has a large extinction coefficient, $\varepsilon \approx 10^5\ M^{-1}cm^{-1}$, and a fluorescence quantum yield close to unity. It is very photostable when it is embedded in solid matrices[16] and polymers[17]. The undistorted terrylene molecule belongs to D_{2h} symmetry, and its planar structure, similar to that of perylene[18-20], makes it an interesting candidate for growing ordered films as well. Thanks to some of these optical, electronic and structural properties, Tr could find some applications as a red pigment or as a semiconductor medium for OFET's[11].

The other very important element in the design of semiconductor devices is the selection of a metallic substrate. Gold has been commonly used as contact material for source and drain electrodes in organic field effect transistors. It is one of the noble metals used as a substrate that presents moderate physisorption interactions with poly-aromatic molecules like terrylene. This is an important property to keep the vibrational and the electronic properties of the deposited molecule as unperturbed as possible[4]. Thus, as the main part of this work we present the characterization of ultra-high vacuum (UHV) deposited films of terrylene on Au (111) surface by means of surface sensitive techniques, mainly with HREELS.

As a very particular aim, we were interested in measuring the energy gap between the ground state and the lowest triplet excited state of terrylene ($S_0 \rightarrow T_1$), as has been done for naphthalene films using HREELS[6]. This information is crucial for the design of the optical experiment that may allow us to switch off the continuous fluorescence photon stream from a single terrylene molecule, by exciting the molecule into this triplet state[21]. In the case of Tr, the energy for the singlet excited state (S_1) is well known[22]. However, to our knowledge, the energy of the lowest triplet state (T_1) has never been measured. The main difficulty in this measurement stems from the weakness of the population yield of T_1 from the excited singlet state, and from the extremely weak yield of the radiative decay (phosphorescence) from the triplet state to the ground singlet state.

We first report the vibrational spectroscopy of terrylene by HREELS. We use different complementary techniques to analyze and discuss the observations, including: Fourier transform infra-red (FTIR) absorption in a KBr pellet doped with Tr in a commercial spectrometer; quantum chemical calculations of terrylene vibrations by DFT B3LYP/6-31G(d,p) method from Deperasińska et al.[23] and the fluorescence spectrum from a single terrylene molecule, in *p*-DCB at 1.5 K[24]. The FTIR spectra showed almost one-to-one correspondence with the HREEL spectrum. However, some fluorescent active modes could also be observed in the HREEL spectrum. Finally, we studied the electronic properties of terrylene films by HREELS and compared to optical spectroscopy.

4.2. Experimental Part

All HREELS experiments were performed in a home-built UHV chamber at a base pressure of 3.0×10^{-10} mbar. A clean Au (111) surface was produced by repeated Ar^+ sputtering cycles and subsequent annealing at 650 °C. The cleanliness of the surface was determined by Auger electron spectroscopy (AES, from 80 - 560 eV) using a single-pass cylindrical mirror analyzer (CMA) with a coaxial electron gun at 2.7 kV (Varian CMSS-981). The presence of a reconstructed Au (111) surface was characterized by LEED with an incident beam energy E_0 = 45 eV. Terrylene powder (purchased from Chiron AS, Norway. Purity 99%) was directly inserted in the Knudsen cell that was separately pumped to 3×10^{-10} mbar. Then, it was baked for 24 hours at 373 K residual pressure of 3×10^{-8} mbar to be outgassed, dried and to eliminate possible carbon-containing compounds of lower molecular weight. The optimal sublimation parameters for terrylene in Au (111) were 469 ± 4 K (196 ± 4°C) at a residual pressure of 8×10^{-10} mbar. Exposure times of ≈ 2 min led to a controlled deposition rate. After each exposure X-ray photoelectron spectroscopy (XPS) and HREELS were recorded one after the other. The α radiation from a Mg source ($h\nu$ =1,253.6 eV) impinge the surface at -20° and the electrons are collected by the Leybold-Heraeus spectrometer under +20° relative to the surface normal. The HREELS experiments were performed with a home-built spectrometer in specular geometry, $\theta_{in} = \theta_{det}$ = can be 53º. The incident beam energy was set at E_0 = 5.0 eV for vibrational spectroscopy and 12 eV for electronic excitation. The

resolution of the spectrometer determined by measuring the FWHM of the elastic peak (loss at 0 meV) was 5 meV and 1.2 meV (40 and 10 cm^{-1}) respectively.

The complete fluorescence spectrum from a single terrylene has been measured using a poly-crystal of *para*-dichlorobenzene (*p*-DCB) as a host-matrix at 1.5 K.[CPC Submitted]. The Fourier-transform infrared spectrum was measured in a commercial FTIR-spectrometer. The sample was a very fine powder of Tr mixed with KBr as excipient, and then pressed to form a thin pellet.

4.3. Results and discussion

4.3.1. Vibrational spectroscopy of Terrylene

When an incident electron beam impacts the surface, the molecule has a probability to be excited to one of the vibrational levels of the ground state. As a result, the scattered electron transfers to the molecule some of its initial energy giving rise to the recorded energy-loss signal in the spectrum.

As a result of the excitation, an oscillating motion of the atoms of the deposited molecule induces a polarization of the gold electrons, creating a surface dipole. For molecular vibrations with atomic displacements perpendicular to the surface plane (out-of-plane modes), the electrostatic images enhance the dipole moment and the transition strength (left side of Scheme 4.1). For molecular vibrations with atomic displacements parallel to the surface (in-plane modes), the electrostatic images suppress the dipole moment (right side of Scheme 4.1). As a result, the intensities of the out-of plane vibrations are enhanced by the induced surface dipole while those of the in-plane vibrations are strongly suppressed as we will discuss along the paper.

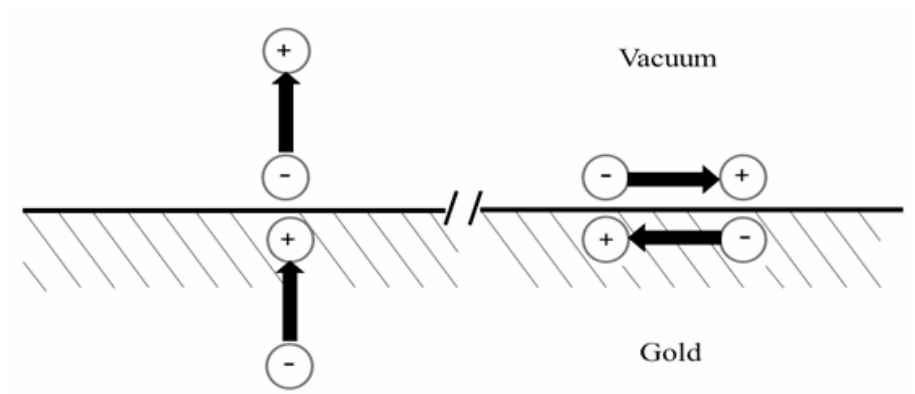

Scheme 4.1: *Shows the effect of electrostatic image charges in the metallic surface on the dipole moments of molecular vibrations. Left: out-of-plane dipole moments are strengthened by the image, enhancing the Coulomb interactions with impinging electrons. Right: for in-plane dipole moments, the image charges shields the field on impinging electrons and the Coulomb interaction with the mode is strongly suppressed.*

Figure 4.1 shows the HREEL (Fig.4.1a), the measured (Fig.4.1b) and the calculated (Fig.4.1c) infrared absorption, and the fluorescence (Fig.4.1d) spectra of Tr measured in the vibrational region from 0-3500 cm^{-1}. In the following, we discuss each of the modes appearing in the HREEL spectrum of a thin film of terrylene (Fig. 4.1a) in increasing frequency and compare to the other spectra. The HREEL spectra were always measured together with the XPS after each exposition time of 2 min.

The first loss signal on the wing of the elastic peak appears at 185 cm^{-1}. Although this region was not accessible to our IR spectrometer, the calculations predict a weakly out-of-plane bending mode, which is IR-active at 181 cm^{-1} and is in very good agreement with the HREEL peak. As expected, this IR-active mode is not observed in fluorescence.

The next loss signal comes at about 259 cm^{-1}. It appears broadened or split. Calculations predict an IR-active mode at 277 cm^{-1}, but also, a totally symmetric (Raman- and fluorescence-active) mode at 246 cm^{-1}. This Raman-mode corresponds to in-plane stretching of the whole molecule[23] along its long axis (strong peak in Fig.4.1d). We could not test whether the calculated IR-active mode appears in the IR spectrum, as our FTIR spectrograph cuts off at 300 cm^{-1}. Therefore, the loss peak at 259 cm^{-1} could arise from either of these modes, or from both.

The next component is a weak and broad (width 80 cm^{-1}) loss peak at 547 cm^{-1}. The corresponding region in the IR absorption spectrum shows multiple peaks at 492, 536 and 560 cm^{-1}. The fluorescence spectrum also shows modes in that region at 496, 542 and 588 cm^{-1}. Because of the low spectral resolution in HREELS (5 meV = 40 cm^{-1}) compared to that on IR absorption spectroscopy (1 cm^{-1}), it is difficult to propose any clear assignment of this broad peak.

The most intense loss peak in the HREEL spectrum around 800 cm^{-1} is observed at very low coverage. We can distinguish a weak shoulder at 690 cm^{-1}, a more intense shoulder at 760 cm^{-1} and the most intense component of all our spectra at resonant frequency of 815 cm^{-1}. The IR spectrum (Fig.4.1b) shows three strong modes at 696, 754 and 808 cm^{-1}. The calculations (Fig.4.1c) predict three modes around 800 cm^{-1}, two of them correspond to out-of-plane modes with frequencies at 765 and 829 cm^{-1} and one at 801 cm^{-1} for an in-plane mode. Figure 4.2 shows the atomic displacements for those three modes ordered by increasing frequency. The fluorescence spectrum shows only one weak peak at 786 cm^{-1}, possibly due to a combination of the long and short-axis deformation modes, corresponding to 544 + 243 cm^{-1} . No other active modes have ever been reported in this region from single molecule fluorescence spectra of terrylene in solid matrices[25-29].

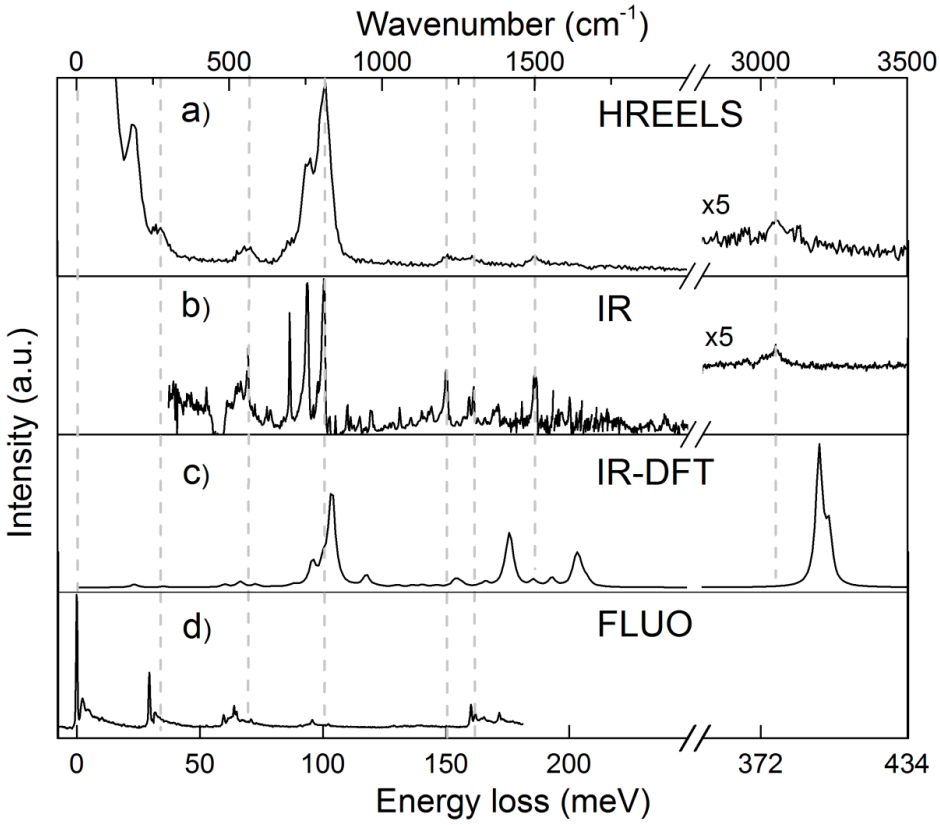

Figure 4.1: *a) specular HREELS of a terrylene film (14 min) on Au (111) recorded with energy beam* E_0 = 5.0 *eV with 5 meV resolution and 30 min acquisition time. b) FTIR of Terrylene in a KBr pellet. c) Calculated IR spectrum considering a FWHM = 25* cm^{-1}*. d) Fluorescence spectrum from one single terrylene molecule at 1.5 K (the zero position corresponds to the zero-phonon line (ZPL) at 577.13 nm or 17327* cm^{-1}*. The dotted lines are guides to follow the peak positions found in each spectrum.*

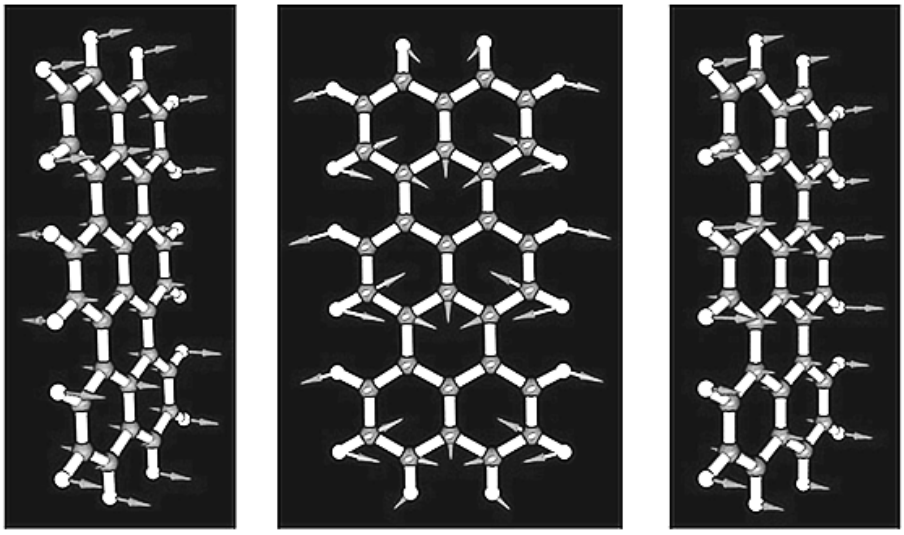

Figure 4.2: *Atomic displacements calculated for molecular vibrations of terrylene at 765 801 and 829 cm^{-1}, from left to right. Those modes might be the ones responsible for the strongest loss peak in EELS experiments. Drawings are made on the basis of calculation results published in [23], for which thank the authors of this work*[23].

The next HREELS signals at 1200 and 1280 cm^{-1} are weak but appear consistently even for very thin films. The corresponding FTIR spectrum presents maxima at 1208 and 1298 cm^{-1}. According to calculations these modes correspond to C-H in-plane wagging. Because the displacements are parallel to the metallic surface, their intensity should be strongly reduced by the electrostatic image effect (Scheme 4.1, right side). In fluorescence, another four in-plane modes appear at higher energies 1272, 1287, 1313 and 1357 cm^{-1}; but these are presumably Raman-active modes.

The next energy interval around 1500 cm^{-1} corresponds to the stretching of the carbon-carbon aromatic bonds. Only one band appears at 1495 cm^{-1} in the HREEL spectrum (Fig.4.1a). The calculations predict several modes within 1300 – 1600 cm^{-1}. Two of them with a significant IR activity are predicted, at 1402 and 1631 cm^{-1}; however a weak one at 1491 cm^{-1} matches the HREEL signal. The measured IR spectrum shows an intense mode at 1496 cm^{-1} in agreement with HREELS and calculations. The fluorescence spectrum does not extend to this frequency area because of the limitation of our spectrometer grating.

Finally, the HREELS shows a weak vibration at 3054 cm^{-1}, which can be attributed to a C-H stretching ν(C-H). This is in good agreement with the FTIR spectrum where this mode appears at 3065 cm^{-1}. However, the DFT calculation finds this mode at 3200 cm^{-1}. The clear frequency difference between calculation and experimental is due to an overestimation of the C-H mode energy, when this mode is used to normalize the whole spectrum, as required in DFT calculations.

All the modes are summarized in Table 4.1. On the whole we notice a fair agreement between the HREEL spectrum and the measured FTIR spectrum, both in position and relative intensity of the bands. It is likely that the HREELS peaks with the highest intensities correspond to out-of-plane modes enhanced by the electrostatic image effect discussed in Scheme 1. Nonetheless, some in-plane modes according to our assignment are visible in the HREEL spectrum and therefore are not completely suppressed by the electrostatic image effect. This may arise from a different excitation mechanism or from molecules that are not completely flat to the surface. Some of the differences in frequencies can arise from the different environments of the molecules, the gold surface in HREELS and the microcrystal environment in the IR KBr pellet measurement.

Table 4.1: *Frequencies (in cm^{-1}) of the main vibrational modes of terrylene found in HREELS on Au (111) surface, measured on terrylene in a KBr pellet by FTIR, calculated IR and fluorescence (or Raman), and from a single-molecule fluorescence spectrum[24], with maximum uncertainty ±5 cm^{-1}.*

Mode assignment	HREELS cm^{-1}	IR cm^{-1}	IR-DFT[23] cm^{-1}	Fluo-DFT[23] cm^{-1}	SMS[24] cm^{-1}
out-of-plane bending	185	-------	181	No active mode	No signal
long-axis stretching	259	-------	277	246	249
short-axis stretching	547	492 536 560	478 528 579	447 544 590	496 522 588
Out-of-plane C-H wagging	690 760 815	696 754 808	765 801 829	No active modes	Very weak 544+246
In-plane C-H bending	1200 1280	1208 1298	1232 1256	No active modes	No peaks
Aromatic C=C stretching	1495	1496 1612	1402 1491 1631	1307 1343 1391 1403	1272 1287 1313 1357
C–H stretching	3054	3065	3200	Not reported	------

In gas phase, fluorescent- (or Raman-) active modes are IR-inactive because of the central symmetry of the molecule[23], therefore "no active mode" is written in the table in case. Dotted lines means not measured due to experimental limitations. "No peaks" corresponds to a part in the spectrum were no components were observed.

4.3.2. HR-EEL spectrum at increasing exposition times

Figure 4.3 shows HREELS spectra for increasing exposure times 14, 30, 70 and 100 min. These spectra display clear changes. The most striking feature in these spectra is the relative intensity decrease of the modes around 800 cm^{-1}, which we assigned to out-of-plane C-H wagging. The decrease in intensity could arise from a different structure of the molecules at larger thickness or from a decrease of the interaction with the surface.

A second feature is the appearance of two new modes for larger thicknesses, at 400 cm^{-1} and around 1090 cm^{-1}. The first one becomes visible after 30 min and stays unchanged at longer exposure times. The second one is in the aromatic stretching area and it could appear because of a change in orientation of the terrylene molecules when the film becomes thicker.

Finally, we observe a shift of the C-H stretch from 3054 cm^{-1} to 2920 cm^{-1}. It is not possible to ensure that these peaks correspond to the same molecular vibration because of the big frequency mismatch. But in case they are the same, the direct change of the electrostatic interaction with the gold surface as the film becomes ticker could explain the frequency shift. As an alternative reason, a different C-H stretch mode could be excited at high thickness because of a different molecular orientation.

From these data, it is hard to understand the origin of the observed spectral changes. But in general, it is likely that the molecules are almost lying flat on the surface at low coverage, but they could rearrange in three-dimensional aggregates at higher coverage. For a better understanding, it will be necessary to probe the structure of the deposited films as a function of thickness, and in particular to determine the orientation of the molecules.

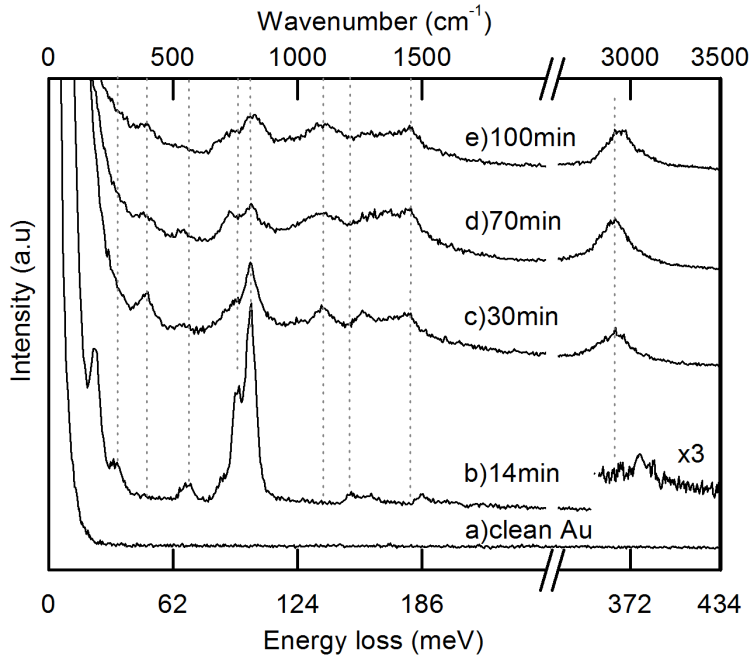

Figure 4.3: *Specular HREELS spectra for increasing terrylene film thickness on top of Au (111). The first spectrum is the base line obtained from a clean Au (111) surface before deposition. The dotted lines are guides to help to follow the peak evolution. The beam energy was* E_0 = 5.0 *eV; and an integration time 30 min.*

4.3.3. EELS probing of electronic excitations of terrylene

Figure 4.4 shows the HREEL spectrum of terrylene thick films for the complete spectral-loss between 0 and 22, 000 cm^{-1}. Intense peaks are clear in the vibrational region between 0 - 4000 cm^{-1} (as discussed in previous sections). Then, it is also possible to distinguish a clear and broad signal in the high-energy loss region between 16,000 and 20,000 cm^{-1} (2.0 and 2.5 eV) which is centered at 18,147 cm^{-1} (2.25 eV). Looking in more detail into this broad feature is it possible to see a maximum loss signal around 2.1 eV. This is in good agreement with the optical spectroscopy (Chapter 3 of this thesis)

and therefore be assigned to the singlet-to-singlet electronic transition. Even further, the other component at 18, 550 cm^{-1} (2.3 eV) agrees with the expected vibro-electronic transition found in the optical spectrum. Next, we look for the spin-forbidden singlet-to-triplet electronic transition of terrylene. This transition has been predicted by quantum chemical calculations to lie at about 8,000±800 cm^{-1} (1±0.1 eV). However, as can be seen in Fig 4.4, no clear signal appears around this interval in the energy loss spectra. It is possible to see a weak feature at 1.8 eV that cannot be assigned to any of the know terrylene electronic states.

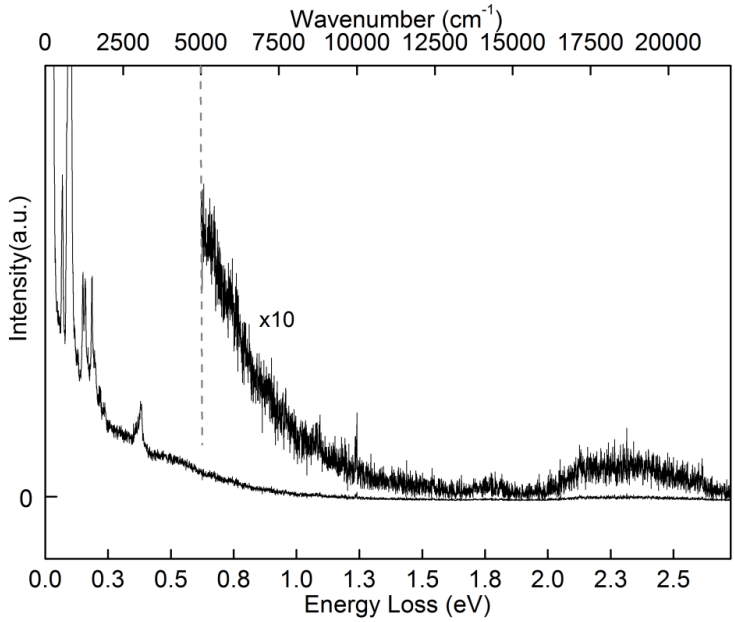

Figure 4.4: *EELS probing of electronic excitations of terrylene. The sample is a thick film (2 hours exposure) of terrylene on Au (111). It was probed with a 12 eV electron beam in specular geometry.*

4.4. Conclusions

HREELS is a surface-sensitive technique which provides information about modes inaccessible by optical means. The selection rules and excitation mechanisms of HREELS are thus complementary to optical spectroscopy. We have succeeded in electronically exciting terrylene to the first excited-singlet state using the HREELS electron beam, but the spin-forbidden transition towards the lowest triplet state remains unknown. The strongest terrylene vibration modes in HREELS appearing around 800 cm^{-1} have never been reported before from fluorescence spectroscopy. The HREEL spectrum agrees fairly well with the IR absorption. With support from calculations, we assign the two strongest modes to C-H out-of-plane wagging (Fig. 4.2). To progress in the assignment of the other HREELS modes, delicate structural studies in the sub-monolayer regime are the natural next steps of this work.

More broadly, we have shown that terrylene is a suitable molecule for controlled deposition in an UHV system. We were able to produce organic films on Au (111) which were stable for many hours of exposure to the electron beam and to X-rays. Terrylene shows a good compatibility and weak interactions with gold which may prove interesting for future organic electronics devices.

4.5. Acknowledgments

We would like to thank to Dr. Irena Deperasinska and Prof. Boleslaw Kozankiewicz, from the Institute of Physics, Polish Academy of Science, Warsaw, Poland for the intense discussions, permission to use the DFT-IR spectrum of terrylene (Figure 4.1c) and the simulated chemical structures used in Figure 4.2 for mode assignment and discussions. We thank Dr. Andreas Köhn, from JGU, Theoretical Chemistry Department on Mainz, who predicted the triplet-state energy of terrylene by DFT calculations (Not published). Special thanks to Anne-Marie Franken, the lab technician in Jülich for the HREELS experiments. This work was supported by the Stichting Fundamenteel Onderzoek der Materie (FOM) project # L2105, which is part of the Nederlandse Organisatie voor Wetenschappelijk Onderzoek (N*W*O).

Reference List

1. Ibach, H.; Balden, M.; Bruchmann, D.; Lehwald, S. Electron-Energy Loss Spectroscopy - Recent Advances in Technology and Application. *Surface Science* **1992,** *269*, 94-102.

2. Tautz, F. Structure and bonding of large aromatic molecules on noble metal surfaces: The example of PTCDA. *Progress in Surface Science* **2007,** *82* (9-12), 479-520.

3. Nakamura, T.; Iwasawa, K.; Kera, S.; Azuma, Y.; Okudaira, K. K.; Ueno, N. Low-energy molecular exciton in indium/perylene-3,4,9, 10-tetracarboxylic dianhydride system observed by electronic energy loss spectroscopy. *Applied Surface Science* **2003,** *212*, 515-519.

4. Shklover, V.; Tautz, F. S.; Scholz, R.; Sloboshanin, S.; Sokolowski, M.; Schaefer, J. A.; Umbach, E. Differences in vibronic and electronic excitations of PTCDA on Ag(111) and Ag(110). *Surface Science* **2000,** *454*, 60-66.

5. Bulovic, V.; Burrows, P. E.; Forrest, S. R.; Cronin, J. A.; Thompson, M. E. Study of localized and extended excitons in 3,4,9,10-perylenetetracarboxylic dianhydride (PTCDA) .1. Spectroscopic properties of thin films and solutions. *Chemical Physics* **1996,** *210* (1-2), 1-12.

6. Swiderek, P.; Michaud, M.; Hohlneicher, G.; Sanche, L. Electron-Energy Loss Spectroscopy of Solid Naphthalene and Acenaphthene - Search for the Low-Lying Triplet-States. *Chemical Physics Letters* **1990,** *175* (6), 667-673.

7. Haas, U.; Thalacker, C.; Adams, J.; Fuhrmann, J.; Riethmuller, S.; Beginn, U.; Ziener, U.; Moller, M.; Dobrawa, R.; Wurthner, F. Fabrication and fluorescence properties of perylene bisimide dye aggregates bound to gold surfaces and nanopatterns. *Journal of Materials Chemistry* **2003,** *13* (4), 767-772.

8. Winder, C.; Matt, G.; Hummelen, J. C.; Janssen, R. A. J.; Sariciftci, N. S.; Brabec, C. J. Sensitization of low bandgap polymer bulk heterojunction solar cells. *Thin Solid Films* **2002,** *403*, 373-379.

9. Kudo, K.; Iizuka, M.; Kuniyoshi, S.; Tanaka, K. Device characteristics of lateral and vertical type organic field effect transistors. *Thin Solid Films* **2001,** *393* (1ΓÇô2), 362-367.

10. Wood, S.; Kim, J. S.; James, D. T.; Tsoi, W. C.; Murphy, C. E.; Kim, J. S. Understanding the relationship between molecular order and charge transport properties in conjugated polymer based organic blend photovoltaic devices. *Journal of Chemical Physics* **2013,** *139* (6).

11. Karl, N. Charge carrier transport in organic semiconductors. *Synthetic Metals* **2003,** *133*, 649-657.

12. Toda, Y.; Yanagi, H. Electroluminescence of epitaxial perylene films. *Applied Physics Letters* **1996,** *69* (16), 2315-2317.

13. Kazmaier, P. M.; Hoffmann, R. A Theoretical-Study of Crystallochromy - Quantum Interference Effects in the Spectra of Perylene Pigments. *Journal of the American Chemical Society* **1994,** *116* (21), 9684-9691.

14. Komolov, S.; Aliaev, Y. Influence of the substrate properties on the electronic structure of organic film-inorganic substrate interfaces. *Technical Physics* **2007,** *52* (9), 1163-1168.

15. Barlow, S. M.; Raval, R. Complex organic molecules at metal surfaces: bonding, organisation and chirality. *Surface Science Reports* **2003,** *50* (6-8), 201-341.

16. Kosciesza, R.; Luzina, E.; Wiacek, D.; Dresner, J.; Kozankiewicz, B. Photo-stability of single terrylene molecules in 2,3-dimethylnaphthalene crystals. *Molecular Physics* **2009,** *107* (18), 1889-1895.

17. Wirtz, A. C.; Dokter, M.; Hofmann, C.; Groenen, E. J. J. Spincoated polyethylene films for single-molecule optics. *Chemical Physics Letters* **2006,** *417* (4-6), 383-388.

18. Unwin, P. J.; Jones, T. S. Vibrational properties of ordered perylene thin films on GaAs(100) and InAs(111)A. *Surface Science* **2003,** *532*, 1011-1016.

19. Gao, L.; Sun, J.; Cheng, Z.; Deng, Z.; Lin, X.; Du, S., X; Gao, H. Structural evolution at the initial growth stage of perylene on Au(111). *Surface Science* **2007,** *601* (15), 3179-3185.

20. Lee, S. K.; Zu, Y. B.; Herrmann, A.; Geerts, Y.; Mullen, K.; Bard, A. J. Electrochemistry, spectroscopy and electrogenerated chemiluminescence of perylene, terrylene, and quaterrylene diimides in aprotic solution. *Journal of the American Chemical Society* **1999,** *121* (14), 3513-3520.

21. Orrit, M. Nano-optics - Quantum light switch. *Nature Physics* **2007,** *3* (11), 755-756.

22. Orrit, M.; Bernard, J.; Zumbusch, A.; Personov, R. I. Stark-Effect on Single Molecules in A Polymer Matrix. *Chemical Physics Letters* **1992,** *196* (6), 595-600.

23. Deperasinska, I.; Zehnacker, A.; Lahmani, F.; Borowicz, P.; Sepiol, J. Fluorescence studies of terrylene in a supersonic jet: Indication of a dark electronic state below the allowed transition. *Journal of Physical Chemistry A* **2007,** *111* (20), 4252-4258.

24. Navarro, P.; Tian, Y.; van Stee, M.; Orrit, M. Stable Single-Molecule Lines of Terrylene in Polycrystalline para-Dichlorobenzene at 1.5 K. *Chemphyschem : a European journal of chemical physics and physical chemistry* **2014,** *15* (14), 3032-3039.

25. Tchenio, P.; Myers, A. B.; Moerner, W. E. Vibrational Analysis of the Dispersed Fluorescence from Single Molecules of Terrylene in Polyethylene. *Chemical Physics Letters* **1993,** *213* (3-4), 325-332.

26. Kummer, S.; Basche, T.; Brauchle, C. Terrylene in P-Terphenyl - A Novel Single-Crystalline System for Single-Molecule Spectroscopy at Low-Temperatures. *Chemical Physics Letters* **1994,** *229* (3), 309-316.

27. Kozankiewicz, B.; Bernard, J.; Orrit, M. Single-Molecule Lines and Spectral Hole-Burning of Terrylene in Different Matrices. *Journal of Chemical Physics* **1994,** *101* (11), 9377-9383.

28. Palewska, K.; Lipinski, J.; Sworakowski, J.; Sepiol, J.; Gygax, H.; Meister, E. C.; Wild, U. P. Total Luminescence Spectroscopy of Terrylene in Low-Temperature Shpolskii Matrices. *Journal of Physical Chemistry* **1995,** *99* (46), 16835-16841.

29. Deperasinska, I.; Kozankiewicz, B.; Biktchantaev, I.; Sepiol, J. Anomalous fluorescence of terrylene in neon matrix. *Journal of Physical Chemistry A* **2001,** *105* (5), 810-814.

CHAPTER 5

Single molecule as a local acoustic detector for mechanical oscillators

A single molecule can serve as a nanometer-sized detector of acoustic strain. Such a nanomicrophone has the great advantage that it can be placed very close to acoustic signal sources and high sensitivities can be achieved. We demonstrate this scheme by monitoring the fluorescence intensity of a single dibenzoterrylene molecule in an anthracene crystal attached to an oscillating tuning fork. The characterization of the vibration amplitude and of the detection sensitivity is a first step towards detection and control of nanomechanical oscillators through optical detection and feedback.

The content of this chapter is published.
Y. Tian, P. Navarro and M. Orrit.
PRL 113, 135505 (2014). Editors suggestion's
Focus article, in Physics 7, 98 (2014) | DOI: 10.1103/Physics.7.98

5.1.Introduction

Acoustic vibrations are central to communication in our daily lives, but also form the basis of many technologies such as sonar, seismography or ultrasound medical imaging. The main advantage of acoustic waves is their faculty to propagate in media which absorb or scatter electromagnetic waves. A major drive to achieving smaller, faster and, more sensitive sound detectors is the perspective of generating, detecting and controlling sound at nanometer scales, which would open new avenues for acoustic microscopy[1,2], as well as for manipulation and cooling of acoustic degrees of freedom down to the quantum regime[3]. Single gold nanoparticles have been shown to be sensitive vibration detectors in solution[4]. In recent years, thanks to spectacular progress in nanoscience, nanometer-scale oscillators have been applied to accurate mass measurements down to the mass of single atoms, and to bacterium screening[5,6]. Nanomechanical oscillators are promising candidates as quantum systems that can be manipulated. The vibration amplitude and phase, and even the quantum state of a nanomechanical oscillator could be read through coupling to a quantum system such as a qubit, an optical cavity, a single-electron transistor, a SQUID or a point contact between two conductors[7-10]. Recently, Puller *et al.* have put forward the theoretical possibility to detect the displacement and to manipulate the state of a nanomechanical oscillator through the optical fluorescence signal of a single molecule[11]. The aim of this chapter is to demonstrate such detection experimentally, and to provide measurements of the sensitivity in a well-controlled and well-understood case. The oscillator will be a quartz crystal tuning fork, causing mechanical deformations of the host crystal around the molecule under optical study.

To selectively detect individual molecules, the molecules have to be separated from each other[12,13]. At cryogenic temperature and in suitable rigid matrixes, the absorption spectrum of a molecule presents an extremely narrow electronic transition that occurs without any creation or annihilation of phonons, and is therefore called the zero-phonon-line (ZPL). Its linewidth is chiefly determined by the lifetime of the excited state and lies in the range of 10-50 MHz for many well-studied host-guest systems[13-19]. Because of its sharpness, the ZPL is extremely sensitive to the molecule's local environment. The frequency of the ZPL can be shifted by mechanical strains or electric fields, including those caused by local degrees of freedom still

active at the cryogenic temperature of the experiment. Such dynamics lead to spectral diffusion or to spectral jumps of the ZPL[20-22], and should therefore be eliminated or minimized for sensing applications. For example, the ZPL is very sensitive to librations of any methyl groups present in the host matrix[23]. Static hydrostatic pressure is also a well-known factor which shifts the ZPLs of single molecules[24-27]. The present work also relates to an earlier discovery by our group of acoustic modes localized at defects of the anthracene crystal[28]. Here, the tuning fork may be regarded as a well-known and well-controlled replacement for one of these localized modes. As we will see, its effects on the single-molecule lines are very comparable to those of the localized defect oscillators described previously.

The sensitivity of a molecular ZPL to the environment has its origin in the short-range interactions between the guest molecules and its first shells of host neighbors. Any variation of the respective positions of the guest and the host molecules induces a shift of the ZPL. Acoustic waves generated by a mechanical oscillator in contact with the sample will couple to the molecular transition and shift the ZPL of the guest molecule. We can thus use a single molecule to detect the local vibrations by monitoring the instantaneous frequency of its ZPL. In the present work, we chose single dibenzoterrylene (DBT) molecules embedded in an anthracene (Ac) crystal because of the stability of their ZPL, of their lifetime-limited linewidth and of their convenient wavelength[16].

5.2.Experimental

The Ac single crystal doped with DBT molecules was glued to a quartz crystal tuning fork with a well-defined resonant oscillation frequency and high quality factor (Q factor), as shown in Fig. 5.1a. By electrically driving the tuning fork, the crystal is stretched or compressed periodically at the driving frequency. Such periodic vibrations change the average distance between molecules inside the crystal. The ZPLs of DBT molecules thus shift correspondingly, as shown in the cartoon of Fig. 5.1. Of course, the deformations of the molecular surroundings are much more complicated in reality and may involve fork's bending, shearing, and molecular

distortions. Any of these deformations, however, will give rise to a periodic shift of the molecular ZPL at the wave's frequency.

When the excitation laser is tuned to the wing of the ZPL as indicated by the dashed vertical line in Fig. 5.1b, a shift of the ZPL changes the molecular absorption and thereby the measured fluorescence intensity. In this way, the molecule's fluorescence can be used as a probe to read out the vibration amplitude, phase and frequency of the tuning fork, by monitoring time-dependent changes in the fluorescence intensity.

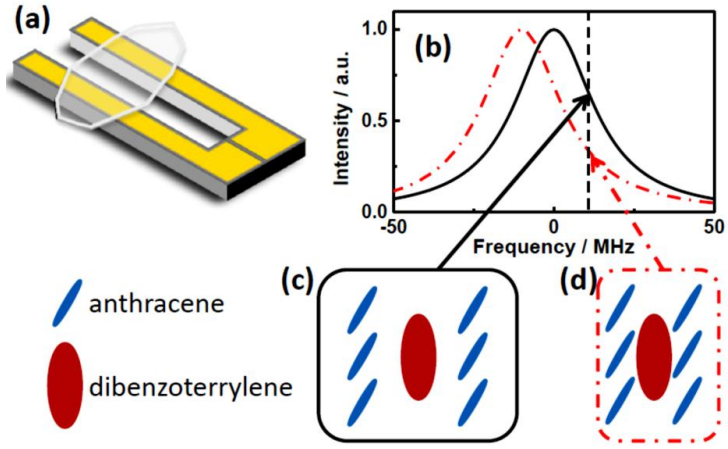

Figure 5.1: *(a) Sample mounting: an anthracene crystal doped with DBT was attached to the quartz crystal tuning fork; (b) the ZPL of a single DBT molecule is shifted upon deformation of its surrounding host crystal, as shown in (c) and (d). The real deformations are three-dimensional and much more complicated, as molecules can also rotate and be distorted.*

First, we characterized the tuning fork optically using the experimental set up described in Scheme 5.1. The excitation laser was focused on the edge of one of the tuning fork prongs. The reflected light was collected and detected by a photodiode, providing a signal modulated at the oscillating frequency of the tuning fork[29]. The lock-in signal thus provides the modulation amplitude of the reflected light at the oscillation frequency of the tuning fork.

For the bare tuning fork in vacuum at 1.5 K, a sharp peak was obtained at frequency of 32.709 kHz with high Q factor of about 40,000 (Fig.5.2d), corresponding to the fundamental flexion mode (symmetrical oscillation of the two prongs)[30]. When the sample crystal was attached, the oscillation of the tuning fork was strongly shifted and damped. Depending on the details of the contact between

the crystal and the fork, the frequency shift could be positive or negative. The Q-factor was always lowered by the crystal. Surprisingly, three peaks rather than a single peak were observed in the range from 10 kHz to 50 kHz, as shown in Fig. 5.2c. Certain crystal defects can present acoustic modes at these frequencies, as was reported in reference[28].

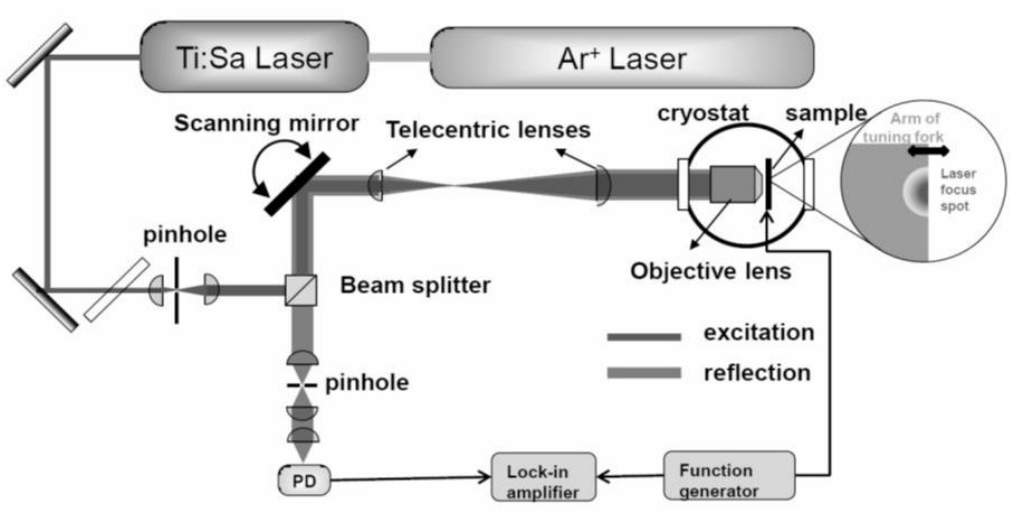

Scheme 5.1: *Diagram of the confocal microscope used for the reflection measurements. The laser beam spot was focused on the edge of the tuning fork prong as shown in the insert. PD stands for photodiode.*

However, our present experiments directly monitor the oscillation of the tuning fork and are therefore less sensitive to localized crystal modes. In addition, we did not observe any significant temperature dependence for these additional modes. We thus assign them to additional deformations of the tuning fork-crystal system, in addition to the strongest resonant peak located at 20.091 kHz which we attribute to the damped fundamental flexion mode. Theoretical calculation and modeling would be needed for a better understanding of the additional modes.

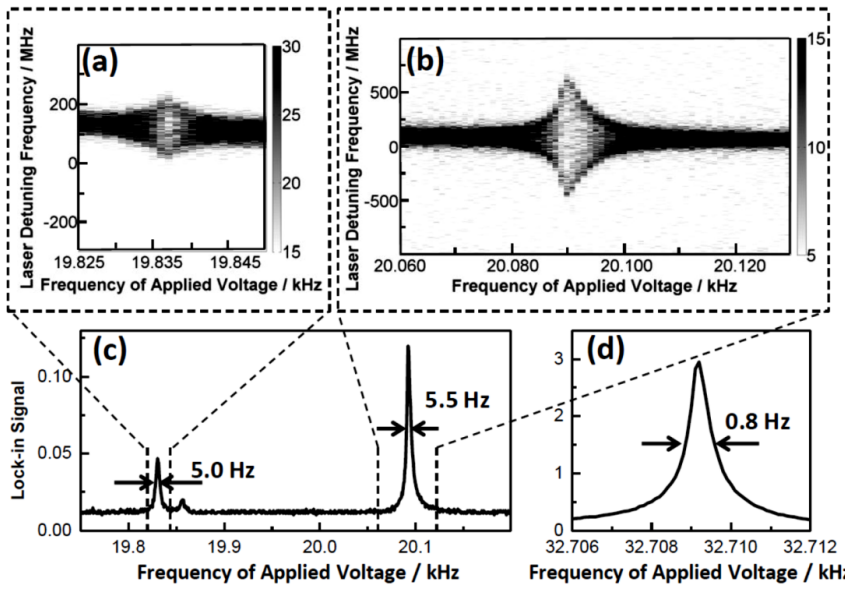

Figure 5.2: a) *Spectral trail of a single DBT molecule as a function of the driving frequency (a) from 19.820 kHz to 19.850 kHz or (b) from 20.060 kHz to 20.130 kHz. The driving voltage was 0.8 V. Lock-in signal of the reflection light intensity from the tuning fork with sample attached (c) and from the bare tuning fork (d). The asymmetry of the main resonance around 20.090 kHz (c) is due to the anharmonicity of the tuning fork's oscillation. All the measurements were done in vacuum at 1.5 K.*

5.3.Results and Discussion

Spectral trails of a single DBT molecule were obtained by repeatedly scanning the laser frequency (2 GHz, 3 s/scan) while slowly varying the driving frequency on the tuning fork (19.820 kHz to 19.850 kHz and 20.060 kHz to 20.130 kHz). Because of the limited fluorescence rate and time resolution, we could not directly monitor the oscillation of the ZPL shift. Instead, the periodical shift of the ZPL was observed as a broadening of the molecular line. As shown in Fig. 5.2a and 5.2b, the broadening of the molecular ZPL resonated at the specific frequencies found by monitoring the displacement of the tuning fork (Fig.5.2c). These results are evidence of the coupling between the DBT molecule and the vibrations generated by the tuning fork in the anthracene crystal. The slight asymmetry of the main peak is observed both on the lock-in signal from the fork (Fig. 5.2c) and on the molecular fluorescence (Fig.5.2b). It is due to a frequency shift at high oscillation amplitudes and indicates anharmonicity of the tuning fork's oscillations. We studied the distortions of the resonance line with the oscillation amplitude, and found that the anharmonic effect is much more pronounced by the presence of the crystal. Similar observations were made on the localized acoustic defect modes[28].

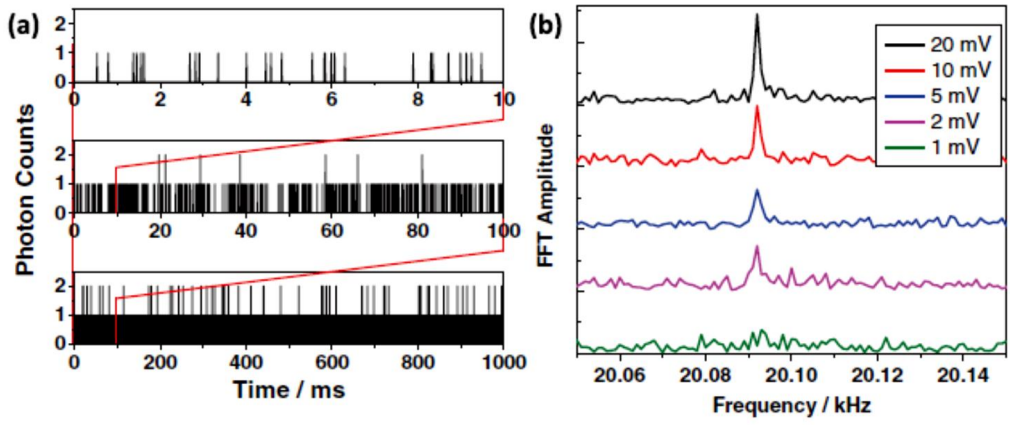

Figure 5.3: *(a) Fluorescence intensity trace of a single DBT molecule (3,300 counts/s) and (b) Fourier transforms of such recordings when the tuning fork was driven at its resonant frequency (20.091 kHz), for various driving voltages (1 mV to 20 mV). The sharp peak at 20.091 kHz*

indicates the modulation due to coupling to the tuning fork. This signal becomes comparable to noise at a driving voltage of 1 mV.

To estimate the detection sensitivity of a single molecule, we fixed the laser frequency to the half maximum position of the ZPL (as shown by the dashed line in Fig. 5.1b) and monitored the fluorescence photons from the molecule by time-tagged single-photon-counting when the tuning fork was driven at resonant frequency (20.091 kHz). The conted photons with bin size of 10μs over 10ms, 100ms and 1s are shown in Fig.5.3a. Because of the low fluorescence signal, we cannot directly see the modulation of the fluorescence intensity trace, not even for the largest oscillation amplitude. However, a fast-Fourier transform (FFT) of the fluorescence intensity trace reveals the weak modulation, as shown in Fig. 5.3b for different oscillation amplitudes. Note that, in spite of the random distribution of single photon detection events, the FFT picks up the weak modulated component unambiguously, just as a lock-in detection would filter an analog signal. The sharp peaks represent the driving frequency (their linewidth is determined by the function generator). The FFT signal amplitude varies linearly with the driving voltage, i.e., with the tuning fork's oscillation amplitude. As a consequence, the FFT signal can no longer be distinguished from noise, for about 1 mV driving voltage with an integration time of 1 s.

Hereafter, we discuss the detection sensitivity following the reasoning and notations of Puller et al.[11]. We measure the oscillator's displacement in relative deformation of the host lattice $\varepsilon = \delta x / x$ rather than the absolute displacement of the nanotube's tip as reported[11]. The sensitivity is determined by the smallest deformation detectable over a time t against shot noise fluctuations of the fluorescence signal, $\sqrt{It}$, where I is the fluorescence rate.

The shift of the molecular frequency is given by

$$\delta\nu = \varepsilon \frac{d\nu}{d\varepsilon}.$$

It gives rise to an intensity change

$$\delta I = I\delta\nu / \Gamma ,$$

where Γ is the linewidth (30 MHz in previous experiments, 80 MHz in our case).

The minimum deformation value at which the signal overcomes the photon noise is thus:

$$\varepsilon_m = \Gamma \frac{d\varepsilon}{d\nu}\sqrt{\frac{t}{I}} .$$

The elastic modulus of anthracene crystal is $E \sim 10^{10}$ N/m^2 corresponding to 10^5 bar. [31,32] The frequency shift induced by pressure change is reported[24] to be ~ 1 GHz/bar, i.e. a 1 GHz shift corresponds to a lattice deformation $\varepsilon = 10^{-5}$.

The coupling constant, corresponding to a change of frequency of the molecular transition per relative deformation of the crystal lattice is thus about

$$\frac{d\nu}{d\varepsilon} = 10^{14} \text{ Hz.}$$

Therefore, the typical values in single-molecule spectroscopy give, a deformation of 1 ppb/$\sqrt{\text{Hz}}$

$$\varepsilon_m = 10^{-9}\sqrt{t}$$

With a low fluorescent rate of 3300 counts/s and a broad linewidth in our experiment, we would expect a sensitivity of about 1.4×10^{-8} Hz$^{-1/2}$. However, the experimental detection limit is rather 7×10^{-7} Hz$^{-1/2}$. We attribute this difference of a factor 50 to the background mechanical vibrations generated by the noisy environment of our cryostat. Indeed, a noise background appears in the FFT of the intensity trace. This noise background was also observed in the reflection measurement where no molecular spectroscopy was involved. Therefore, the oscillations of the tuning fork are driven by these noise sources.

We estimated the energy of these background oscillations. For this, we need the minimum detectable oscillation amplitude of the prongs, which was 0.1 nm. So the oscillation energy associated with this amplitude, can be deduced from the spring constant of the tuning fork

(k = 10 000 N/m), to be around 10^{-17} J and found them to be much larger than thermal fluctuations (10^{-23} J) expected at our experimental temperature (1.5 K). These vibrations ought to be eliminated to reach the shot-noise limited sensitivity of our single-molecule acoustic detector.

We now discuss the theoretical detection limits for various oscillators. But first, we need to estimate the amplitude of the tuning fork with crystal under the experimental conditions. Assuming that the edges of the prongs are similar, the displacement of the prong would be linear with the lock-in signal. We then estimate the displacement of 0.14 nm/mV from the slope of the linear fit, by comparing the lock-in signal for the bare tuning fork and the tuning fork with crystal.

It is worth to note that the edge of the tuning fork is not perfectly sharp at the nanometer scale. In this experiment, we have made some assumptions: 1) the focal spot has the same size for the bare tuning fork and for the tuning fork with crystal; 2) the edges of the prongs for both cases are the same; 3) by keeping the reflection intensity the same, we assume that the effect of laser power is excluded; 4) the lock-in signal is linearly dependent on displacement and linearly dependent on the driving voltage in this range.

Now that we know the vibration amplitude of the tuning fork's prongs, and that linearly depends on the driving voltage[33-35], we can estimate the experimental sensitivity of the fork prong's displacement to be 0.14 nm/$\sqrt{\text{Hz}}$.

Thus, in our experiments, the detection sensitivity is 0.14 nm/$\sqrt{\text{Hz}}$, corresponding to a relative deformation of the host lattice of 7×10^{-7} (crystal size 200 μm).

If the shot-noise-limited sensitivity is achieved, much weaker displacements still are detectable with the molecule. Assuming the oscillation to be a mode delocalized over the whole crystal, typically 100 μm in size (as presented in previous work[28]), the detectable displacement would be about 1.4 pm/$\sqrt{\text{Hz}}$ in our present conditions, and would reach 100 fm/$\sqrt{\text{Hz}}$ with improvements in the fluorescence collection efficiency.

A nano-oscillator with 10 nm in size located around the molecule would give a sensitivity of 10 am/$\sqrt{\text{Hz}}$. This sensitivity exceeds that of the device proposed by Puller et al. based on an oscillating carbon nanotube placed in the vicinity of the molecule[11].

Another important feature of our acoustic detector is its time resolution. The frequency of nanomechanical oscillators covers a large range from MHz to THz[36,37]. The time resolution of our current setup is limited to 25 MHz by the dead time of our photodetector. Even with faster photodetector, the time resolution will be limited to some hundreds of MHz by the fluorescence lifetime of the molecules. Higher bandwidths would require faster emitters, for example molecules coupled to plasmonic antennas.

As a final remark, we rule out the possibility of a Stark shift of the molecular transition due to the applied electric field for driving the tuning fork[38,39]. Indeed, Fig. 5.2 shows that the resonant acoustic effect is much larger than the frequency-independent Stark effect. Moreover, we can estimate the electric field created around the molecule to be 5 kV/m, for an applied voltage of 0.8 V on the tuning fork. Such a weak field cannot induce a significant Stark effect on the molecule[28,39]. The observed ZPL shift of the DBT molecule is therefore exclusively due to the mechanical coupling between the molecule and the tuning fork.

5.4.Conclusion

In conclusion, we measured the coupling of a single organic molecule to acoustic strain generated by a macroscopic mechanical oscillator. Exciting the fluorescence at half-maximum gave rise to an intensity modulation of the fluorescence intensity trace. Such a weak was successfully detected trough a fast Fourier transform that works as a lock-in amplifier for a digital signal. The sensitivity threshold to relative deformation reached in our current experiments was about 7×10^{-7} $\text{Hz}^{-1/2}$, limited by mechanical experimental noise. However, for a shot-noise-limited detection of the vibrations of a nanomechanical oscillator, the sensitivity should reach the level of 1 fm/$\sqrt{\text{Hz}}$, comparable to the theoretical sensitivity proposed by Puller et al[11]. Such a high sensitivity is promising for reading out the quantum states of nanomechanical devices. Even though the detection sensitivity is not exceptionally high compared to other techniques, the main advantage of single-molecule detection is the small size of the sensor (sub-

nanometer in size). These small probes can be placed in the elastic strain field of the oscillator, enabling high coupling to artificial nanomechanical oscillators[11] or to natural oscillators found around defects in crystals[28] and defects in disordered solids[42].

Acknowledgements

This work is supported the Stichting voor Fundamenteel Onderzoek der Materie (FOM), which is part of the Dutch Science Funding Organization NWO.

Reference List

1. Dunn, F. Ultrasonic Absorption Microscope. *J. Acoust. Soc. Am.* **1959,** 31**,** 632.
2. R. G. Maev, *Acoustic Microscopy* (Wiley-VCH Verlag GmbH & Co. KGaA, Weinheim, Germany, **2008**).
3. J. Gieseler, B. Deutsch, R. Quidant, and L. Novotny, *Phys. Rev. Lett*. **109,** 103603 (**2012**).
4. A. Ohlinger, A. Deak, A. A. Lutich, and J. Feldmann, Phys. Rev. Lett. **108,** 018101 (**2012**).
5. Calleja, and J. Tamayo, *Nat. Nanotechnol*. **2010,** 5, 641.
6. G. Longo, L. Alonso-Sarduy, L. M. Rio, A. Bizzini, A. Trampuz, J. Notz, G. Dietler, and S. Kasas, *Nat. Nanotechnol*. **2013,** 8, 522.
7. N. Flowers-Jacobs, D. Schmidt, and K. Lehnert, *Phys. Rev. Lett*. **98,** 096804 (**2007**).
8. S. Etaki, M. Poot, I. Mahboob, K. Onomitsu, H. Yamaguchi, and H. S. J. van der Zant, *Nat. Phys.* **2008,** 4, 785.
9. R. G. Knobel and A. N. Cleland, *Nature***. 2003,** 424, 291.
10. M. D. LaHaye, J. Suh, P. M. Echternach, K. C. Schwab, and M. L. Roukes, *Nature*. **2009,** 459, 960.
11. V. Puller, B. Lounis, and F. Pistolesi, *Phys. Rev. Lett*. **110,** 125501 (**2013**).
12. W. E. Moerner and M. Orrit, *Science*. **1999,** 283, 1670.

13. M. Orrit and J. Bernard, *Phys. Rev. Lett*. **65**, 2716 (**1990**).
14. A.-M. Boiron, F. Jelezko, Y. Durand, B. Lounis, and M. Orrit, *Mol. Cryst. Liq. Cryst. Sci. Technol. Sect. A.* **1996,** 291, 41.
15. F. Jelezko, P. Tamarat, B. Lounis, and M. Orrit, *J. Phys. Chem*. **1996,**100, 13892 ().
16. A. A. L. Nicolet, C. Hofmann, M. A. Kol'chenko, B. Kozankiewicz, and M. Orrit, *ChemPhysChem* **2007,** 8, 1215.
17. A. A. Gorshelev, A. V Naumov, I. Y. Eremchev, Y. G. Vainer, L. Kador, and J. Köhler, *ChemPhysChem*. **2010,** 11, 182.
18. A. Walser, A. Renn, S. Götzinger, and V. Sandoghdar, *Chem. Phys. Lett*. **2009,** 472, 44.
19. P. Navarro, Y. Tian, M. van Stee, and M. Orrit, *Chem.Phys.Chem.* **2014,** 15, 3032-3039.
20. W. P. Ambrose and W. E. Moerner, *Nature*. **1991,** 349, 225.
21. T. Basché, S. Kummer, and C. Bräuchle, *Nature*. **1995,** 373, 132.
22. F. Kulzer, S. Kummer, R. Matzke, C. Brauchle, and T. Basché, *Nature.* **1997,** 387, 688.
23. Y. Tian, P. Navarro, B. Kozankiewicz, and M. Orrit, *ChemPhysChem***. 2012,** 13, 3510.
24. A. A. L. Nicolet, P. Bordat, C. Hofmann, M. A. Kol'chenko, B. Kozankiewicz, R. Brown, and M. Orrit, *ChemPhysChem*. **2007,** 8, 1929.
25. M. Croci, H.-J. Müschenborn, F. Güttler, A. Renn, and U. P. Wild, *Chem. Phys. Lett.* **1993,** 212, 71.
26. T. Iwamoto, A. Kurita, and T. Kushida, *Chem. Phys. Lett.* **1998,** 284, 147.
27. A. Müller, W. Richter, and L. Kador, *Chem. Phys. Lett.* **1995**, 241, 547.
28. M. A. Kol'chenko, A. A. L. Nicolet, M. D. Galouzis, C. Hofmann, B. Kozankiewicz, and M. Orrit, *New J. Phys.* **2009,** 11, 023037.
29. D. van Vörden, M. Lange, M. Schmuck, N. Schmidt, and R. Möller, Beilstein *J. Nanotechnol.* **2012,** 3, 809.
30. J.-M. Friedt and E. Carry, *Am. J. Phys.* **2007,** 75, 415.
31. R. C. Dye and C. J. Eckhardt, *J. Chem. Phys.* **1989,** 90, 2090.
32. H. B. Huntington, *J. Chem. Phys.* **1969,** 50, 3844.
33. A. Castellanos-Gomez, C. R. Arroyo, N. Agraït, and G. Rubio-Bollinger, *Microsc. Microanal.* **2012,** 18, 353.
34. P. Sandoz, J.-M. Friedt, and E. Carry, *Rev. Sci. Instrum.* **2008,** 79, 086102.

35. A. G. Ruiter, K. O. van der Werf, J. A. Veerman, M. F. Garcia-Parajo, W. H. Rensen, and N. F. van Hulst, *Ultramicroscopy.* **1998,** 71, 149.
36. G. Anetsberger, O. Arcizet, Q. P. Unterreithmeier, R. Rivière, A. Schliesser, E. M. Weig, J. P. Kotthaus, and T. J. Kippenberg, *Nat. Phys.* **2009,** 5, 909.
37. V. V. Temnov, *Nat. Photonics.* **2012,** 6, 728.
38. M. Orrit, J. Bernard, A. Zumbusch, and R. I. Personov, *Chem. Phys. Lett.* **1992,**196, 595.
39. C. Brunel, P. Tamarat, B. Lounis, J. C. Woehl, and M. Orrit, *J. Phys. Chem. A*. **1999**, 103, 2429.
40. Y. Vainer, A. Naumov, M. Bauer, and L. Kador, *Phys. Rev. Lett.* **97**, 185501 **(2006).**

CHAPTER 6

Lifetime-limited excitation linewidths from single perylene molecules at 1.5 K

Lifetime-limited lines were never reported before for perylene. We have investigated single perylene molecules in *ortho*-dichlorobenzene (*o*-DCB) by fluorescence excitation spectroscopy at 1.5 K. Several different hosts were systematically tested before deciding for *o*-DCB as a promising host. We found excitation lines of 20 MHz width which agrees with the expected value corresponding to a fluorescence lifetime of 7 ± 2 ns. Detected emission rates in the order of 6×10^4 count/s have been obtained at saturation. The observation of stable narrow lines showed a strong dependence on the sample history. Because the system is a liquid mixture at room temperature, it is possible to fill long glass capillaries. This system could be used as the first source of single photons from a molecule in the blue part of the electromagnetic spectrum, between 445 and 450 nm.

6.1. Introduction

Stable and lifetime-limited quantum emitters are of fundamental importance for the development of quantum optics and nanophotonics. The emitted photons within the zero-phonon line are indistinguishable[1,2] and their resonance can be tuned by Stark-effect when applying an electric field[3]. Once spectrally filtered, the single photons from the ZPL have been used to perform spectroscopy on a second single molecule[4], to excite plasmonic structures[5], to interface with alkali atoms[6] and lately have been proposed to excite or cool nano-mechanical resonators down to their ground state[7]. However, the chemical and physical properties of the host play a crucial role in the optical properties of the fluorescent single molecule.

In order to observe stable molecule lines, the coupling between the host phonon bath and the electronic transition of the quantum system has to be optimized. This has been achieved for organic single crystals such as naphthalene[8], *para*-terphenyl[9,10] or anthracene[11] that were co-sublimated with selected dyes. These crystals have no active optical phonons at 1.5 K that interact with the dye vibrational modes. Besides the weak phonon coupling, the crystalline environment of the host induces well-defined insertion sites with a polarized emission[12] in single crystals because guest molecules are aligned[13]. Lately, the same host-guest systems have been prepared by simply melting or spin coating the mixture instead of the more complicated co-sublimation. The results show still lifetime-limited linewidths[14,15] but due to the poly-crystallinity in such systems, the orientation is random, and the inhomogeneous distribution is clearly broadened.

The next most extensively studied hosts for SMS have been Shpol'skii matrices in which spectral hole-burning experiments had shown narrow spectral features. The size matching between the length of the host alkane chain and the length and width of the guest dye turned out to be a very important parameter in the observed stability of single molecules, as tested systematically for many systems[16-20]. Lifetime-limited linewidths can be obtained, but at the same time clear spectral jumps and broad inhomogeneous distributions were observed. The apparent reason for inhomogeneous distribution was

that in case of size mismatch between host-guest, the insertion sites of the guests were not very well defined. The spectral jumps evidence the presence of interacting two-level systems (TLS's) which can be created from tunneling or from hindered rotations of the methyl groups between alkane molecules.

Doped-polymers could find applications for the development of flexible electronic devices such as organic field-effect transistors (OFET's) [18,21-23]. The optical isolation of single molecules in polymers thus provides nanometer-scale probes of the structure and dynamics of these important materials. However, it is well known that amorphous hosts present a variety of spectral diffusion processes. When spectral diffusion is faster than the experimental recording time, the excitation line is broadened. For slow spectral diffusion, discontinuous spectral jumps of the resonant frequency of a single molecule up to 10-1000 MHz can be observed, which are sometimes reversible.

Over more than 20 years of single-molecule spectroscopy at low temperature, many host-guest systems have been discovered and studied. The main suitable dyes with high fluorescence quantum yield, photo-stability and low ISC that are commonly used in single molecule spectroscopy (SMS) range in frequency from the near infrared with dibenzoterrylene (785 nm, DBT) towards higher transition energies with terrylene diimide (630 nm, TDI,), pentacene (592 nm, Pc), dibenzanthanthrene (590 nm, DBATT), tertbutyl-terrylene (580 nm, TBT), terrylene (572 nm, Tr), perylene diimide (500 nm, PDI), perylene (445 nm, Pr), and diphenyloctatetraene (400 nm, DPOT).

Perylene is the only dye for which lifetime-limited lines have not yet been reported. Perylene has been studied in the organic crystals biphenyl and anthracene[24]. In biphenyl[25], spectral diffusion caused broadening of the lines between 140 - 300 MHz. When anthracene was used as a host, no fluorescence could be detected[24]. This result has been attributed to an "intermolecular" intersystem crossing (ISC) process from the singlet (S_1) of perylene to the triplet (T_1) of the host that quenches the fluorescence. A similar result was reported for terrylene in anthracene[26]. However, this latter process enabled the detection of phosphorescence from the triplet of perylene after a "reverse intermolecular"

ISC, which has not been reported from a direct measurement[24]. Reports on perylene in *n*-nonane (C_9) matrix showed clear spectral jumps[27]. In spite of these jumps, the stability of the lines was sufficient to measure the linear shift of the lines in response to an applied electric field in a Stark-effect experiment[28]. Perylene was also studied in *n*-heptane (C_7) by persistent hole burning showing 1 GHz holes[29]. In particular perylene was studied in polyethylene[30,31] (PE) showing a variety of spectral diffusion effects for the first time. Fast spectral diffusion induced a broadening of the excitation lines from 50 to 140 MHz and TLS caused discontinuous jumps in the order of 10-1000 MHz on a slower time scale.

Despite extensive efforts towards isolating perylene single molecules with lifetime-limited lines and high spectral stability, no proper host has ever been reported. Here we present our observations of single perylene molecules in *ortho*-dichlorobenzene at 1.5 K. We report the systematic procedure we followed to determine *o*-DCB as a suitable matrix to perform SMS experiments. The sample preparation plays a crucial role in the observation of narrow lines of single perylene molecules.

6.2. Experimental

The sample precursor can be prepared by mixing the desired amount of perylene in the required amount of host (*o*-DCB) as the solvent. The solubility of perylene in *o*-DCB can reach mM concentrations. We start with a 100 μM solution concentration and dilute till we reach 0.01 μM or a lower concentration depending in the experiment. Figure 6.1 shows the type of samples that can be prepared with this mixture. Samples made with capillaries (b, c, d) were more suitable for SMS experiments than those in between glass slides. Also, the use of capillaries allowed us to put more than one sample (i.e. different concentrations) in the sample holder and study them in the same cooling cycle. At room temperature, *o*-DCB is a liquid but solidifies below -18°C (255K) forming a crystalline phase with monoclinic unit cell[32].

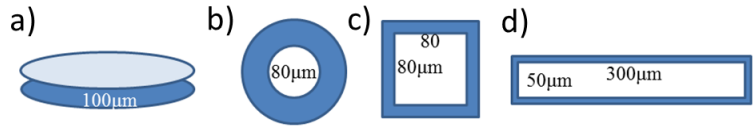

Figure 6.1: *Two coverslips (2.5 cm diam.) to produce a film as thin as 10 µm, a cross section of a cylindrical glass capillary (b) of a squared capillary (c) and of a rectangular capillary (d).*

All the experiments were performed in a home-built confocal fluorescence microscope. The objective (Microthek, 60x, N.A = 0.85) is mounted inside the cryostat in inverted geometry. Confocal fluorescence imaging was performed by spatially scanning the excitation beam over the sample at a fixed frequency. By using a piezo-actuated mirror (New-Port) and a tele-centric system (described in Fig. 6.2a) a maximum field of view of $150 \times 150\ \mu m^2$ is achieved. An avalanche phothodiode (SPCM-AQR - 16) in confocal geometry is used to record the fluorescence signal. When required, a flip mirror can be set in the collection path, and the fluorescence signal is sent then into a multi-mode optical fiber which is coupled to a Princeton Instruments i500 spectrograph to record the spectrum (150 or 300 grooves/mm).

In order to perform wide-field illumination microscopy, a third lens (Fig 6.2) is introduced before the scanning mirror to collimate the excitation beam over the sample. For detection, a CCD camera with a maximum image acquisition rate of 65 kHz (Orca 4.0 from Hamamatsu) is accessible by placing a flip mirror on the detection path instead of the APD.

a)

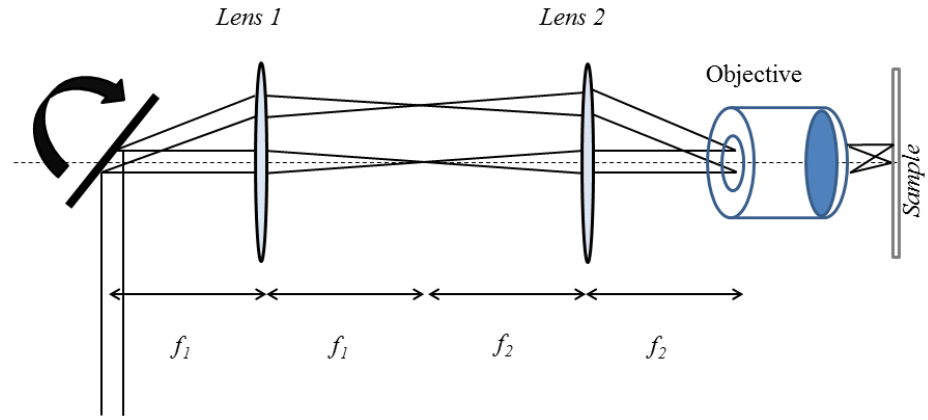

b)

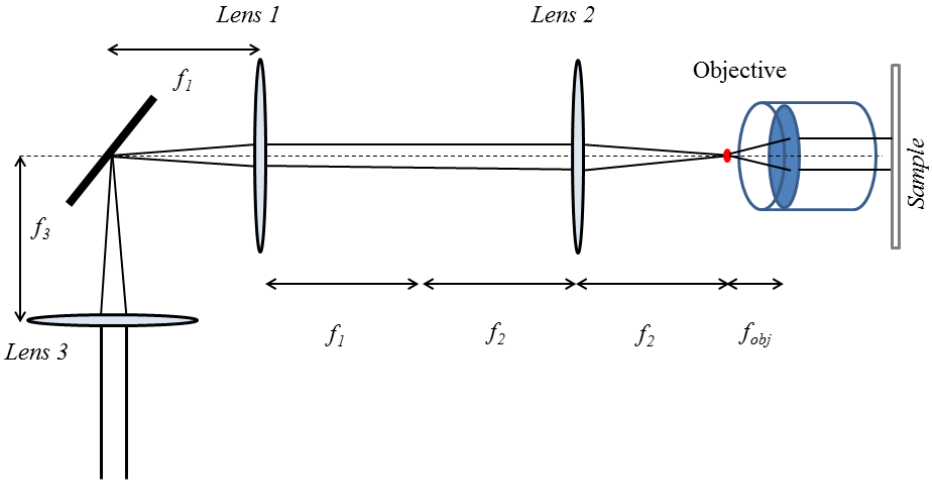

Figure 6.2: *a) Telecentric system for beam-scanning on a confocal microscope. The scanning mirror is mounted on a galvanometric stage (10 V). The focal lengths are: f_1 = 10 cm, f_2 = 20 cm and for the objective, f_3 = 3 mm. The set-up has a magnification of $M = f_1 / f_{obj} = 6$. b) Wide-field illumination set up. Lens 3 focuses the beam at the center of the mirror, and this is at the focus of lens 1.*

The excitation laser source is selected according to the kind of experiment to be performed. The bulk fluorescence spectrum of all the host guest systems here, were collected by exciting with a broad band laser at 405 nm because it allows for recording the complete spectrum. For the fluorescence excitation line-narrowing experiments, a single-frequency laser at 443.3 nm was used with a 450 long-pass filters.

In order to perform the fluorescence-excitation spectroscopy of single molecules in the confocal microscope, a grating-stabilized external cavity diode laser (ECDL) in Littrow configuration from the "*DL pro HP series"* of Toptica was used (Figure 6.3a). It has a central wavelength of 446 nm and a coarse tuning range of ±2 nm. The laser linewidth that determines the maximum spectral resolution is 900 kHz (factory settings), and is shown in the right side of Fig 6.3b. The grating and the semiconductor gain profile determine the new external lasing mode. The output of the laser is immediately coupled to a Fiber Patchcord (SM/FC 400-640 nm) and directed to the microscope.

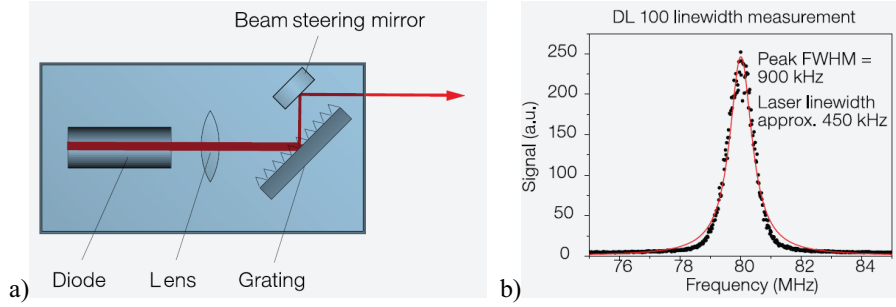

Figure 6.3: *This is very schematic and can be removed at this stage, redrawn later. Representation of our ECDL in a Littrow configuration (Left). Factory recording of the laser output spectrum with a full width at half-maximum of 900 kHz.*

The main emission wavelength of the laser is determined by the current applied in the diode (as shown in Fig. 6.4) at a very well-defined temperature (set at 20±0.1°C). The diode has a measured lasing current threshold at 25.1 mA (factory sheet 24.0 mA). The output power is also linear with current. At 72 mA the power reaches 60.2 mW before the

fiber and 37 mW after it. At the optimal scanning conditions of 66.8 mA it gives 55.6 mW before and 32.0 mW after. The transmission efficiency of all the optical elements in the optical table, considering the objective transmission of 30 %, is just 7.2 % from the power measured.

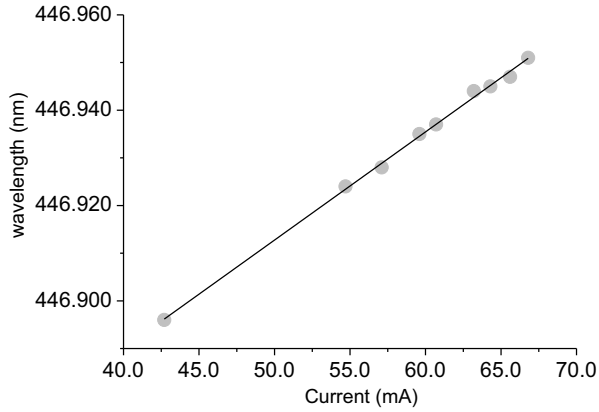

Figure 6.4: *The measured central wavelength as a function of current follows a linear dependence with a slope of 0.0022 nm / mA. The power after the 24 mA threshold value also increases linearly (data not shown).*

To perform the spectroscopy of single excitation lines of perylene, the diode current is fixed at 66.8 mA. The maximum hopping-free scan width from specifications is 22 GHz for 8 Volts (applied to the piezo). For our experiments the piezo was driven with 200 mV which corresponds to 550 MHz (± 275 MHz around the central wavelength). The scanning rate was set at 0.1 Hz. At the same time, detection was made in wide-field using the CCD camera. The integration time was set to 100 ms (Mega pixel 2x2). So, it takes 10 seconds to scan 200 mV (550 MHz) and 100 frames are taken in this time. This leads to a minimum step size of 5.5 MHz for all the reported fluorescence excitation spectra.

6.3. Results

6.3.1. Bulk spectroscopy

There are no strict rules for the selection of a host-guest system that ensure great stability and narrow lines from the guest molecules. However, in this section we discuss some trends that can be followed step-by-step in order to search for suitable host-guest systems yielding lifetime-limited excitation lines of single molecules.

We studied several samples of perylene at different temperatures and with different excitation sources. The emission maximum of perylene at 5 K under 405 nm excitation, appears in *p*-DCB at 436.4 nm, in *o*-DCB at 450.1 nm, and in fluorene at 457.9 nm. The electronic transition of any aromatic guest molecule in a solid is expected to be blue-shifted with respect to the gas phase value[33]. Inside a solid, the guest molecule feels a local strain field exerted by the surrounding molecules that determines the position of the maximum emission wavelength.

In the case of *o*-DCB, host molecules are not-centrosymmetric, static dipole-dipole interactions are very likely to be present and to affect the spectral position of the 450 nm emission of perylene. *p*-DCB, on the other hand, is centrosymmetric and forms a polycrystalline solid with a well-defined γ-phase at T < 100 K which is different from the α-phase at room temperature. A special feature of *p*-DCB is the formation of "molecular sheets" between adjacent crystalline planes[34]. The strong shift (14 nm) of the emission in *p*-DCB compared to *o*-DCB could be explained assuming that perylene molecules are embedded exactly in those molecular planes, and therefore feel strong *pi*-stacking interactions with the neighboring *p*-DCB molecules of adjacent planes[35].

In non-polar organic crystals the dispersion (London) interactions that contribute to the stabilization of the excited state depend on the polarizability of the guest and host molecules. These Van der Waals interactions decay fast with the intermolecular distances, as $1/r^6$. They also depend on the relative orientation of the molecules.

pi-stacking interactions between aromatic host and guest can lead to the large red shift observed for perylene in fluorene (Fig.6.5).

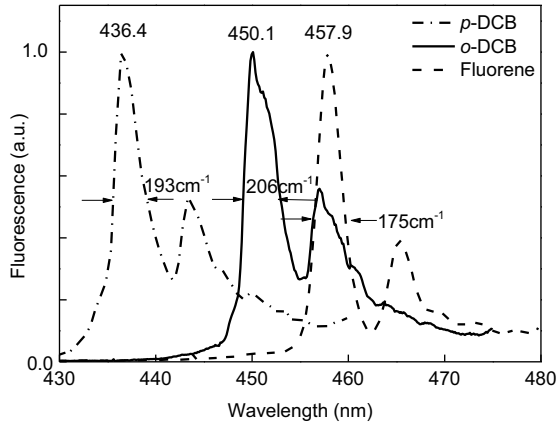

Figure 6.5: *Bulk fluorescence spectra of perylene at 5 K in para-, ortho-dichlorobenzene and fluorene hosts. The excitation source is a broad-band 405 nm laser at 5 K. Linewidth has a FWHM of 2 nm.*

Even though the maxima in the emission spectra are very different for each system of Fig. 6.5, all spectra shows fairly narrow inhomogeneous band with a width of about 2 nm. Fluorene shows the narrower inhomogeneous distribution. In Fig 6.6, perylene in hexadecane (C_{16}) and methylmethacrylate (MMA) show broader linewidths, 3.3 and 5.5 nm, respectively.

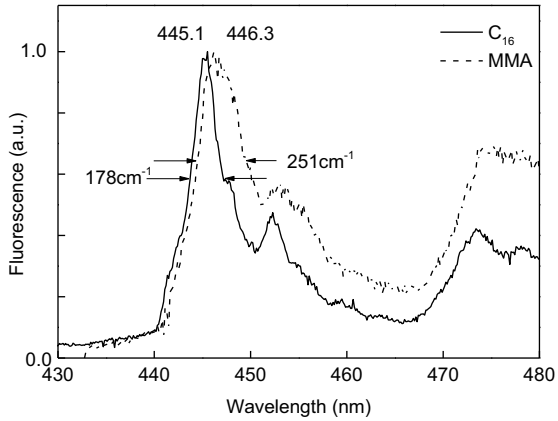

Figure 6.6: *Bulk fluorescence spectra of perylene at 5 K in hexadecane and methylmethacrylate hosts. Using 405 nm as excitation and a 435 nm long-pass filter allowed the collection of the complete fluorescence spectra.*

The next experiment was to perform line-narrowing excitation spectroscopy in the three samples of Fig. 6.5. When we perform spectroscopy using a broad excitation source, the number of molecules that are excited within the inhomogenous distribution is large. As a result, the emission spectra show also broad linewidths. In order to choose a host and decide which single-frequency laser to buy, we needed an accuracy of about ±1.5 nm for the position of the ZPL for these three systems. A single-frequency excitation source at 443 nm was used to record the fluorescence line-narrowing excitation spectra shown in Fig. 6.7 for fluorene and for *o*-DCB samples. However, the use of a 450 long-pass filter limited the direct detection of the ZPL_{00} of the *o*-DCB. Therefore the spectrum of *o*-DCB begins with the first vibrational component of perylene that appears at 453.7 nm (sharp line in the gray spectrum of Fig.6.7) and the ZPL does not appear in this spectrum.

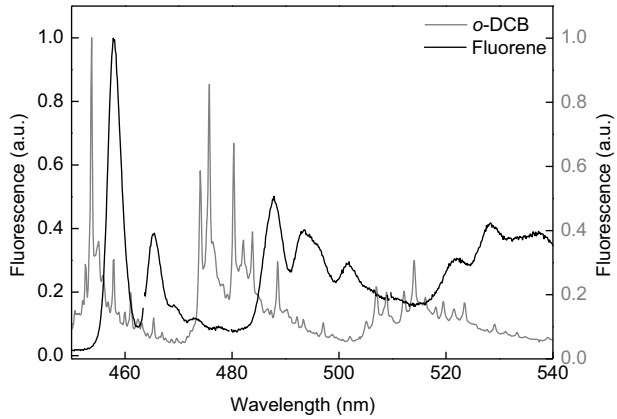

Figure 6.7: *Line narrowing fluorescence spectra of perylene in fluorene and o-DCB. Excitation by a single-frequency laser at 443 nm. The temperature was 1.5 K.*

From the complete spectrum in fluorene with a maximum at 457.9 nm and the first vibronic component at 465.3 nm, it is possible to calculate a 347 cm^{-1} frequency for the first vibrational mode, which correspond to a stretching of the molecule along the long axis[36]. So, considering that the sharp peak from Pr/*o*-DCB (Fig.6.7) corresponds to this longitudinal mode at 347 cm^{-1} with an accuracy of ±20 cm^{-1} is possible to determine that the energy at the ZPL_{00} of perylene in *o*-DCB must appear at 446±2 nm.

Even though fluorene showed a broad site in the bulk sample, we did not observe any narrowing of the spectrum when we used the single frequency excitation laser, in contrast to *o*-DCB (see Fig 6.7). This observation indicates that this host-guest system does not present narrow sites. Indeed, excitation at 443 nm of a bulk spectrum starting at 457.9 nm (0-0 peak) requires dissipation of 735 cm^{-1} in vibrational energy. This frequency does not correspond to any expected normal mode of perylene and should excite all molecules in the inhomogeneous profile equally efficiently. The absence of narrow sites could arise from a large inhomogeneous width, for example because of disorder in the fluorene crystal. In that case, selective spectroscopy would still be

possible, and single-molecule lines would be observable. A second possibility, however, is that the single molecule lines are subject to active spectral diffusion, in which case single-molecule lines would be exceedingly broad. Although mechanisms for spectral diffusion are difficult to imagine with the compact molecule fluorene, we did not take the risk of finding spectral diffusion and discarded the fluorene matrix.

We found the sharp lines in *o*-DCB and the reported data [24,27,29,30] convincing enough to decide for a diode laser at 446±1.5 nm. Moreover, such a laser could still be used in other hosts in the possible case that lifetime-limited lines could not be found in the *o*-DCB experiment. This would have been much more difficult for the red-shifted fluorene system.

6.3.2. Single molecule spectroscopy

Real-time wide-field imaging of the samples showed some positions in the sample along the capillaries where strong fluorescence signals were observed. At the same time, the laser frequency was scanned (22 GHz, 8 V) while moving the samples with the piezo-stages. By doing this, it was possible to find portions of *o*-DCB crystals inside the capillaries containing blinking spots when the laser was scanned, indicating the presence of narrow spectral lines. We found that capillaries showed in general better crystallization and therefore nicer sites with blinking perylene molecules. The thin films samples, although showing bright fluorescent spots, never gave rise to such blinking signals, probably indicating a red-shifted site and excitation of perylene through broad vibronic transitions. Flat capillary samples allowed exploring larger area while the cylindrical ones create geometric aberrations due to the curved surface.

Single shot images are shown in Fig 6.8. An isolated molecule appears in the center of the sample (6.8a). When changing the central frequency of the laser for about 1000 MHz (0.36 mV in the piezo), the spot in the center of the image disappeared and other spots appear (Fig 6.8b). This is a good indication that the bright spots are emitter sources that have high sensitivity to changes in frequency. Qualitatively, the fact that the

spots disappeared after detuning the laser, at least indicated that the linewidth of such a single perylene must be narrower than this 1000 MHz.

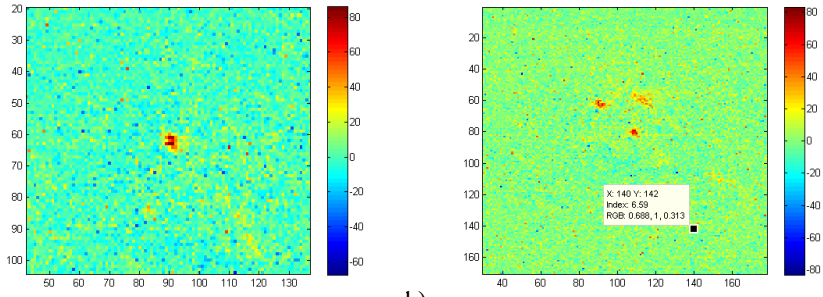

a) b)

Figure 6.8: *Wide field images of an area of 20 x20 μm^2. a is taken at 446.8 nm using 0 volts in the piezo, and b) is taken applying 0.36 mV to the piezo, which is a frequency detuning of 1 GHz. Excitation intensity 1 μW and integration time 100 ms.*

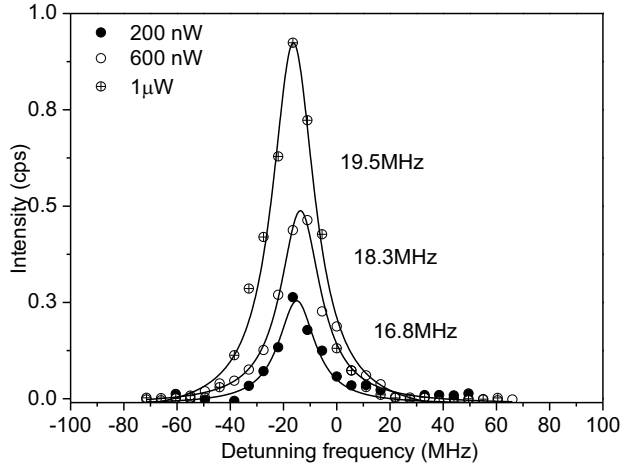

Figure 6.9: *Fluorescence excitation spectra of the single perylene molecule at 1.5 K. The spectra were measured for 200 mV at 0.1 Hz (Piezo) and integration time, 100 ms (300 frames). Three increasing excitation intensities. Solid lines are Lorentzian fits.*

The fluorescence excitation lines as obtained from the experiment are shown in Fig. 6.9. The data in the figure corresponds to the excitation line of the same single molecule at three increasing excitation powers. A slight line broadening due to excitation effects can be observed. The lines are well fitted with Lorentzian profiles, yielding $\gamma = 16.8$ MHz for the weakest excitation intensity of 200 nW (full circles). At 600 nW the width is 18.3 MHz (empty circles) at 1 μW, 19.5 MHz. (crossed circles). Considering the fluorescence lifetime of 7 ± 2 ns reported for perylene in *n*-octane at 4.2 K[31,37], the expected γ_0 linewidth is 22.7 ± 6 MHz. This shows that our measurements provide lifetime-limited linewidths for perylene in *o*-DCB at 1.5 K.

As we could record the data repeatedly for the same molecule to draw a saturation curve is a qualitative proof of the stability of the molecular lines on frequency and of the absence of photobleaching. The fluorescence excitation shown in Fig.6.10 for 350 μW shows a broadening of a factor of 8 compared to the lifetime limited value. The noisy profile may be due to triplet bunching, which will be investigated in future work.

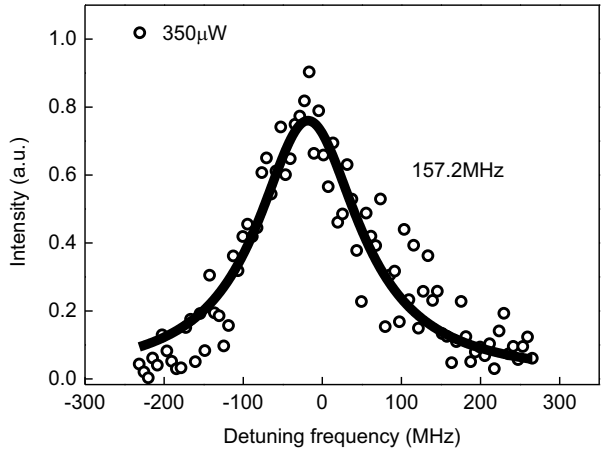

Figure 6.10: *Fluorescence excitation spectrum of the single molecule of Fig. 6.9 for 350 μW excitation intensity. Integration time 100 ms per frame.*

Saturation curve for perylene in o-DCB.

Further to characterize this new system, we looked at the saturation behavior of a single perylene molecule line as a function of intensity. Figure 6.11 shows the variations of the linewidth of the molecule with excitation power, from 23 MHz up at 200 nW to more than 1 GHz at 1 mW excitation power. A fit with the proper saturation expression (Eq.6) yields a saturation intensity ≤ 1 W/ cm^2 for perylene in *o*-DCB. Extrapolating the fit to low excitation powers provides a homogeneous linewidth γ_0=18 MHz.

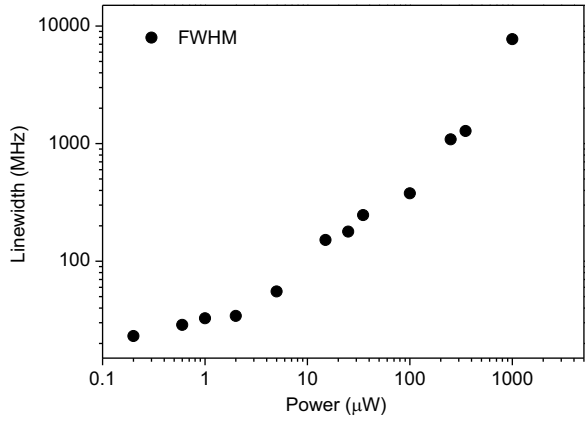

Figure 6.11: *Averaged fluorescence excitation linewidth as a function of excitation power (0.2, 0.6, 1, 2, 5, 15 25, 35, 100, 250, 350 and 1000 μW). The sample was illuminated over a 20×20 μm^2 area.*

The linewidth γ changes due to intensity increasing or decreasing, *I,* according to:

$$\gamma = \gamma_0 \sqrt{1 + \frac{I}{I_S}} \quad ,$$

where γ_0 is the intrinsic linewidth at zero intensity. An important parameter to characterize perylene as a single emitter is the saturation intensity I_s at which the linewidth equals $\gamma_0\sqrt{2}$.

After background subtraction, we obtain the maximum intensity of the peak from the same Lorentzian fits. Figure 6.12 shows the dependence of the detected emission rate of a single perylene with increasing excitation intensity. The last parameter that can be obtained from saturation curves is the fluorescence count rate at saturation $R_\infty \approx 6.3\times10^4$ count/s, after fitting. This rate determines the maximum number of photons (cps) that can be emitted from a single perylene molecule in *o*-DCB when excited on resonance at excitation intensity $I > I_{sat}$.

$$R(I) = R_\infty \frac{I}{I + I_s} \quad ,$$

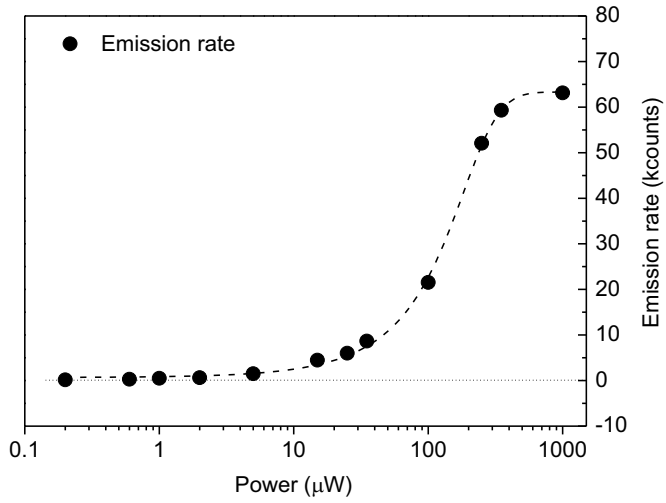

Figure 6.12: *Detected fluorescence count rate at increasing excitation powers (0.2, 0.6, 1, 2, 5, 15, 25, 35, 100, 250, 350 and 1000 μW). The detection rate of fluorescence photons reaches 63,300 cps at saturation.*

Assuming that the triplet bottleneck is negligible, the detection yield can be calculated by considering the excitation linewidth of 16 MHz as lifetime-limited, which corresponds to a maximum emission rate of 6.2×10^{8} count/s. Then, for a very bad detection yield of about 6×10^{-4} one can determine the expected emission photons at saturation, 3.7×10^{8} count/s. This agrees with typical detection yields in low-temperature experiments, which range between 10^{-2} and 10^{-3}. Our lower value is due to extra losses in the transmission of the optics in the blue spectral region where perylene emits (440-460 nm).

Another way to present the saturation study of a single molecule is by looking to the profile by plotting the linewidth vs the line intensity. It shows a very god agreement with the expected saturation laws.

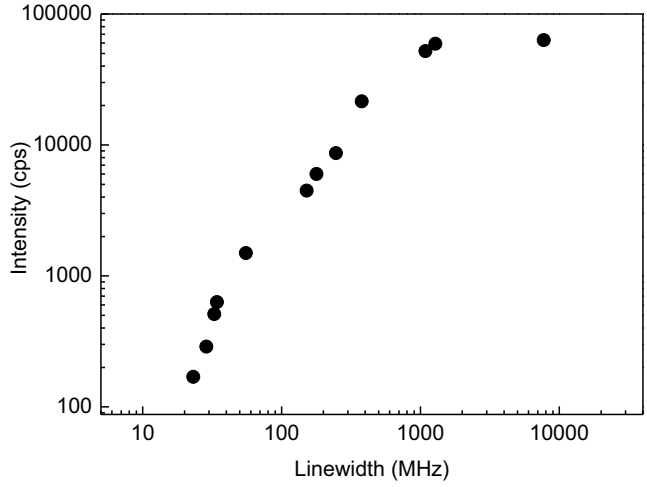

Figure 6.13: *Plot of the maximum fluorescence signal of a single molecule line vs its linewidth for various excitation intensities.*

6.4. Discussion

Ortho-DCB as a host presents high excitation energies of its singlet (256 nm) and of its triplet (about 353 nm) [38]. Therefore, these host electronic states are well above the singlet excitation energies of many different guests (DBT, terrylene) but also of Perylene (singlet at 443 nm). Therefore, the guest fluorescence cannot be quenched by energy transfer or intermolecular intersystem crossing[24,26].

The use of capillaries may induce a better crystallization of the liquid mixture when is cooled down. It defines better insertion sites and the single molecules lines are narrower. In thin film in coverslips, the main problem was to manipulate the sample at room temperature because of leaking problems and of sublimation. With capillaries it is possible to study multiple samples at the same time. Very thin hollow fibers or cavities can be filled with this simple mixture and then cooled down.

6.5. Conclusion

Lifetime-limited lines of perylene have been observed in this work for the first time. *o*-DCB, *p*-DCB and fluorene all showed sharp features in the bulk spectrum at 5 K and therefore maybe stable and narrow single molecules could be found. However we do not have the right lasers to pursue these studies.

Reference List

1. Lettow, R.; Rezus, Y. L. A.; Renn, A.; Zumofen, G.; Ikonen, E.; G+¦tzinger, S.; Sandoghdar, V. Quantum Interference of Tunably Indistinguishable Photons from Remote Organic Molecules. *Phys. Rev. Lett.* **2010,** *104* (12), 123605.

2. Trebbia, J. B.; Tamarat, P.; Lounis, B. Indistinguishable near-infrared single photons from an individual organic molecule. *Physical Review A* **2010,** *82* (6).

3. Orrit, M.; Bernard, J.; Zumbusch, A.; Personov, R. I. Stark-Effect on Single Molecules in A Polymer Matrix. *Chemical Physics Letters* **1992,** *196* (6), 595-600.

4. Rezus, Y.; Walt, S.; Lettow, R.; Renn, A.; Zumofen, G.; Goetzinger, S.; Sandoghdar, V. Single-Photon Spectroscopy of a Single Molecule. *Physical Review Letters* **2012,** *108* (9).

5. Kumar, S.; Kristiansen, N. I.; Huck, A.; Andersen, U. L. Generation and Controlled Routing of Single Plasmons on a Chip. *Nano Letters* **2014,** *14* (2), 663-669.

6. Siyushev, P.; Stein, G.; Wrachtrup, J.; Gerhardt, I. Molecular photons interfaced with alkali atoms. *Nature* **2014,** *509* (7498), 66-+.

7. Puller, V.; Lounis, B.; Pistolesi, F. Single Molecule Detection of Nanomechanical Motion. *Physical Review Letters* **2013,** *110* (12).

8. Jelezko, F.; Tamarat, P.; Lounis, B.; Orrit, M. Dibenzoterrylene in naphthalene: A new crystalline system for single molecule spectroscopy in the near infrared. *Journal of Physical Chemistry* **1996,** *100* (33), 13892-13894.

9. Orrit, M.; Bernard, J. Single Pentacene Molecules Detected by Fluorescence Excitation in A Para-Terphenyl Crystal. *Physical Review Letters* **1990,** *65* (21), 2716-2719.

10. Kummer, S.; Basche, T.; Brauchle, C. Terrylene in P-Terphenyl - A Novel Single-Crystalline System for Single-Molecule Spectroscopy at Low-Temperatures. *Chemical Physics Letters* **1994,** *229* (3), 309-316.

11. Nicolet, A. A.; Hofmann, C.; Kol'chenko, M. A.; Kozankiewicz, B.; Orrit, M. Single dibenzoterrylene molecules in an anthracene crystal: Spectroscopy and photophysics. *Chemphyschem* **2007,** *8* (8), 1215-1220.

12. Guttler, F.; Croci, M.; Renn, A.; Wild, U. P. Single molecule polarization spectroscopy: Pentacene in p-terphenyl. *Chemical Physics* **1996,** *211* (1-3), 421-430.

13. Nicolet, A. A.; Bordat, P.; Hofmann, C.; Kol'chenko, M. A.; Kozankiewicz, B.; Brown, R.; Orrit, M. Single dibenzoterrylene molecules in an anthracene crystal: Main insertion sites. *Chemphyschem* **2007,** *8* (13), 1929-1936.

14. Toninelli, C.; Early, K.; Bremi, J.; Renn, A.; Goetzinger, S.; Sandoghdar, V. Near-infrared single-photons from aligned molecules in ultrathin crystalline films at room temperature. *Optics Express* **2010,** *18* (7), 6577-6582.

15. Pfab, R. J.; Zimmermann, J.; Hettich, C.; Gerhardt, I.; Renn, A.; Sandoghdar, V. Aligned terrylene molecules in a spin-coated ultrathin crystalline film of p-terphenyl. *Chemical Physics Letters* **2004,** *387* (4-6), 490-495.

16. Moerner, W. E.; Plakhotnik, T.; Irngartinger, T.; Croci, M.; Palm, V.; Wild, U. P. Optical Probing of Single Molecules of Terrylene in A Shpolskii Matrix - A 2-State Single-Molecule Switch. *Journal of Physical Chemistry* **1994,** *98* (30), 7382-7389.

17. Palewska, K.; Lipinski, J.; Sworakowski, J.; Sepiol, J.; Gygax, H.; Meister, E. C.; Wild, U. P. Total Luminescence Spectroscopy of Terrylene in Low-Temperature Shpolskii Matrices. *Journal of Physical Chemistry* **1995,** *99* (46), 16835-16841.

18. Kozankiewicz, B.; Bernard, J.; Orrit, M. Single-Molecule Lines and Spectral Hole-Burning of Terrylene in Different Matrices. *Journal of Chemical Physics* **1994,** *101* (11), 9377-9383.

19. Vacha, M.; Liu, Y.; Nakatsuka, H.; Tani, T. Inhomogeneous and single molecule line broadening of terrylene in a series of crystalline n-alkanes. *Journal of Chemical Physics* **1997,** *106* (20), 8324-8331.

20. Durand, Y.; Bloess, A.; Kohler, J.; Groenen, E. J. J.; Schmidt, J. Spectral diffusion of individual pentacene, terrylene, and dibenzanthanthrene molecules in n-tetradecane. *Journal of Chemical Physics* **2001,** *114* (15), 6843-6850.

21. Tchenio, P.; Myers, A. B.; Moerner, W. E. Vibrational Analysis of the Dispersed Fluorescence from Single Molecules of Terrylene in Polyethylene. *Chemical Physics Letters* **1993,** *213* (3-4), 325-332.

22. Tchenio, P.; Myers, A. B.; Moerner, W. E. Optical Studies of Single Terrylene Molecules in Polyethylene. *Journal of Luminescence* **1993,** *56* (1-6), 1-14.

23. Fleury, L.; Zumbusch, A.; Orrit, M.; Brown, R.; Bernard, J. Spectral Diffusion and Individual 2-Level Systems Probed by Fluorescence of Single Terrylene Molecules in A Polyethylene Matrix. *Journal of Luminescence* **1993,** *56* (1-6), 15-28.

24. Walla, P. J.; Jelezko, F.; Tamarat, P.; Lounis, B.; Orrit, M. Perylene in biphenyl and anthracene crystals: an example of the influence of the host on single-molecule signals. *Chemical Physics* **1998,** *233* (1), 117-125.

25. Zazubovich, V.; Suisalu, A.; Leiger, K.; Laisaar, A.; Kuznetsov, A.; Kikas, J. Pressure effects on the spectra of dye molecules in incommensurate and commensurate phases of biphenyl. *Chemical Physics* **2003,** *288* (1), 57-68.

26. Nicolet, A.; Kol'chenko, M. A.; Kozankiewicz, B.; Orrit, M. Intermolecular intersystem crossing in single-molecule spectroscopy: Terrylene in anthracene crystal. *Journal of Chemical Physics* **2006,** *124* (16).

27. Pirotta, M.; Renn, A.; Werts, M. H. V.; Wild, U. P. Single molecule spectroscopy, perylene in the Shpol'skii matrix n-nonane. *Chemical Physics Letters* **1996,** *250* (5-6), 576-582.

28. Pirotta, M.; Renn, A.; Wild, U. P. Stark effect measurements on single perylene molecules. *Helvetica Physica Acta* **1996,** *69*, 7-8.

29. Attenberger, T.; Bogner, U.; Maier, M. Electric-Field Effects on Persistent Spectral Holes - Perylene in the Shpolskii Matrix Normal-Heptane. *Chemical Physics Letters* **1991,** *180* (3), 207-210.

30. Basche, T.; Moerner, W. E. Optical Modification of A Single Impurity Molecule in A Solid. *Nature* **1992,** *355* (6358), 335-337.

31. Basche, T.; Ambrose, W. P.; Moerner, W. E. Optical-Spectra and Kinetics of Single Impurity Molecules in A Polymer - Spectral Diffusion and Persistent Spectral Hole Burning. *Journal of the Optical Society of America B-Optical Physics* **1992,** *9* (5), 829-836.

32. Boese, R.; Kirchner, M. T.; Dunitz, J. D.; Filippini, G.; Gavezzotti, A. Solid-state behaviour of the dichlorobenzenes: Actual, semi-virtual and virtual crystallography. *Helvetica Chimica Acta* **2001,** *84* (6), 1561-1577.

33. Sesselmann, T.; Richter, W.; Haarer, D.; Morawitz, H. Spectroscopic studies of impurity-host interactions in dye-doped polymers: Hydrostatic-pressure effects versus temperature effects. *Phys. Rev. B* **1987,** *36* (14), 7601-7611.

34. Thiery, M. M.; Rerat, C. Calculation of crystal and molecular structures of the temperature and pressure polymorphs of para-dichlorobenzene p-C6H4Cl2. *Journal of Chemical Physics* **2003,** *118* (24), 11100-11110.

35. Wheeler, G. L.; Colson, S. D. Intermolecular Interactions in Polymorphic P-Dichlorobenzene Crystals - Alpha, Beta, and Gamma Phases at 100Degreesk. *Journal of Chemical Physics* **1976,** *65* (4), 1227-1235.

36. Unwin, P. J.; Jones, T. S. Vibrational properties of ordered perylene thin films on GaAs(100) and InAs(111)A. *Surface Science* **2003,** *532*, 1011-1016.

37. Abram, I. I.; Auerbach, R. A.; Birge, R. R.; Kohler, B. E.; Stevenson, J. M. Narrow-Line Fluorescence-Spectra of Perylene As A Function of Excitation Wavelength. *Journal of Chemical Physics* **1975,** *63* (6), 2473-2478.

38. Alfassi, Z. B.; Previtali, C. M. Triplet state properties of dichlorobenzenes. *Journal of Photochemistry* **1985,** *30* (2), 127-132.

Summary

The field of single-molecule spectroscopy and microscopy at room temperature relies mainly on the dilution of a dye in a solid or solvent such that only one fluorescent molecule is expected within the diffraction-limited spot size. At room temperature the absorption cross section is low because the excitation line is broadened due to electron decoherence. However, when the molecule in a non-interacting solid host is cooled down to 1.5 K (as was done in the research described in this thesis), the suppression of decoherence processes leads to a narrowing of the excitation line (down to the lifetime-limited or Fourier-limited width) and to an increased absorption cross section. Finally, because the purely electronic transition of the molecule occurs without the creation or annihilation of phonons (zero-phonon line), the single molecule can be described as a single-quantum two-level system.

Part of this thesis concerns the spectroscopic properties (the distribution of excitation linewidths, the frequency stability, the saturation profile) of single dibenzoterrylene (DBT, chapter 2), terrylene (chapter 3) and perylene (chapter 6) molecules embedded in different solid hosts in order to characterize these new host-guest systems for single-molecule spectroscopy. By looking at the distribution of the excitation linewidths of selected single molecules, obtained at zero intensity, we correlate the experimental observations with physical phenomena in the local environment of the single fluorophore.

From recording intensity-time traces from a single molecule and by looking at the corresponding auto-correlation functions, we were able to study dynamic processes that occur in the surrounding of the dye molecule at different time scales. Results of such studies are described in chapters 2 and 5.

Further in chapter 5, we use the lifetime-limited linewidths of DBT in an anthracene crystal to perform experiments on a host-guest system that is externally

disturbed in a controlled way. The resonant excitation line serves as an ultra-sensitive vibrational sensor to detect the tiny oscillations of an electrically driven quartz tuning fork. Moreover, the stable single molecules reported in this thesis are suitable isolated quantum systems, which could be used as single photon sources, as optical transistors, as all-optical switches based on non-linear optical phenomena and for optical read-out of the quantum state of nano-mechanical oscillators.

In order to prepare for a proposed experiment on a two-color optical transistor, we need the transition energy from the ground singlet state to the excited triplet state. For perylene embedded in anthracene this transition was measured at 778 nm. For terrylene this transition has never been observed because of the low probability of intersystem crossing. In the work reported in chapter 4, we tried to induce the singlet to triplet transition in this molecule by using an electron beam instead of optical excitation. Besides electron-energy-loss spectroscopy, other techniques were used to study the vibrational and electronic properties of terrylene. Despite all efforts, the energy of the triplet state of terrylene remains unknown.

Samenvatting

Spectroscopie en microscopie aan individuele moleculen bij kamertemperatuur is voornamelijk gebaseerd op het verdunnen van een kleurstof in een oplosmiddel of vaste stof totdat er nog maar één molecuul over is in een volume ter grootte van de optische diffractielimiet. Bij kamertemperatuur is de absorptiedoorsnede van het molecuul klein omdat de spectrale lijnen breed zijn vanwege elektron decoherentie. Echter, wanneer men het molecuul oplost in een vaste matrix waarmee de wisselwerking klein is (zoals we hebben gedaan in de experimenten die in dit proefschrift worden besproken), leidt de onderdrukking van decoherentieprocessen tot een versmalling van de lijn (tot aan de levensduur ofwel Fourier gelimiteerde lijnbreedte) en tot een vergroting van de absorptiedoorsnede. Tenslotte, doordat de optische overgang binnen een molecuul optreedt tussen twee zuivere elektronische toestanden, en zonder de creatie of annihilatie van fononen (de zogeheten nul-fononlijn), kan het individuele molecuul beschouwd worden als een kwantum twee-niveausysteem.

In een deel van dit proefschrift beschrijven wij de spectroscopische eigenschappen (de verdeling van lijnbreedtes, de stabiliteit van de resonantiefrequentie, het verzadigingsprofiel) van individuele dibenzoterryleen (DBT, hoofdstuk 2), terryleen (hoofdstuk 3) en peryleen (hoofdstuk 6) moleculen, ingebed in verschillende vaste stoffen om zo nieuwe combinaties van gast en gastheer te karakteriseren als systemen voor spectroscopie aan individuele moleculen. Door te kijken naar de verdeling van lijnbreedtes van geselecteerde moleculen bij een intensiteit van nul kunnen we de experimentele observaties correleren aan fysische fenomenen die plaatsvinden in de directe omgeving van het kleurstofmolecuul.

Door de lichtintensiteit van een individueel molecuul te volgen in de tijd en te kijken naar de corresponderende autocorrelatie functie, waren we in staat dynamische processen in de omgeving van het kleurstofmolecuul op verschillende tijdschalen te bestuderen. Deze experimenten bespreken we in de hoofdstukken 2 en 5.

Daarnaast gebruiken we in hoofdstuk 5 de levensduur gelimiteerde lijnbreedte van DBT in een anthraceen kristal om de effecten waar te nemen van een externe storing. Daarbij

functioneert de resonante excitatielijn als een ultra-gevoelige sensor om kleine oscillaties van een elektrisch aangedreven stemvork van kwarts te detecteren. Bovendien kunnen de stabiele moleculen die worden beschreven in dit proefschrift mogelijk gebruikt worden als bron van individuele fotonen, als optische transistor, als volledig optische schakelaar gebaseerd op niet-lineaire optische fenomenen en voor het volledig optisch uitlezen van de kwantumtoestand van een nanoscopische mechanische oscillator.

Ter voorbereiding van een voorgesteld experiment met een twee-kleuren optische transistor, is het nodig om het energieverschil tussen de singlet grondtoestand en de triplet aangeslagen toestand te bepalen. Voor peryleen in anthraceen is bekend dat de corresponderende overgang bij 778 nm ligt. Echter voor terryleen kon deze overgang niet waargenomen worden vanwege de lage waarschijnlijkheid van "intersystem crossing" voor dit molecuul. We hebben daarom, als beschreven in hoofdstuk 4, getracht om de singlet-triplet overgang te induceren met behulp van een bundel elektronen. Daarnaast hebben we andere technieken gebruikt voor de bepaling van vibrationele en elektronische eigenschappen van terryleen. Ondanks alle inspanningen weten we de energie van de laagste triplettoestand van terryleen nog steeds niet.

Curriculum Vitae

of Pedro Navarro Pérez, born in México City on the 23rd November 1982.

In 2008, Pedro Navarro graduated from the National Autonomous University of Mexico (UNAM) upon receiving his BSc diploma in Chemistry. His thesis was entitled "*Synthesis of useful chromophores to study energy transfer processes"*. He then enrolled in the MSc program in Physical Chemistry at the same University. In 2009 he received his MSc diploma upon completion of the thesis *"Femto-second studies of internal conversion rates of poly-aromatic hydrocarbons in solution"*. During his MSc studies he was a teaching assistant for a theoretical and practical course in organic synthesis.

In September 2010, he joined the MoNOS group at Leiden University as a PhD candidate under supervision of Prof. dr M. Orrit. In his research project he studied the optical and spectroscopic properties of well-known fluorescent molecules at room and cryogenic temperatures embedded in different solids. By carefully analyzing the fluorescence excitation spectra of isolated single molecules, he studied the nanometer-scale inhomogeneities in the immediate surroundings of the fluorescent molecules. He discovered new systems in which single molecules can be spectrally isolated and studied over extended times. Moreover, he used one of these systems to demonstrate the coupling between a macroscopic mechanical oscillator and a single molecule. He did an internship in the group of Prof. dr S. Tautz, at the Peter Grünberg Institut (PGI-3), Forschungszentrum Jülich, Germany to perform experiments on electron energy-loss spectroscopy of vacuum-deposited terrylene films under ultra-high vacuum conditions. During his time in Leiden he assisted Dr M. Huber three times with the course "Introduction to Quantum Chemistry", which is part of the BSc program "Life science and technology" at Leiden University.

Soon he will join the group of Prof. J. Peón at UNAM in Mexico City, to develop a new family of photo-activatable dyes that may be used for a variety of optical super-resolution techniques such as STORM, *d*STORM, PALM and SOFI.

List of Publications

- J. Zugazagoitia, M. Maya, C. D. Zea, P. Navarro, H.I. Beltrán and J. Peon: "Excited-state dynamics and two-photon absorption cross sections of fluorescent diphenyl-tin(IV) derivatives with schiff bases: a comparative study of the effect of chelation from the ultrafast to the steady-state time scale". *J. Phys. Chem. A* **2010** 114, 704–714.

- Y. Tian, P. Navarro, B. Kozankiewicz and M. Orrit: "Spectral Diffusion of Single Dibenzoterrylene Molecules in 2,3-Dimethylanthracene". *ChemPhysChem* **2012** 13, 3510 – 3515.

- W. Rodríguez-Córdoba, R. Noria-Moreno, P. Navarro and J. Peon: "Ultrafast fluorescence study of the effect of carboxylic and carboxylate substituents on the excited state properties of anthracene". *Journal of Luminescence* **2014** 145, 697-707.

- P. Navarro, Y. Tian, M. van Stee and M. Orrit: "Stable Single-Molecule Lines of Terrylene in Polycrystalline para-Dichlorobenzene at 1.5 K". *ChemPhysChem* **2014** 15, 3032-3039.

- Y. Tian, P. Navarro and M. Orrit: "A Single Molecule as a Local Acoustic Detector for Mechanical Oscillators". *Phys. Rev. Lett.* **2014**. 113, 135505.

- P. Navarro, F.C. Bocquet, I. Deperasinska, G. Pirug, F. S. Tautz and M. Orrit. "Electron energy loss of terrylene deposited on Au (111): Vibrational and electronic spectroscopy". *J. Phys. Chem. C*, accepted for publication.

Acknowledgements

Although the cover of this thesis bears my name only, many people have contributed to the work described in this thesis. There are also people who have contributed to my life in the Netherlands; I gladly acknowledge their contributions here.

During the four years in Leiden, I have seen many people come and go. Even though I cannot name them all, I hope they know that I have not forgotten them.

The experimental work would not have been possible without the fantastic contributions of the high-quality technical support people at the "Leiden Instituut voor Onderzoek in de Natuurkunde" (LION). I thank the people from the mechanical workshop for developing essential components, the people from the cryogenic department for supplying a constant flow of liquid Helium, and the people from the electronic department for keeping the computer equipment in LION updated and for the maintenance of all the lab equipment. I wish to thank Henriëtte van Leeuwen for her great organizational skills, and all my colleges from MoNOS, the Quantum Optics group, and the Biophysics groups at both the Huygens and the Cell Observatory. And I wish to thank all the others with who I interacted for a longer or shorter time while being in Leiden. I had the opportunity to work together with a set of very special people: Dr. Tian, Dr. Yorulmaz, Dr. Zijlstra, Dr. Ruijgrok, Dr. Faez, Dr. Khatua; to all of you I say: thanks.

I would like to thank my supervisor Prof. Dr. Michel Orrit, who invited me to the Netherlands to study single molecules; without him I would never have come to Leiden. Michel, it was a pleasure to work with you! I wish to thank all the members of my family, especially my mom and dad, Pilar and Pedro, my brother Pablo and my uncle Amaury. Also, I would like to thank my good Dutch friends who helped me to fit into the daily life in the Netherlands. Special thanks to the International Student Network in Leiden. Thanks also to all the Mexican friends for sharing with me more than friendship; to all my German friends for their splendid kindness; to the Spanish group for the fruitful discussions and Dutch friends who were around me during the 4 years. And to all of you who read this lines, thanks.